

THE UNIVERSITY OF MANITOBA

EQUIVALENT BANDPASS FILTERS IN
CANONIC LADDER STRUCTURE

BY

EUIWON KIM

A THESIS

SUBMITTED TO THE FACULTY OF GRADUATE STUDIES
IN PARTIAL FULFILLMENT OF THE REQUIREMENTS FOR THE DEGREE OF
DOCTOR OF PHILOSOPHY

DEPARTMENT OF ELECTRICAL ENGINEERING

WINNIPEG, MANITOBA

February 1980

EQUIVALENT BANDPASS FILTERS IN
CANONIC LADDER STRUCTURE

BY

EUIWON KIM

A thesis submitted to the Faculty of Graduate Studies of
the University of Manitoba in partial fulfillment of the requirements
of the degree of

DOCTOR OF PHILOSOPHY

© 1980

Permission has been granted to the LIBRARY OF THE UNIVERSITY OF MANITOBA to lend or sell copies of this thesis, to the NATIONAL LIBRARY OF CANADA to microfilm this thesis and to lend or sell copies of the film, and UNIVERSITY MICROFILMS to publish an abstract of this thesis.

The author reserves other publication rights, and neither the thesis nor extensive extracts from it may be printed or otherwise reproduced without the author's written permission.

ABSTRACT

This thesis is an exhaustive study of equivalent bandpass filters in canonic ladder structure. Theorems are developed to determine and generate the exact number of equivalent canonic ladder networks based on the sequence of transmission zero removal at extreme frequencies. It is proven that there exists a unique equivalent network corresponding to each independent sequence of the transmission zero removal. A straightforward procedure is developed that synthesizes the two-element-kind driving-point functions in all possible canonic ladder structures. The procedure is applied to the realization of equivalent canonic ladder networks for a given bandpass transfer function. An explicit formula is established for the exact number of singly terminated equivalent canonic ladder networks. Comparisons of equivalent networks are made for the 4th and 6th order bandpass functions with respect to certain criteria.

A direct conversion from the single termination to double termination is investigated for the normal bandpass transfer function, i.e., the transfer function with an equal distribution of transmission zeros at $s=0$ and $s=\infty$. It is proven that there always exists a $p(s)$, the zeros of which satisfying a quadrantal symmetry requirement, and the ladder two-ports directly derived from the singly terminated networks form a complete set of doubly terminated equivalent canonic ladder two-ports. It is also shown that those equivalent networks are conformable to the bandpass characteristic within a multiplicative constant. A comparison among equivalent networks for certain specified criteria is given with the emphasis on the magnitude sensitivity of the

transfer function with respect to component value variations.

The equivalent canonic ladder networks are subsequently used as reference prototype networks for transforming, by means of component simulation techniques, into a corresponding set of active filters. A similar approach, using a bilinear transformation, is taken to obtain wave digital filters, all in canonic ladder structures. In the wave digital filter realization, a new analysis method for the transfer function magnitude sensitivity with respect to multiplier coefficient is presented and an actual sensitivity comparison is made for the 4th order maximally flat bandpass filter as an example.

It is concluded that newly generated canonic bandpass ladder networks reveal superior features in comparison with the conventional network in the passive filter realization. The superior characteristics are preserved in both active RC and wave digital filters which are directly derived from the prototype reference networks.

LIST OF FIGURES

<u>FIGURE</u>	<u>Page</u>
2.1 Reduction of Z_C and Z_D types into Z_A or Z_B Types	8
2.2 (a) Degree reduction cycle for Z_A or Z_B type (b) Table to be used to sketch all equivalent canonic ladders	13
2.3 (a) Schematic reduction procedure for the canonic ladder realizations of Z_A type (b) The same for Z_B type	15
2.4 Illustration of the rule	17
2.5 General configurations of BS type canonic ladder networks	18
3.1 Singly terminated LC two-port networks	25
3.2 Grouping of transmission zero pairs	27
3.3 Sketch of seven equivalent BP networks	32
3.4 Plot of magnitude sensitivity - Load terminated	37
3.5 The Darlington circuit structure	40
3.6 Equival normal BP canonic networks (a) for $n=2$ (b) for $n=3$	48
3.7 Doubly terminated networks with interchanged LC two-ports and terminations	49
3.8 Equivalent T network of Fig. 3.7(a)	49
3.9 Zero-pair distribution of $\rho(s)$	52
3.10 Zero-pair distribution of $\rho(s)$	58
3.11 (a) Doubly terminated and (b) Singly terminated filter . . .	67
3.12 Locus of $\rho(j\omega)$	68
3.13 Plot of magnitude sensitivity - Doubly terminated	73

<u>FIGURE</u>		<u>Page</u>
4.1	The Antoniou GIC embedded in an arbitrary network	78
4.2	The Antoniou GIC used to realize a grounded inductor	82
4.3	Simulation of an inductive network N through the connection of a topologically identical resistive network N' and n GICs	84
4.4	Active realizations with optimum GICs for $B_n = 0.1$	85
4.5	Doubly terminated lossless network	90
4.6	Definition of port variables	91
4.7	(a) 4th order canonic bandpass filter (b) Corresponding wave digital filter using two four-port adaptors (c) Corresponding wave digital filter using four three-port wave adaptors	97
4.8	(a) 4th order canonic bandpass filter (b) Corresponding wave digital filter	98
4.9	(a) 4th order canonic bandpass filter (b) Corresponding wave digital filter	98
4.10	Magnitude sensitivity with respect to multiplier coefficients; (a) for N_{31} , (b) for N_{33}	103

ACKNOWLEDGEMENT

The author wishes to express his deepest gratitude to his supervisor Professor H.K. Kim for his advising the thesis, invaluable guidance, encouragement and kind assistance throughout the entire course of his post-graduate study.

The author also wishes to acknowledge gratefully Mr. B.A. German for his laborious proof-reading and valuable advices. Special thanks are due to author's wife, Hyun-Ock, who took care of two-year old boy alone while carrying her own graduate study during the preparation of this thesis.

The financial assistance from the National Research Council and the University of Manitoba is gratefully acknowledged.

TABLE OF CONTENTS

	<u>Page</u>
ABSTRACT	i
LIST OF FIGURES	iii
ACKNOWLEDGEMENT	v
CHAPTER	
I INTRODUCTION	1
II EQUIVALENT CANONIC LADDER NETWORKS OF TWO- ELEMENT-KIND	5
2.1 Canonic Ladder Realization of LC Driving-Point Functions	7
2.1.1 Classification and Definition	7
2.1.2 Properties of LC Driving-Point Impedance of $Z_A(s)$ and $Z_B(s)$ Type	9
2.1.3 Total Number of Canonic LC Ladder Networks	10
2.2 Canonic Ladder Realization of RC and RL Driving- Point Functions	20
2.2.1 RC Driving-Point Functions	20
2.2.2 RL Driving-Point Functions	22
III GENERATION OF EQUIVALENT BANDPASS LADDER NETWORKS IN CANONIC FORM	23
3.1 Formulation of Problem	24
3.2 Singly Terminated BP Canonic Ladder Realization Based on Transmission Zero Removal Sequences	24
3.2.1 Realization Procedure	24
3.2.2 Normal BP Networks	30
3.2.3 Comparison of Equivalent Networks	32

	<u>Page</u>
3.3 Direct Derivation of Doubly Terminated Canonic BP Ladder Networks	38
3.3.1 Doubly Terminated Network	39
3.3.2 Canonic Ladder Realization Procedure	43
3.3.3 Total Number of Doubly Terminated Canonic Ladders	47
3.3.4 Constraint on Terminating Resistance	51
3.3.5 Sensitivity Considerations in Doubly Terminated Networks	62
3.3.6 Comparison of Equivalent Networks	71
IV DIRECT CONVERSION TO ACTIVE AND DIGITAL FILTERS IN CANONIC LADDER STRUCTURES	74
4.1 Active Canonic Filters	75
4.1.1 Component Simulation - Optimum GIC	76
4.1.2 Active Realizations - GIC Ladder Embedding Technique	83
4.2 Digital Canonic Filters	86
4.2.1 Wave Digital Filter	88
4.2.2 Wave Digital Filter Realization	90
4.2.3 Sensitivity Considerations and Comparisons . .	96
V CONCLUSION	104
APPENDIX I	107
APPENDIX II	110
APPENDIX III	112
REFERENCES	119

CHAPTER I

INTRODUCTION

A filter, in the most general sense, is a device or a system that alters in a prescribed way the input that passes through it. Since the basic concept of a filter was originally introduced by G. Campbell and K. Wagner independently in 1915, the development of filter knowledge and filter technologies has been and is still expanding. Today, filters have permeated the electronic technology so much that it is difficult to think of any system or device that does not employ a filter in one form or another.

The filter synthesis involves two phases: one, called the approximation phase, consists of finding a realizable network function which approximates the specifications, while the other, the realization phase, deals with the synthesis of the obtained network function. After the approximation problem is solved and a realizable network function (driving-point or transfer) is at hand, what remains to be found is a suitable network having the given function as its driving-point or transfer function. In this study, we assume that the network functions are given, therefore, we deal with the second phase exclusively.

Historically the first and still the most widely used network structure is the ladder network. It is a restricted form of network in that it can have transmission zeros only in the region of the complex s -plane where the poles of the driving-point immittances are located. Hence, in an LC ladder, all the transmission zeros must lie on the imaginary axis, including the origin and infinity.

Since S. Darlington [11] presented an insertion loss synthesis method, the doubly terminated LC ladder networks have been widely used in filter design. The ladder networks exhibit excellent sensitivity characteristics and also render easy tunability. Furthermore, due to the nature of the structure they are readily amenable for conversion into active and digital filters, retaining all the desirable features of the ladder networks.

The network class which utilizes a minimum number of elements is said to be canonic. For economical reasons, the canonic networks are attractive. The first canonic realization was described by Foster for the LC immittance function, however, the circuit configuration was not of much practical applications. The canonic ladder forms presented by Cauer, however, have been used extensively in filter designs, because they yield ladder structures of high-pass or low-pass characteristics. For the bandpass realization, it has been a general practice to obtain a prototype low-pass network first and apply the frequency transformation element by element. Recently, Kim [23] presented a formula for the generation of equivalent bandpass ladder networks and suggested possible comparisons of equivalent networks for specified merits.

This thesis is a thorough investigation of the single terminated canonic ladder structures and their direct transformation into doubly terminated equivalent bandpass networks within the canonicity. As a consequence, numerous non-conventional networks are generated that satisfy superior design criteria. Subsequently, these equivalent networks are used as prototypes for the realization of RC active and digital filters.

In Chapter II, theorems are presented that determine and generate the

exact number of equivalent canonic realizations of driving-point immittance functions of two-element-kind.

Chapter III extends the theorems developed in Chapter II to generate all the equivalent canonic LC ladder two-ports for the specified pattern of the transmission zeros. Singly terminated LC ladder two-ports are first developed and various design parameters are tabulated for comparison. The results are directly applied to generate doubly terminated equivalent canonic ladder networks. It has been proved that the process of equivalent network generation is exhaustive and complete. A straightforward synthesis procedure is advanced with illustrative examples. A brief introduction on sensitivity functions is presented to make comparisons among equivalent networks.

In Chapter IV, using those equivalent canonic LC ladder two-ports as reference prototypes, a method of direct conversion into active RC and digital filters is developed. In the first section, an optimum Generalized Immittance Converter (GIC) is discussed and a component simulation technique is applied to the prototype ladder networks to generate equivalent active RC bandpass filters. The ladder embedding technique is employed for the minimum number of optimum GICs. In the second section, a wave digital filter realization method is introduced and the equivalent reference canonic ladders are directly converted into true ladder wave digital filters that are canonic in both the number of delays and multipliers. A new analysis method for transfer function sensitivity with respect to multiplier coefficient variations is presented. An example is provided to illustrate the basis for comparison among canonic equivalent wave digital filters in ladder structures.

Concluding remarks are made and subsequent extension to the design of precision monolithic high-order filters using MOS switched capacitor techniques is suggested in Chapter V.

CHAPTER II

EQUIVALENT CANONIC LADDER NETWORKS OF TWO-ELEMENT-KIND

Networks containing the minimum number of elements to meet given specifications are said to be canonic. A method for the realization of driving-point functions of two-element-kind networks into canonic form was first proposed by Foster for LC networks. The procedure is straightforward: a partial-fraction expansion is applied on either impedance $Z(s)$ or admittance $Y(s)$, and each term is synthesized, and interconnected accordingly either in series (the first Foster form) or in parallel (the second Foster form). The other two canonic realizations named after Cauer, are based on the continued-fraction expansion. The first type is the continuous removal of the pole at $s = \infty$ and the second type of the expansion removes the poles at $s = 0$ continuously. The corresponding ladder networks are called the first Cauer form and the second Cauer form, respectively [1 - 2].

Generation of new canonic structures, for obvious reasons, has always been a topic of interest. Lee [8, 9] recently showed the existence of other canonic structures; one is the non-symmetrical lattice, where the series elements are of opposite kinds and the other is the bridged-T structure. In both cases, the canonic cycle reduces the order of reactance function by four.

More recently, Ramachandran, et. al. [10] presented a new canonic realization cycle of order six for the realization of lossless immittance

functions, which is based on a twin-T network.

In practice, often one canonic form may be deemed preferable to others under specified criteria such as element size, compensation for parasitic effects, element value spread, tunability, structure, etc. The canonic network in the ladder structure is most preferred by filter designers for a number of reasons:

The ladder is a network structure which has a topology such that the alternating series and shunt arms are made up of simple L or C elements, or simple combinations of these. As a consequence, each arm is responsible for creating a transmission zero, and, vice versa, each finite non-zero transmission zero can be identified with a branch. This makes the tuning of the ladder filter relatively simple. Equally important, due to this property, the transmission zeros of ladders are fairly insensitive to element variations, as compared to the transmission zeros in circuits which depend on a bridge-type balance of several branch impedances to obtain a zero of transmission. Above all, most applications require a filter with a common ground (i.e., unbalanced structure) for which the ladder structure is a natural choice.

The realization of the required reactive ladder networks can be reduced to the synthesis of the associated driving-point function implementing simultaneously the given transmission zeros. Therefore, the theory of LC driving-point function synthesis and its applications were well developed [1 - 7].

It is essential to generate all the possible equivalent canonic ladder networks if we are to compare various meritorious features for a specific

application. In this chapter, a new straightforward procedure is developed that synthesizes the two-element-kind driving-point network functions into canonic ladder structure. A closed form formula is presented to determine the exact number of equivalent canonic ladder networks for the specified driving-point function.

2.1 CANONIC LADDER REALIZATION OF LC DRIVING-POINT FUNCTIONS

2.1.1 Classification and Definitions

The LC driving-point impedances are rational polynomial functions of the complex frequency variable, and can be classified into four distinct types as follows:

$$Z_A(s) = \frac{a_{2n}s^{2n} + a_{2n-2}s^{2n-2} + \dots + a_2s^2 + a_0}{a_{2n-1}s^{2n-1} + a_{2n-3}s^{2n-3} + \dots + a_3s^3 + a_1s} \quad (2.1a)$$

$$Z_B(s) = \frac{a_{2n-1}s^{2n-1} + a_{2n-3}s^{2n-3} + \dots + a_3s^3 + a_1s}{a_{2n}s^{2n} + a_{2n-2}s^{2n-2} + \dots + a_2s^2 + a_0} \quad (2.1b)$$

$$Z_C(s) = \frac{a_{2n+1}s^{2n+1} + a_{2n-1}s^{2n-3} + \dots + a_3s^3 + a_1s}{a_{2n}s^{2n} + a_{2n-2}s^{2n-2} + \dots + a_2s^2 + a_0} \quad (2.1c)$$

$$Z_D(s) = \frac{a_{2n}s^{2n} + a_{2n-2}s^{2n-2} + \dots + a_2s^2 + a_0}{a_{2n+1}s^{2n+1} + a_{2n-1}s^{2n-1} + \dots + a_3s^3 + a_1s} \quad (2.1d)$$

It is to be noted that Z_A and Z_B are of even order, and structurally dual to each other. They possess the properties:

$$Z_A(0) = Z_A(\infty) = \infty \quad \text{and} \quad Z_B(0) = Z_B(\infty) = 0 .$$

On the other hand, Z_C and Z_D are of odd order, and structurally dual to each other exhibiting the properties:

$$Z_C(0) = Z_C(\infty) = \infty \quad \text{and} \quad Z_D(0) = Z_D(\infty) = 0 .$$

It is easily seen that Z_C and Z_D can be reduced to Z_A , or Z_B type, by simply removing a single element as shown in Fig. 2.1. Because of this reduction,

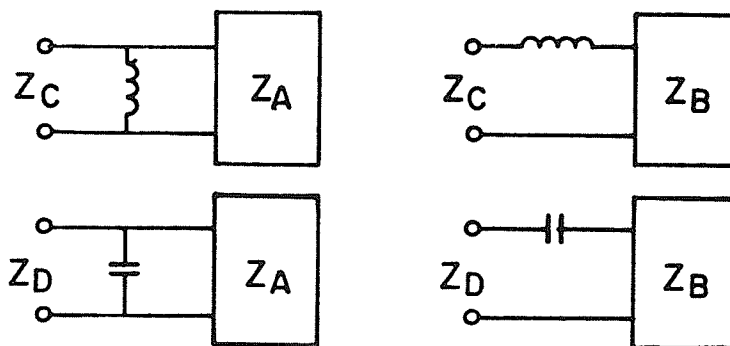


Fig. 2.1 Reduction of Z_C and Z_D types into Z_A or Z_B types.

the synthesis procedure developed for Z_A and Z_B types can be directly applicable to the realization of Z_C and Z_D types. Therefore, we will consider only the synthesis of Z_A and Z_B types of order $2n$.

To realize the LC driving-point impedance of order $2n$ into a canonic form, $2n$ elements are required, and all the transmission zeros occur on the $j\omega$ axis. Depending on the location of transmission zeros on the $j\omega$ axis, LC canonic ladder network can be classified as follows:

- (1) Low Pass (LP) Network; all the transmission zeros are at $s = \infty$ (first Cauer form).
- (2) High Pass (HP) Network; all the transmission zeros are at $s = 0$ (second Cauer form).
- (3) Band Pass (BP) Network; an equal or non-equal distribution of transmission zeros at $s = \infty$ and $s = 0$. We shall call the one that has an equal distribution "normal BP network" to distinguish from others.
- (4) Band Stop (BS) Type; all the transmission zeros are at non-zero finite frequencies.

The networks for LP and HP are well known as Cauer forms, and they are unique. However, the networks for BP are structurally diverse, thus suggesting the possible equivalent networks. The canonic realization in BS type results in a unique structure, but element values differ depending on the order of realization of the non-zero finite frequencies.

2.1.2 Properties of LC Driving-Point Impedance of Z_A and Z_B Type

The driving-point impedances of type Z_A and Z_B are the special kinds of positive real functions. They have the following properties:

- (i) The numerator and denominator of Z_A are even and odd, respectively, and $Z_B(s)$ is the dual of $Z_A(s)$. Consequently,

$$Z_A(s) = -Z_A(-s) \quad Z_B(s) = -Z_B(-s) .$$

- (ii) The degree of the numerator and denominator polynomials differs by one at most.
- (iii) All the poles are simple with real and positive residues, and occur only on the imaginary axis of the s -plane. Since the inverse of Z_A or Z_B is functionally identical, the same statements hold for the zeros of the functions.
- (iv) The poles and zeros must always interlace on the imaginary axis.

2.1.3 Total Number of Canonic LC Ladder Networks

The fundamental operation of passive network synthesis is the pole removal operation. Poles are removed implementing simultaneously the transmission zeros [1 - 7].

The canonic ladder realization of the LC driving-point immittance function of order $2n$ requires that:

- (i) Due to canonicity, the number of elements is $2n$.
- (ii) Due to structure, the transmission zeros are realized as the poles of series arm impedances or shunt arm admittances.

The requirement (i), in turn, implies that $2n$ full removal operations are required if removed at $s = 0$ and/or $s = \infty$ only, and n full operations if removed at non-zero finite frequencies only.

Let us first consider the variety involved in the removal of poles at extreme frequencies, viz. at $s = 0$ and $s = \infty$. It is straightforward to show that by removing the pole of the LC immittance function twice either at infinity, at the origin or at both, we can reduce the order of the function by two.

The following development for the systematic order reduction is based on the property that "the LC immittance has a zero at $s = 0$ ($s = \infty$) if it is devoid of a pole at $s = 0$ ($s = \infty$)".

Let us consider Z_A type first, $Z_A(s)$ has a pole at $s = 0$ and another at $s = \infty$. After removing the pole at $s = 0$, $Z_1(s)$ has a zero at $s = 0$ retaining the pole at $s = \infty$

$$Z_A(s) = \frac{1/C_0}{s} + Z_1(s) \quad . \quad (2.2)$$

Then, by removing the pole of $Y_1(s)$ at $s = 0$, we have, ($Y_1(s) = 1/Z_1(s)$)

$$Y_1(s) = \frac{1/L_0}{s} + Y_R(s) \quad (2.3)$$

where $Y_R(s)$ has a zero at $s = 0$ retaining the zero at $s = \infty$. Thus, the remainder function $Z_R(s)$ of order $2(n-1)$ is of Z_A type.

Secondly, if we remove the pole at $s = \infty$ first we have

$$Z_A(s) = L_\infty s + Z_1(s) \quad (2.4)$$

where $Z_1(s)$ now possesses a zero at $s = \infty$, retaining the pole $s = 0$.

Further removing a pole of $Y_1(s)$ at $s = \infty$, we write

$$Y_1(s) = C_\infty s + Y_R(s) \quad (2.5)$$

where $Y_R(s)$ has a zero at $s = \infty$, retaining the zero at $s = 0$. Thus, the remainder function $Z_R(s)$ of order $2(n-1)$ is again of Z_A type.

For the last case, we may remove the two extreme poles of $Z_A(s)$ simultaneously; i.e.,

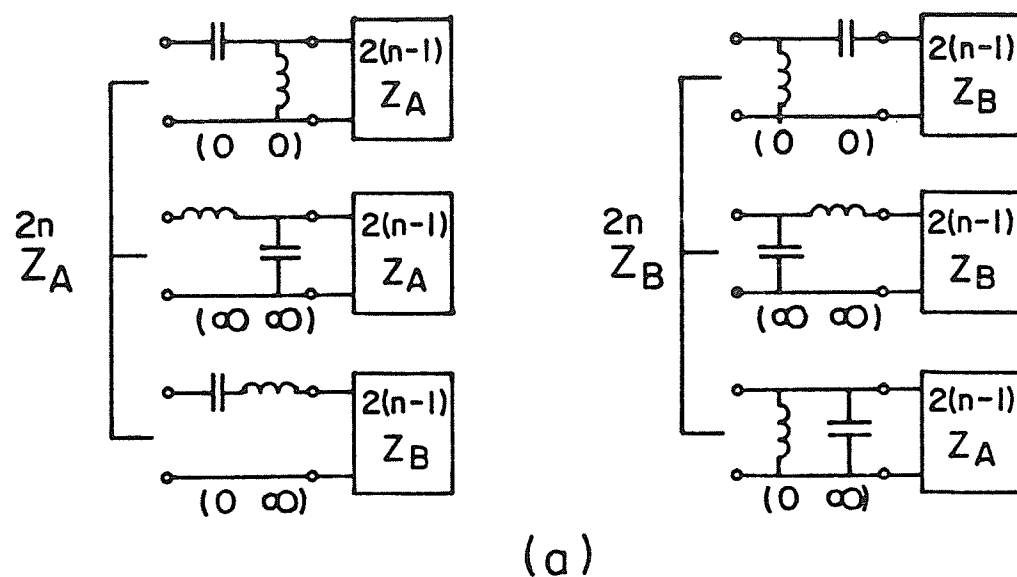
$$Z_A(s) = \frac{1/C_0}{s} + L_\infty s + Z_R(s) \quad (2.6)$$

then, the remainder function $Z_R(s)$ has a zero at $s = 0$, and another zero at $s = \infty$, resulting in the Z_B type.

We can conclude that the type of impedance function changes only when a pole is removed alternately at $s = 0$ and $s = \infty$. Since Z_B type is a dual of Z_A type, the same statement holds with a dual configuration.

These processes of reducing the order of a given function by two are named three reduction cycles, and they are summarized in Fig. 2.2(a) for both Z_A and Z_B types.

The reduction cycles may be classified by the two homogeneous pairs (00) , $(\infty\infty)$ of the transmission zeros and a heterogeneous pair (0∞) as shown in Fig. 2.2(b) depending on the type of the impedance function to be realized.



	(0 0)	(∞ ∞)	(0 ∞)
A			
B			

(b)

Fig. 2.2 (a) Degree reduction cycle for Z_A or Z_B type

(b) Table to be used to sketch all equivalent canonic ladders.

Recalling the fact that a canonic ladder network is realized by a process of continuous pole removal in a specific way, with the aid of the table in Fig. 2.2(b) we can easily show that a different combination of pairs in sequence will produce a different canonic ladder. For example, the sequence consisting of only $(\infty\infty)$ pairs produces the first Cauer form and consisting of only (00) pairs, the second Cauer form. The sequence that is made of only (0∞) pairs yields a normal BP network.

Now, we will present theorems by which we can determine the exact number of independent sequences, therefore, the exact number of equivalent canonic ladder networks.

Theorem 2.1

Given an LC driving-point impedance function of $Z_A(s)$ or $Z_B(s)$ type of order $2n$, there exist 3^{n-1} canonic ladder realizations.

Proof:

For simplicity let us represent Z_A and Z_B by symbols A and B , and each reduction cycle by transmission zero pairs. Then we can develop the schematic reduction procedures as illustrated in Fig. 2.3. At each reduction cycle, three new networks are generated and hence, presumably 3^n networks in total. However, since the last element in the driving-point function synthesis is to be closed, three sections in row A and row B in Fig. 2.2(b) degenerate into one identical section. Thus the total number of canonic ladder realization is 3^{n-1} .

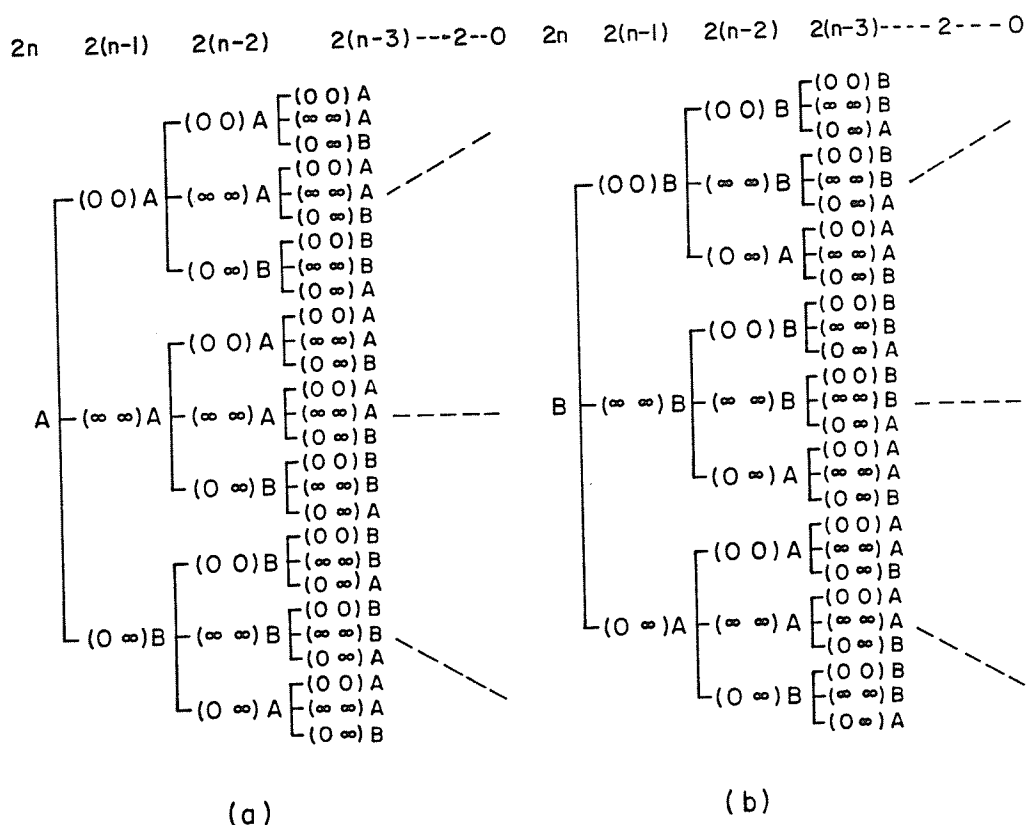


Fig. 2.3 (a) Schematic reduction procedure for the canonic ladder realizations of Z_A type. (b) The same for Z_B type.

Corollary 2.1

Given an LC driving-point impedance function of $Z_C(s)$ or $Z_D(s)$ type of order $2n+1$, there exist $2 \times 3^{n-1}$ canonic ladder realizations.

Proof:

We make use of the proof of theorem 2.1. Since there are two ways of reducing $Z_C(s)$ (or $Z_D(s)$) to $Z_A(s)$ or $Z_B(s)$ type of order $2n$ as illustrated in Fig. 2.1, there exist $2 \times 3^{n-1}$ equivalent canonic ladder networks.

Excluded is the BS type canonic ladder network. This is obtained when pole removal operations are carried out only at non-zero finite pole frequencies. Structurally, there exists a single network for the BS type, but by changing the sequence of resonant pole removal, for the functions of third order or greater, at each reduction step, a family of networks of

identical configuration with different element values may be generated. However, in this case, to ensure that all the transmission zeros are realized at non-zero finite frequencies, a rule is to be imposed on the choice of elements in the first arm. This can be best explained by example.

Example 2.1

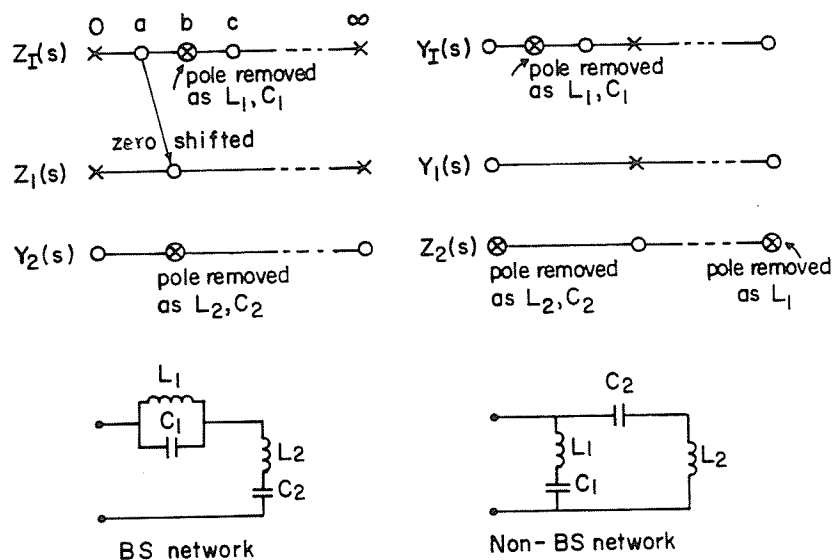
Let us consider LC driving-point impedance functions;

$$Z_I(s) = \frac{(s^2 + a^2)(s^2 + c^2)}{s(s^2 + b^2)} \quad (a)$$

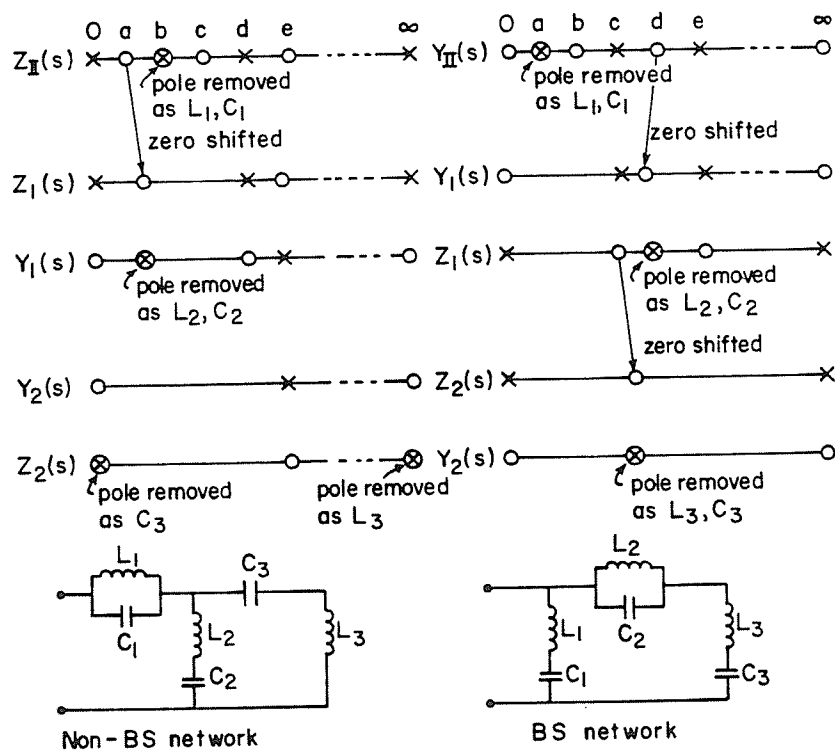
$$Z_{II}(s) = \frac{(s^2 + a^2)(s^2 + c^2)(s^2 + e^2)}{s(s^2 + b^2)(s^2 + d^2)} \quad (b)$$

These functions are of Z_A type with $n=2$ and $n=3$, respectively. As illustrated in Fig. 2.4 for $Z_I(s)$, the first arm must be a series arm of the ladder, otherwise, the resulting network is not of BS type. For the same reason, the first arm of $Z_{II}(s)$ must be a shunt arm.

From this example, we can derive general configurations of BS type canonic networks as shown in Fig. 2.5 depending on the value of n . It can be easily seen in Fig. 2.4(b) that if the first shunt arm is derived from removing the pole e instead of a , then a different set of element values is obtained.

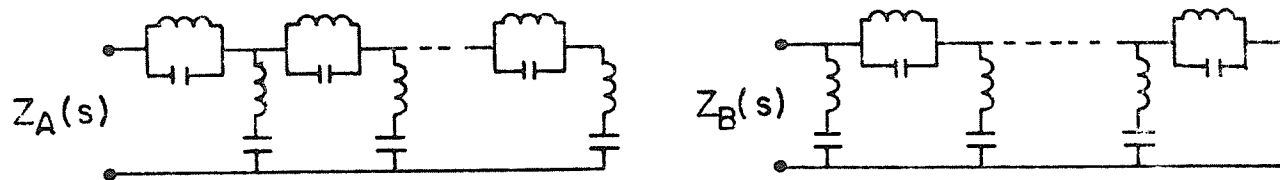


$$(a) Z_I(s) = \frac{(s^2 + a^2)(s^2 + c^2)}{s(s^2 + b^2)}, \quad Y(s) = 1/Z_I(s)$$

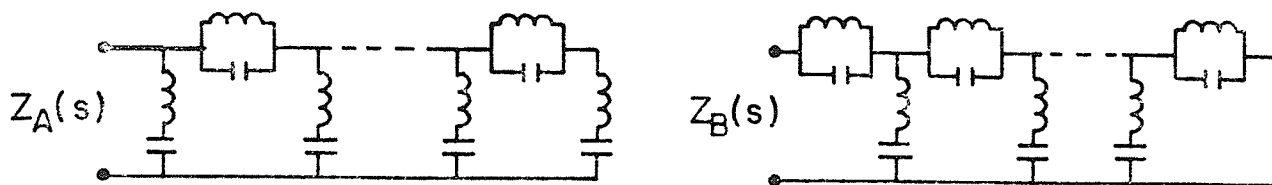


$$(b) Z_{II}(s) = \frac{(s^2 + a^2)(s^2 + c^2)(s^2 + e^2)}{(s^2 + b^2)(s^2 + d^2)}, \quad Y_{II}(s) = 1/Z_{II}(s)$$

Fig. 2.4. Illustration of the rule.



(a) when n is even



(b) when n is odd

Fig. 2.5 General configurations of BS type canonic ladder networks.

Theorem 2.2

Given an LC driving-point impedance function of $Z_A(s)$ or $Z_B(s)$ type of order $2n$, there exist N different sets of element values in a family of BS type canonic ladder networks, determined by

$$N = \prod_{k=0}^{\frac{n-2}{2}} [n-(2k+1)]^2 \quad (\text{for even } n) \quad (2.7a)$$

$$N = n \prod_{k=1}^{\frac{n-1}{2}} (n-2k)^2 \quad (\text{for odd } n) \quad (2.7b)$$

Proof:

Let us consider the case of even n first for the Z_A type function. The Z_A has n pairs of zeros and $(n-1)$ pairs of poles at non-zero finite frequencies. Let us denote this characteristic as

$$Z_A = \frac{[n]}{[n-1]} .$$

From Fig. 2.5, the first arm must be in series. Since there are $(n-1)$ finite poles, we have $(n-1)$ different ways to remove a finite pole. This will result in Z_1 such that

$$Z_1 = \frac{[n-1]}{[n-2]} .$$

Then, the inverse of Z_1 is

$$Y_1 = \frac{[n-2]}{[n-1]} .$$

Therefore, again there are $(n-1)$ different ways to remove a finite pole from Y_1 . After a removal of a finite pole from Y_1 , then, the remainder Y_2 is

$$Y_2 = \frac{[n-3]}{[n-2]} .$$

The inverse of Y_2 , then, allows $(n-3)$ different ways to remove finite poles. This process is continued until a given function is exhausted. It is now obvious that the total number of ways to remove finite poles is,

$$(n-1)(n-1)(n-3)(n-3)(n-5)(n-5) \dots$$

A similar argument may be made for the case of odd n , resulting in

$$n(n-2)(n-2)(n-4)(n-4) \dots$$

Since Z_B type is a dual of Z_A type, the total number is the same.

2.2 CANONIC LADDER REALIZATION OF RC AND RL DRIVING-POINT FUNCTIONS

2.2.1 RC Driving-Point Functions

There are four types of RC driving-point impedance functions:

$$\bar{Z}_A(s) = \frac{c_n s^n + c_{n-1} s^{n-1} + \dots + c_1 s + c_0}{b_n s^n + b_{n-1} s^{n-1} + \dots + b_1 s} \quad (2.8a)$$

$$\bar{Z}_B(s) = \frac{c_{n-1} s^{n-1} + c_{n-2} s^{n-2} + \dots + c_1 s + c_0}{b_n s^n + b_{n-1} s^{n-1} + \dots + b_1 s + b_0} \quad (2.8b)$$

$$\bar{Z}_C(s) = \frac{c_n s^n + c_{n-1} s^{n-1} + \dots + c_1 s + c_0}{b_n s^n + b_{n-1} s^{n-1} + \dots + b_1 s + b_0} \quad (2.8c)$$

$$\bar{Z}_D(s) = \frac{c_n s^n + c_{n-1} s^{n-1} + \dots + c_1 s + c_0}{b_{n+1} s^{n+1} + b_n s^n + \dots + b_2 s^2 + b_1 s} \quad (2.8d)$$

Making use of RC : LC transformation, we will present a theorem by which we can determine the exact number of canonic ladder network realizations.

Theorem 2.3

Given an RC driving-point impedance of $\bar{Z}_A(s)$ or $\bar{Z}_B(s)$ type of order n , there exist 3^{n-1} canonic ladder realizations excluding the BS type ladder.

Proof:

Applying RC : LC transformation, we obtain

$$s [\bar{Z}_A(p)]_{p \rightarrow s^2} = Z_A(s) \quad (2.9a)$$

$$s [\bar{Z}_B(p)]_{p \rightarrow s^2} = Z_B(s) . \quad (2.9b)$$

Therefore, instead of \bar{Z}_A or \bar{Z}_B , we may realize Z_A or Z_B and then replace the inductance of L henries by a resistor L ohms keeping all capacitors unchanged. Since there exist 3^{n-1} canonic ladder networks for Z_A or Z_B , there must exist 3^{n-1} realizations for \bar{Z}_A or \bar{Z}_B .

Corollary 2.2

Given an RC driving-point impedance of $\bar{Z}_C(s)$ or $\bar{Z}_D(s)$ type of order $n+1$, there exist $2 \times 3^{n-1}$ canonic ladder realizations excluding the BS type ladder.

Proof is obtained as a consequence of Corollary 2.1 and theorem 2.3.

2.2.2 RL Driving-Point Functions

Recalling the fact that the RL impedance expression has the same form as the RC admittance expression and RL admittance is identical in form to RC impedance, the conclusions reached for the RC impedance are directly applicable to the RL admittance and vice versa. Therefore, the theorems and the associated corollaries for RL functions are omitted for brevity.

CHAPTER III

GENERATION OF EQUIVALENT BAND-PASS LADDER NETWORKS IN CANONIC FORM

Resistively-terminated LC two-port ladder networks have been used most commonly in realizing transfer functions which exhibit such characteristics as low-pass, high-pass, band-pass, band-stop, etc. The reason for this is mainly due to the fact that the two-port LC ladder has a common ground (i.e., unbalanced network) and transmission zeros may be easily implemented and adjusted by the proper choice of LC impedances in the series and shunt arms. In parallel with the theory of LC driving-point function synthesis, the theory of LC two-port ladder realization has been well developed, and an extensive tabulation has been prepared for filter designs [1 - 7, 11 - 22]. However, the utilizations of canonic LC ladders were somewhat limited to the realizations of LP and HP networks. For the realization of BP filters it has been the general practice to directly replace the elements of prototype LP networks by means of LP-BP frequency transformation.

Recently, however, Kim [23] presented a formula for determining the number of equivalent LC canonic ladder networks for the case of singly terminated networks.

In this chapter, we deal with the canonic ladder realizations of a voltage transfer function of BP type in general. Theorems are developed to determine the number of equivalent canonic ladders for the singly terminated networks and the results are directly extended to cover the case for the doubly terminated normal BP networks. Examples are provided to illustrate the

possibility of comparing the equivalent canonic ladders with respect to certain specified merits.

3.1 FORMULATION OF PROBLEM

Let us consider a voltage transfer function of order $2n$,

$$\frac{V_2}{V_1} = \frac{k s^m}{a_{2n}s^{2n} + a_{2n-1}s^{2n-1} + \dots + a_1s + a_0} \quad (3.1)$$

where $0 \leq m \leq 2n$. The above function encompasses LP ($m=0$), HP ($m=2n$) and BP ($0 < m < 2n$).

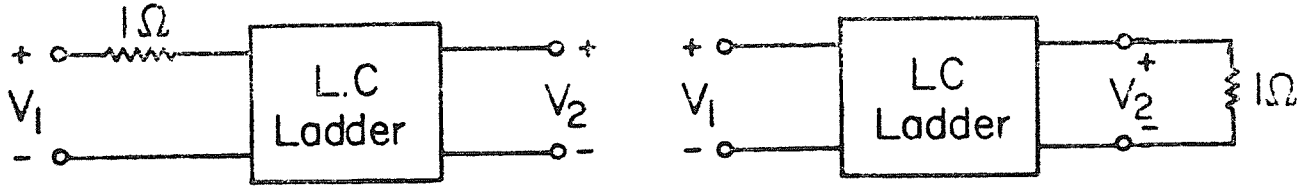
This transfer function is to be realized into terminated canonic ladder structures implementing m transmission zeros at the origin and $(2n-m)$ transmission zeros at infinity.

The objective of this investigation is to generate all the equivalent canonic ladder two-ports and to develop a closed form formula for obtaining the exact number of such equivalent networks that may be compared under specified criteria [20].

3.2 SINGLY TERMINATED BP CANONIC LADDER REALIZATION BASED ON TRANSMISSION ZERO REMOVAL SEQUENCES

3.2.1 Realization Procedure

The two-port parameters z_{ij} and y_{ij} may be used to obtain general expressions for the various network functions. For the singly terminated networks shown in Fig. 3.1, we have



(a) Source termination

(b) Load termination

Fig. 3.1 Singly terminated LC two-port networks

$$\frac{V_2}{V_1} = \frac{z_{12}}{1 + z_{11}} \quad \text{for Fig. 3.1(a)} \quad (3.2)$$

$$\frac{V_2}{V_1} = \frac{-y_{21}}{1 + y_{22}} \quad \text{for Fig. 3.1(b).} \quad (3.3)$$

For LC ladder networks, it is necessary that z_{12} ($-y_{21}$) be the quotient of odd to even or even to odd polynomials to satisfy the coefficient conditions [12]. Thus, from (3.1), (3.2) and (3.3), we can easily identify:

for even m

$$\frac{a_{2n}s^{2n} + a_{2n-2}s^{2n-2} + \dots + a_2s^2 + a_0}{a_{2n-1}s^{2n-1} + a_{2n-3}s^{2n-3} + \dots + a_3s^3 + a_1s}$$

$$= z_{11} \quad \text{for Fig. 3.1(a)}$$

$$= y_{22} \quad \text{for Fig. 3.1(b) .}$$

for odd m

$$\frac{a_{2n-1}s^{2n-1} + a_{2n-3}s^{2n-3} + \dots + a_3s^3 + a_1s}{a_{2n}s^{2n} + a_{2n-2}s^{2n-2} + \dots + a_2s^2 + a_0}$$

$$= z_{11} \text{ for Fig. 3.1(a)}$$

$$= y_{22} \text{ for Fig. 3.1(b) .}$$

The properties that $z_{11}(0) = z_{11}(\infty) = \infty$ and $y_{22}(0) = y_{22}(\infty) = \infty$ indicate that $z_{11}(s)$ and $y_{22}(s)$ are of $Z_A(s)$ and $Y_B(s)$ types, respectively. Thus, the realization of (3.1) is reduced to the realization of the driving point function z_{11} or y_{22} implementing the m transmission zeros at the origin, and $(2n-m)$ transmission zeros at infinity.

Theorem 3.1

In the singly terminated canonic ladder realization of the voltage transfer function of (3.1), there exist N equivalent networks determined by

$$N = \sum_{i=0}^{\left[\frac{m}{2}\right]} \frac{n!}{(n+i-m)! i! (m-2i)!} \quad (3.4)$$

where $\left[\frac{m}{2}\right]$ takes on the nearest integer on the lower side, and the terms with negative integers are ignored.

Proof:

Using Fig. 2.2, we can devise the schematic reduction charts as shown in Fig. 2.3 for Type A and Type B. With the aid of charts we may obtain the groups as shown in Fig. 3.2, each having different combinations of homogeneous and heterogeneous pairs, but all possessing m zeros at the origin. The number

of independent sequences is determined from each group by the rule of permutation. Let $N_0, N_1 \dots N_{k/2}$ be the number of independent sequences of group 1, 2, ... $k/2$, respectively, then we have

$$N_0 = \frac{n!}{(n-m)! 0! (m-0)!}$$

$$N_1 = \frac{n!}{\{(n-(m-1))\}! 1! (m-2)!}$$

$$N\left[\frac{m}{2}\right] = \frac{n!}{\{n - [\frac{m}{2}]\}! [\frac{m}{2}]! 0!}$$

and

$$N = \sum_{i=0}^{\left[\frac{m}{2}\right]} N_i = \sum_{i=0}^{\left[\frac{m}{2}\right]} \frac{n!}{\{n + (i-m)\}! i! (m-2i)!}.$$

It is to be noted that for $m > n$, $N_0, N_1, \dots, N_{m-n-1}$ are ignored in the summation because they require the order to exceed $2n$.

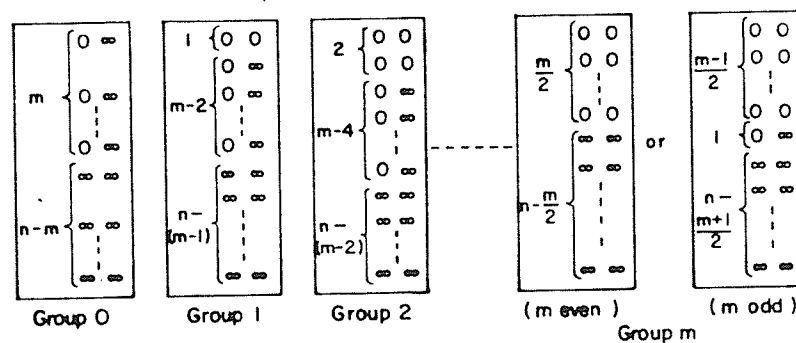


Fig. 3.2 Grouping of transmission zero pairs.

Theorem 3.2

In the singly terminated canonic ladder realization of the voltage transfer function

$$\frac{V_2}{V_1} = \frac{K s^m}{a_{2n+1}s^{2n+1} + a_{2n}s^n + \dots + a_1s + a_0} \quad (3.5)$$

there exist N equivalent networks determined by

$$N = \sum_{i=0}^{\left[\frac{m-1}{2}\right]} \frac{n!}{\{n+i-(m-1)\}! i! \{(m-1)-2i\}!} + \sum_{i=0}^{\left[\frac{m}{2}\right]} \frac{n!}{(n-m+i)! i! (m-2i)!} \quad \text{for odd } m \text{ and} \quad (3.6a)$$

$$N = \sum_{i=0}^{\frac{m}{2}} \frac{n!}{(n-m+i)! i! (m-2i)!} + \sum_{i=0}^{\left[\frac{m-1}{2}\right]} \frac{n!}{\{n-(m-1)+i\}! i! \{(m-1)-2i\}!} \quad \text{for even } m. \quad (3.6b)$$

where $[]$ takes on the lower side integer, and $-q! (q > 0) = \infty$.

Proof:

When m is odd, we can identify

$$z_{11} \text{ or } y_{22} = \frac{a_{2n+1}s^{2n+1} + a_{2n-1}s^{2n-1} + \dots + a_1s}{a_{2n}s^{2n} + \dots + a_2s^2 + a_0} \quad (3.7)$$

$z_{11}(0) = 0$ $z_{11}(\infty) = \infty$ implies $z_{11}(s)$ is of Z_C type. Since Z_C type can be reduced to Z_A and/or Z_B type, we use Corollary 2.1 and Theorem 3.1 to prove Theorem 3.2.

With the table in Fig. 2.2(b), it is now straightforward to generate the unique network corresponding to each independent sequence observing the following conditions:

(1) No degeneration of elements is to occur at the cascading junction of two pairs; e.g., $A(00)$ - $B(00)$, $B(00)$ - $A(00)$, $A(\infty\infty)$ - $B(\infty\infty)$, $B(\infty\infty)$ - $A(\infty\infty)$, $A(0\infty)$ - $A(0\infty)$, $B(0\infty)$ - $B(0\infty)$, etc. are to be avoided.

(2) The connection patterns, such as $A(00)$ - $B(\infty\infty)$, $B(\infty\infty)$ - $A(00)$, $B(00)$ - $A(\infty\infty)$, $A(\infty\infty)$ - $B(00)$, etc., are not permitted. This is because the pole has been fully removed in the previous pair, hence, it is simply impossible for these patterns to occur.

(3) Since $z_{11}(0) = z_{11}(\infty) = \infty$ for even m (i.e., Z_A type), and $z_{11}(0) = z_{11}(\infty) = 0$ for odd m (i.e., Z_B type), the first pair in $z_{11}(s)$ realization shall be one of A type pairs for even m , and B type pairs for odd m , respectively.

(4) The last section, in accordance with the definition of z_{11} (i.e., open-circuit driving-point impedance), is to be either $A(00)$, $A(\infty\infty)$ or $B(0\infty)$ pair. A similar argument may be made for the realization of y_{22} .

Thus, it is impossible to generate another network for a given independent sequence without violating conditions stipulated above.

The realization procedure, then, may be summarized as follows:

- (i) Given the BP voltage transfer function of (3.1), identify $z_{11}(s)$ or $y_{22}(s)$ in accordance with the integer m .
- (ii) Classify $z_{11}(s)$ or $y_{22}(s)$ into one of four types of LC impedance functions and find the number of independent sequences according to Theorem 3.1 or 3.2 whichever the case may be.
- (iii) Conforming with the interconnection conditions, sketch the combination of reduction cycle pairs in accordance with an independent sequence.
- (iv) Find elements values by applying the continued fraction expansion to $z_{11}(s)$ or $y_{22}(s)$ following the sketch obtained in (iii).

3.2.2 Normal BP Networks

The normal BP networks are used more widely than any other kind of filter network. For the normal BP, (3.1) can be written as

$$\frac{V_2}{V_1} = \frac{k s^n}{s^{2n} + a_{2n-1}s^{2n-1} + \dots + a_1s + a_0} \quad (3.8)$$

and from (3.4), the total number of equivalent canonic ladder networks N is,

$$N = \sum_{i=0}^{\left[\frac{n}{2}\right]} \frac{n!}{[i!]^2 (n - 2i)!} \quad (3.9)$$

It should be noted that the number of equivalent canonic ladder networks increases rapidly with order n of the function as shown in Table 3.1.

Table 3.1 Number of Equivalent Canonic Ladder Networks.

n	2	3	4	5	6	7
N	3	7	19	51	141	393

Example 3.1

For the illustration purpose, let us generate all equivalent networks for $n=3$; i.e.,

$$\frac{V_2}{V_1} = \frac{k s^3}{s^6 + a_5 s^5 + \dots + a_1 s + a_0}$$

For the case of 1Ω load termination, we can proceed as follows:

(i) Identify $y_{22}(s)$ as

$$y_{22}(s) = \frac{a_5 s^5 + a_3 s^3 + a_1 s}{s^6 + a_4 s^4 + a_2 s^2 + a_0}$$

(ii) Since $y_{22}(0) = y_{22}(\infty) = 0$, $y_{22}(s)$ is of $Y_A(s)$ type. For $n=3$, there are 7 independent sequences as follows,

1. $(\infty, 00, 0\infty)$
2. $(\infty, 0\infty, 00)$
3. $(00, \infty, 0\infty)$
4. $(00, 0\infty, \infty)$
5. $(0\infty, \infty, 00)$
6. $(0\infty, 00, \infty)$
7. $(0\infty, 0\infty, 0\infty)$.

Note that in each sequence, there are exactly three transmission zeros at the origin and three at infinity.

(iii) Since $y_{22}(0) = y_{22}(\infty) = 0$, the first pair must be one of A type, and since $y_{22}(s)$ is a short circuit admittance, the last pair must be one of B type. The intermediate pairs are chosen so as to avoid degeneration

of elements at the junctions. The sketch of equivalent networks corresponding to each independent sequence is shown in Fig. 3.3

- (iv) Now element values can be easily obtained by applying the continued fraction expansion on $y_{22}(s)$ in accordance with the sketch.

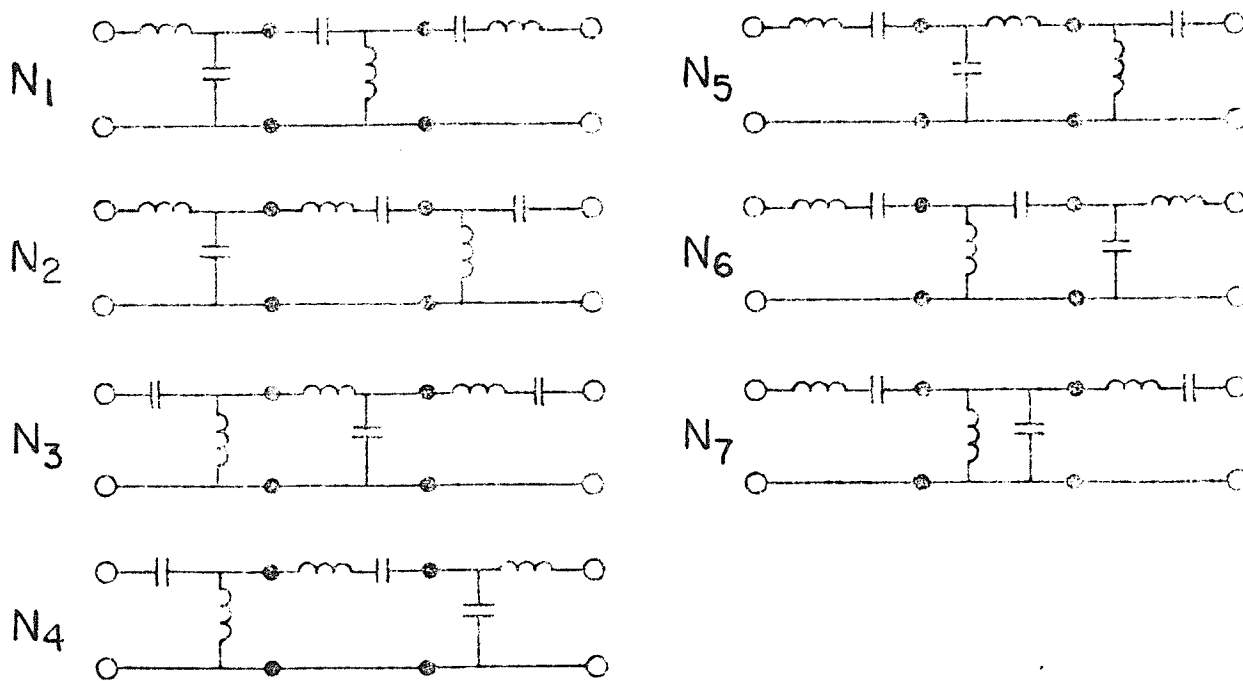


Fig. 3.3 Sketch of seven equivalent BP networks.
(Excluding the terminating resistor)

3.2.3 Comparison of Equivalent Networks

Let us realize the maximally flat 4th order BP filter with bandwidth B , and center frequency ω_0 . We start with 2nd order Butterworth lowpass function

$$H_{LP}(p) = \frac{k}{p^2 + \sqrt{2} p + 1} \quad (3.10)$$

and apply the transformation $p \rightarrow (s^2 + 1)/B_n s$ where, for convenience, the bandwidth is normalized as $B_n = B/\omega_0$. Then the required BP function is

$$H(s) = \frac{Ks^2}{s^4 + \sqrt{2} B_n s^3 + (B_n^2 + 2) s^2 + \sqrt{2} B_n s + 1} \quad (3.11)$$

and for the load-terminated case y_{22} is identified as

$$y_{22} = \frac{s^4 + (B_n^2 + 2) s^2 + 1}{\sqrt{2} B_n s^3 + \sqrt{2} B_n s} \quad (3.12)$$

Independent sequences for transmission zero removal are $(\infty \infty 00)$, $(00, \infty \infty)$ and $(\infty 0 \infty 0)$. Three equivalent networks, and their element values, and other parameters are given in terms of normalized bandwidth B_n in Table 3.2.

A similar approach may be carried out for the case of a source-terminated network. Table 3.3 shows three equivalent networks, their element values, and other parameters in terms of the normalized bandwidth B_n .

It is to be noted that networks N_{11} and N_{21} coincide with BP networks directly obtainable from an LP network by the element transformation.

Table 3.2 Equivalent Networks and their Parameters - Load Terminated

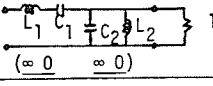
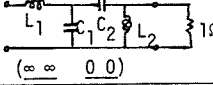
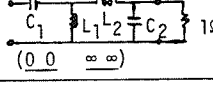
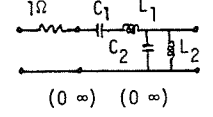
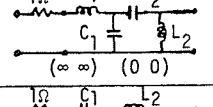
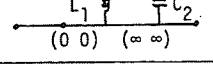
	EQUIVALENT NETWORKS	L_1	L_2	C_1	C_2	ΣL_i	ΣC_i	K
N_{11}		$\frac{\sqrt{2}}{B_n}$	$\sqrt{2}B_n$	$\frac{B_n}{\sqrt{2}}$	$\frac{1}{\sqrt{2}B_n}$	$\frac{\sqrt{2}(B_n^2+1)}{B_n}$	$\frac{B_n^2+1}{\sqrt{2}B_n}$	B_n^2
N_{12}		$\frac{\sqrt{2}B_n^3}{(B_n^2+1)^2}$	$\sqrt{2}B_n$	$\frac{B_n^2+1}{\sqrt{2}B_n^3}$	$\frac{B_n^2+1}{\sqrt{2}B_n}$	$\frac{\sqrt{2}B_n(B_n^4+3B_n^2+1)}{(B_n^2+1)^2}$	$\frac{(B_n^2+1)^2}{\sqrt{2}B_n^3}$	B_n^2+1
N_{13}		$\frac{\sqrt{2}B_n^3}{B_n^2+1}$	$\frac{\sqrt{2}B_n}{B_n^2+1}$	$\frac{(B_n^2+1)^2}{\sqrt{2}B_n^3}$	$\frac{1}{\sqrt{2}B_n}$	$\sqrt{2}B_n$	$\frac{B_n^4+3B_n^2+1}{\sqrt{2}B_n^3}$	B_n^2+1

Table 3.3 Equivalent Networks and their Parameters - Source Terminated

	EQUIVALENT NETWORKS	L_1	L_2	C_1	C_2	ΣL_i	ΣC_i	K
N_{21}		$\frac{1}{\sqrt{2}B_n}$	$\frac{B_n}{\sqrt{2}}$	$\sqrt{2}B_n$	$\frac{\sqrt{2}}{B_n}$	$\frac{B_n^2+1}{\sqrt{2}B_n}$	$\frac{\sqrt{2}(1+B_n^2)}{B_n}$	B_n^2
N_{22}		$\frac{1}{\sqrt{2}B_n}$	$\frac{(1+B_n^2)^2}{\sqrt{2}B_n^3}$	$\frac{\sqrt{2}B_n}{1+B_n^2}$	$\frac{\sqrt{2}B_n^3}{1+B_n^2}$	$\frac{B_n^4+3B_n^2+1}{\sqrt{2}B_n^3}$	$\sqrt{2}B_n$	$1+B_n^2$
N_{23}		$\frac{1+B_n^2}{\sqrt{2}B_n}$	$\frac{1+B_n^2}{\sqrt{2}B_n^3}$	$\sqrt{2}B_n$	$\frac{\sqrt{2}B_n^2}{(1+B_n^2)^2}$	$\frac{(1+B_n^2)^2}{\sqrt{2}B_n^3}$	$\frac{\sqrt{2}B_n(B_n^4+3B_n^2+1)}{(1+B_n^2)^2}$	$1+B_n^2$

The equivalent networks may be compared with respect to certain criteria such as:

(i) Total inductance ΣL

N_{13} has the smallest ΣL as calculated in the following

$$\Sigma L(N_{12}) = \Sigma L(N_{13}) + \frac{\sqrt{2} B_n^3}{(B_n^2 + 1)^2}, \quad \Sigma L(N_{11}) = \Sigma L(N_{12}) + \frac{\sqrt{2}}{B_n (B_n^2 + 1)^2}$$

$$\therefore \Sigma L(N_{13}) < \Sigma L(N_{12}) < \Sigma L(N_{11}) \quad . \quad (3.13)$$

(ii) Total capacitance ΣC

$$\Sigma C(N_{12}) = \Sigma C(N_{11}) + \frac{B_n^2 + 1}{\sqrt{2} B_n^3}, \quad \Sigma C(N_{13}) = \Sigma C(N_{12}) + \frac{1}{\sqrt{2} B_n}$$

$$\therefore \Sigma C(N_{11}) < \Sigma C(N_{12}) < \Sigma C(N_{13}) \quad . \quad (3.14)$$

(iii) Relative gain K

$$K(N_{12}) = K(N_{13}) > K(N_{11}) \quad . \quad (3.15)$$

In the narrow band case of $B_n \ll 1$, the gain of N_{11} becomes very low.

It is also seen that the element value spread is roughly comparable among the three networks.

If we define the cost function as

$$f = \alpha \Sigma L + \beta \Sigma C + \gamma (K_{\max} - K)$$

where α = cost of inductance/Henry, β = cost of capacitance/farad,

K_{\max} = maximum gain among the equivalent networks,

N_{13} will normally be favored because of the higher per unit cost of the inductance.

(iv) Sensitivities

The magnitude sensitivities with respect to the component variations are calculated and plotted for the load terminated case in Fig. 3.4, for $B_n = 0.1$. As can be observed, the magnitude sensitivities are roughly comparable among equivalent networks. It is observed that the magnitude sensitivity with respect to L_1 almost coincides with that of C_1 and so does the magnitude sensitivity with respect to L_2 with that of C_2 .

Similar comparison may be made for the case of a source-terminated network. It is omitted here for brevity.

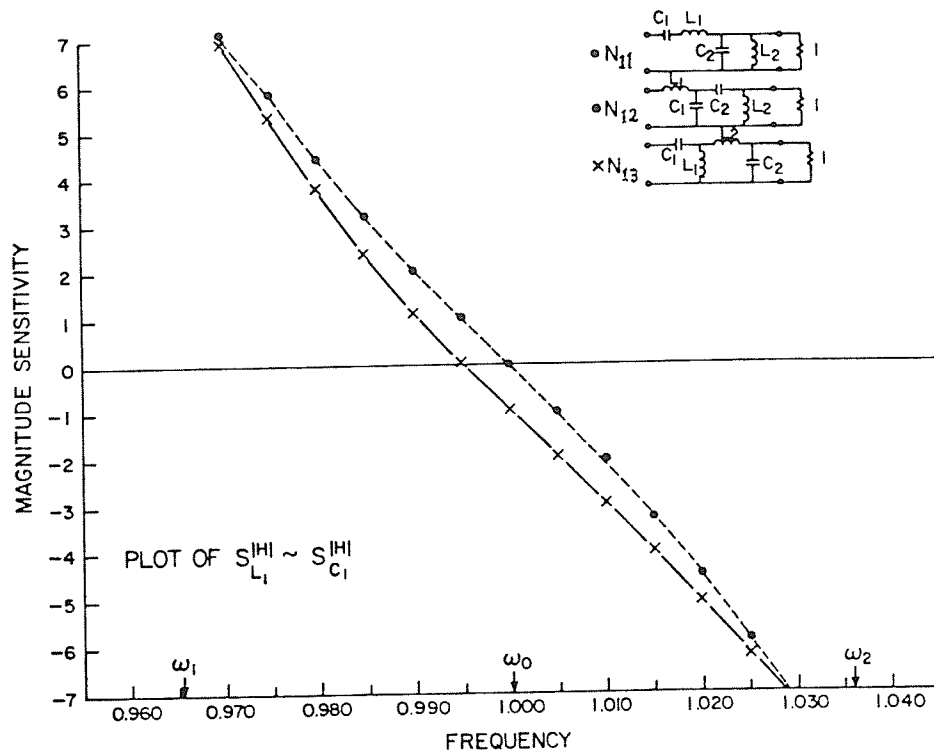
A similar comparison table is provided in Appendix I for $n=3$; i.e.,

$$H(s) = \frac{K s^3}{s^6 + a_1 s^5 + a_2 s^4 + a_3 s^3 + a_2 s^2 + a_1 s + 1}.$$

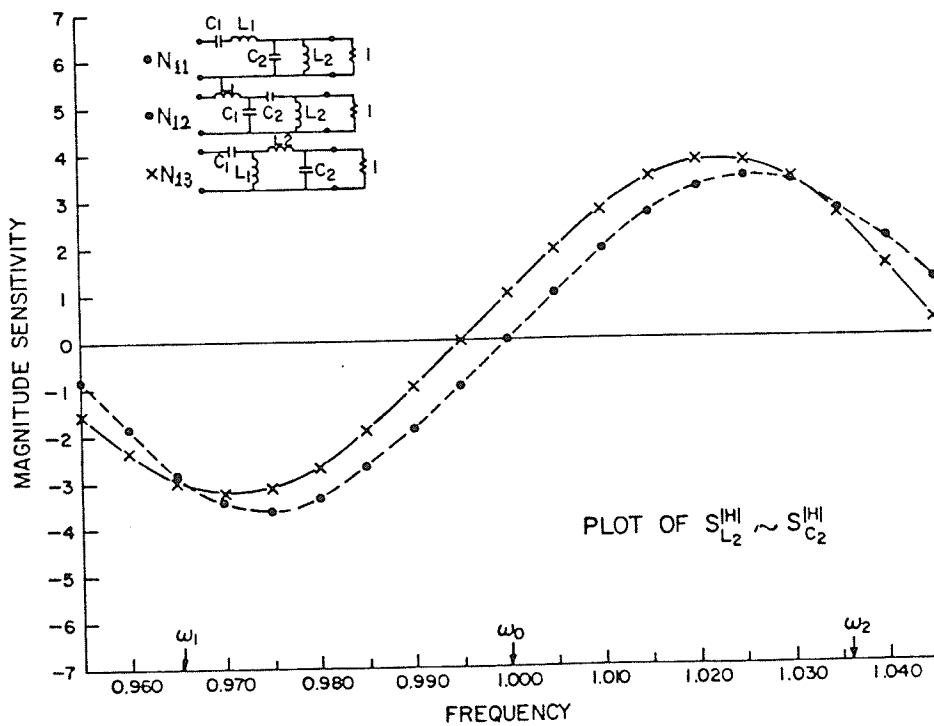
It is to be noted that

(i) The descending order of ΣL_i is

$$N_6 > N_5 > N_7 > N_4 > N_2 > N_1 > N_3$$



(a)



(b)

Fig. 3.4 Plot of magnitude sensitivity - Load terminated.

(ii) The descending order of ΣC_i is

$$N_3 > N_1 > N_7 > N_2 = N_4 > N_5 > N_6$$

(iii) The descending order of gain K is

$$N_1 = N_3 > N_2 = N_4 > N_7 > N_5 = N_6 .$$

Since $\omega_0 = L_1 L_2 L_3 C_1 C_2 C_3 = 1$, in each network the value of L_i 's is inversely proportional to that of C_i 's. Thus, it can be seen from (i) and (ii) that the total inductance increases, the total capacitance decreases, i.e., N_3 has the smallest total inductance, but has the largest total capacitance. The networks tend to have less total inductance when they are realized by homogeneous reduction cycle pairs first (see N_1 , N_3 and N_5 , N_6).

Also, from (i) and (iii) we can see that there is an inverse relationship between total inductance and gain, i.e., the less the total inductance, the greater the gain K . From these comparisons, we can conclude that the conventional network N_7 is not necessarily a good choice. The network N_3 appears to be the best, because it has the smallest total inductance and the highest gain.

3.3 DIRECT DERIVATION OF DOUBLY TERMINATED NORMAL BP CANONIC LADDER NETWORKS

Since Darlington [11] presented a synthesis method based on the insertion loss characteristics, the doubly-terminated LC network has been well accepted

as the preferable structure in filter realization. Such a network is capable of producing any physically realizable loss response with a near minimum number of components for most filter specifications [1 - 2, 14 - 17]. More importantly, the sensitivity of the transfer function to changes in the element values is minimized [24 - 30]. Another advantage includes a possibility of ladder network realization which is mostly preferred in practical applications.

One of the reasons for extensive use of ladder is due to the fact that in the multipath structures such as lattice, bridged-T, twin-T or parallel ladders, transmission zeros are generated by cancellation of energies arriving at the output terminals along different paths. These cancellations are very sensitive to element variations. Due to the structure, such cancellation cannot occur in the ladder networks. On the other hand, because of this fact an LC ladder must have all its transmission zeros on the imaginary axis only.

Although normal BP ladders can easily be obtainable from the LP prototype by means of the element transformation, we may instead find the BP function through frequency transformation and investigate various ways of realizing the BP function. Watanabe [14], however, derived sufficient conditions for the possibility of constructing an LC ladder BP filter with the use of an ideal transformer.

In this section, we deal with the canonic realization of the doubly terminated LC ladder two-port directly from a given transfer function. We shall restrict ourselves to the case of the normal BP network.

3.3.1 Doubly-Terminated Network

Basically, Darlington's synthesis method [11] is to reduce the problem of realizing a transfer function to that of a driving point impedance function

$Z_{in}(s)$ of the Fig. 3.5. This configuration has been a focal point in filter synthesis mainly due to its excellent low sensitivity of the transfer function to changes in the element values of the LC networks [24 - 30].

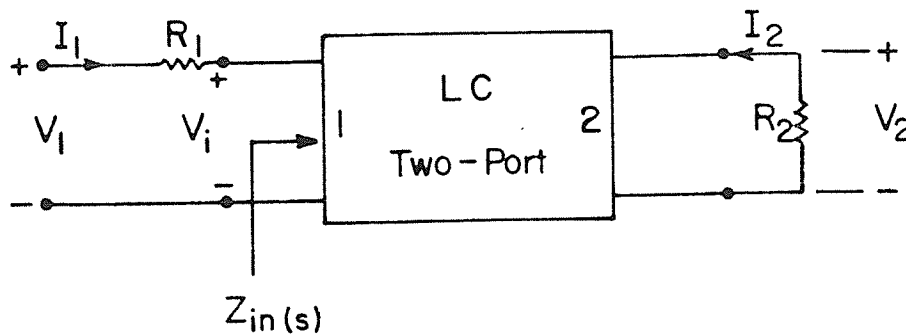


Fig. 3.5 The Darlington circuit structure

In order to extend the applications of the theorems developed previously, we need to introduce the two coefficients: the transmission coefficient, and the reflection coefficient. The transmission coefficient is defined as the ratio of the output power P_o being dissipated in R_2 to the maximum available power P_a from the source with source resistance R_1 . Without loss of generality let us designate $R_1 = 1$ and $R_2 = R$. Then, we obtain

$$P_o(j\omega) = \frac{|V_2(j\omega)|^2}{R} \quad (3.16)$$

and

$$P_a(j\omega) = \frac{|V_1(j\omega)|^2}{4} . \quad (3.17)$$

Hence, the transmission coefficient is given by

$$\begin{aligned} |t(j\omega)|^2 &= \frac{P_o(j\omega)}{P_a(j\omega)} = \frac{4}{R} \cdot \frac{|V_2(j\omega)|^2}{|V_1(j\omega)|^2} \\ &= \frac{4}{R} \cdot |H(j\omega)|^2 \end{aligned} \quad (3.18)$$

where $H(s)$ is the voltage-ratio transfer function

$$H(s) = \frac{V_2(s)}{V_1(s)} .$$

Because the power sent to R from the source must be less than or equal to the maximum power available from the source, we have

$$|t(j\omega)|^2 \leq 1 . \quad (3.19)$$

The reflection coefficient is defined simply to be the complement of the transmission coefficient as

$$|t(j\omega)|^2 + |\rho(j\omega)|^2 = 1 . \quad (3.20)$$

In sinusoidal steady-state, the power P_i supplied to port 1 of the lossless two-port is equal to the power P_o supplied to the load, where

$$P_i = R_e[Z_{in}(s)] |I_1(j\omega)|^2 . \quad (3.21)$$

From the Fig. 3.5 we have

$$\frac{V_1}{I_1} = 1 + Z_{in}(s)$$

which together with (3.21) yields

$$|H(j\omega)|^2 = \frac{R \cdot R_e[Z_{in}(j\omega)]}{|1 + Z_{in}(j\omega)|^2} \quad (3.22)$$

Substituting (3.22) into (3.18) and the resulting expression into (3.20) we obtain

$$\begin{aligned} \rho(j\omega) \cdot \rho(-j\omega) &= |\rho(j\omega)|^2 \\ &= 1 - |t(j\omega)|^2 \\ &= 1 - \frac{4}{R} \cdot \frac{R \cdot R_e[Z_{in}(j\omega)]}{|1 + Z_{in}(j\omega)|^2} \end{aligned} \quad (3.23)$$

By writing $Z_{in}(j\omega)$ as

$$Z_{in}(j\omega) = R(\omega) + j X(\omega)$$

and substituting this into (3.23) we have

$$\rho(j\omega) \rho(-j\omega) = \frac{|Z_{in}(j\omega) - 1|^2}{|Z_{in}(j\omega) + 1|^2}.$$

This implies that

$$\rho(s) = \pm \frac{Z_{in}(s) - 1}{Z_{in}(s) + 1} \quad (3.24)$$

or that



$$Z_{in}(s) = \frac{1 + \rho(s)}{1 - \rho(s)} . \quad (3.25)$$

Through the coefficients $t(j\omega)$ and $\rho(j\omega)$, we have reduced the problem of realizing a voltage-transfer function $H(s)$ to that of realizing a driving point function $Z_{in}(s)$ of (3.25), bearing in mind the locations of the transmission zeros of $H(s)$. We have noted that in the process of obtaining $Z_{in}(s)$, we have two possible values of $\rho(s)$ and therefore two values of $Z_{in}(s)$. Also we should select a Hurwitz denominator, as in the case of transfer functions, since from (3.18) we conclude that $t(s)$ has the same Hurwitz denominator as $H(s)$ and from (3.23) we can see that $\rho(s)$ will also have this denominator.

3.3.2 Canonic Ladder Realization Procedure

Based on the preceding discussion, we can describe a step-by-step procedure for the canonic realization of the doubly-terminated ladder network as follows.

Step 1: Find the $\rho(s)$ from a given $H(s)$.

From (3.18) and (3.24), we have

$$\rho(s) - \rho(-s) = 1 - \frac{4}{R} H(s) H(-s) . \quad (3.26)$$

Finding $\rho(s)$ is the most important step in the realization procedure. To start with, (3.26) may not have solutions.

Let

$$F(s) \triangleq \rho(s) - \rho(-s) \quad (3.27)$$

and

$$G(s) \triangleq 1 - \frac{4}{R} H(s) H(-s) . \quad (3.28)$$

It is apparent that both the poles and zeros of $F(s)$ are required to occur with quadrantal symmetry. However, since $H(s)$ shares the same denominator, the poles of $G(s)$ will also exhibit quadrantal symmetry but not necessarily the zeros. This is because the numerator of $G(s)$ is only an even polynomial, not necessarily with quadrantal symmetry. If the zeros of $G(s)$ do not occur with quadrantal symmetry, then we cannot find $\rho(s)$ from (3.26), and the procedure that we are describing will not realize a circuit for $H(s)$.

Step 2: Find $Z_{in}(s)$.

Once $\rho(s)$ is determined, we write

$$Z_{in}(s) = \frac{1 + \rho(s)}{1 - \rho(s)} \quad \text{or} \quad Z_{in}(s) = \frac{1 - \rho(s)}{1 + \rho(s)} . \quad (3.29)$$

There are two choices for $Z_{in}(s)$. Since one choice is the inverse of the other we can expect that one will give R , and the other will yield $1/R$ as the terminating load resistance. If the terminating load is to be R , then only one choice of $Z_{in}(s)$ will give the desired solution.

Step 3: Realization of $Z_{in}(s)$ into canonic ladder network.

With this procedure in mind, let us now consider a normal BP type transfer function of order $2n$. This type of transfer functions are generated from the LP transfer functions by means of a simple LP-BP frequency transformation. The transformation requires the replacement of the variable s in the LP function with the variable $(s^2 + 1)/B_n s$, where for convenience, the bandwidth is normalized as $B_n = B/\omega_0$. The constants ω_0 and B represent the center frequency and the bandwidth of the BP filter, respectively.

Let us start with the all pole LP transfer function of order n ,

$$H_{LP}(s) = \frac{G b_0}{s^n + b_{n-1}s^{n-1} + \dots + b_1s + b_0} \quad (3.30)$$

where the denominator is strictly Hurwitz.

A LP-BP frequency transformation gives a normal type of BP transfer function,

$$H(s) = \frac{k s^n}{s^{2n} + a_{2n-1}s^{2n-1} + \dots + a_1s + 1} \quad (3.31)$$

where the denominator is also strictly Hurwitz and, due to the nature of the transformation, possesses the property of the so-called reciprocal polynomial (i.e., $a_{2n-i} = a_i$) [13].

Now let us consider the existence of the solution for (3.26).

Theorem 3.3

Given a realizable BP function

$$H(s) = \frac{k s^n}{s^{2n} + a_{2n-1}s^{2n-1} + \dots + a_1s + 1} \quad (3.32)$$

where the denominator is a reciprocal polynomial, and

$$G(s) \triangleq 1 - \frac{4}{R} H(s) H(-s) \quad (3.33)$$

there exist a set of zeros of $G(s)$ which satisfy the quadrantal symmetry requirement.

Proof:

Let us write

$$H(s) = \frac{k s^n}{M(s) + N(s)} \quad (3.34)$$

where $M(s)$ and $N(s)$ are the even and odd parts of the denominator.

Substituting (3.34) into (3.33), we obtain

$$G(s) = \frac{M^2(s) - N^2(s) - \frac{4}{R} k^2 (s)^n (-s)^n}{M^2(s) - N^2(s)} . \quad (3.35)$$

Suppose that s_0 is a zero of $M + N$ so that $M(s_0) + N(s_0) = 0$. Then since M is even and N is odd, $M(-s_0) - N(-s_0) = M(s_0) + N(s_0) = 0$ and we see that $-s_0$ is a zero of $M - N$. Thus the poles of $G(s)$ appear in pairs, one always being the negative of the other. Since $M + N$ is strictly Hurwitz, the zeros of $M^2 - N^2$ occur in a quadruple manner, i.e., in a quadrantal symmetry.

Let

$$A(s) = M^2(s) - N^2(s) - \frac{4}{R} k^2 (s)^n (-s)^n . \quad (3.36)$$

Since M and N are reciprocal polynomials of order $2n$ and $2n-1$, respectively, $M^2 - N^2$ is an even and reciprocal polynomial of order $4n$. The last term in (3.36) can be added or subtracted depending on the integer n , however, since the center of coefficient symmetry is the coefficient of s^{2n} , this term does not disturb the nature of the reciprocal polynomial. In other words, $A(s)$ is an even, reciprocal polynomial of order $4n$. Since $A(s)$ is even, $2n$ zeros must be in the left half plane and the other $2n$ in the right half plane. Furthermore, since $A(s)$ is reciprocal, if s_k is a zero then so is $\frac{1}{s_k}$. Recalling that zeros of polynomials with real coefficients occur in conjugate, we can see that zeros of $A(s)$ occur in quadrantal symmetry.

3.3.3. Number of Doubly-Terminated Canonic Ladders

In the section 3.2.2 we have shown that there exist N equivalent singly terminated canonic ladder two-ports determined by (3.9) in the synthesis of a normal BP transfer function. As far as the lossless two-ports are concerned, the equivalent networks of source termination and those of load termination are structurally identical for even n , and dual in the case of odd n . Since the topological dual exists for the case of even n , the total of $2N$ equivalent canonic networks can always be generated in the doubly terminated ladder configurations within certain constraints on the load resistances. For $n=2$ and $n=3$, for example, there are $2N=6$, and $2N=14$ canonic ladder structures, respectively, as shown in Fig. 3.6. Two networks in the first rows are the conventional BP filters directly obtainable from the LP networks through the element transformation. The rest are the equivalent networks with different sequence of the transmission zero removal.

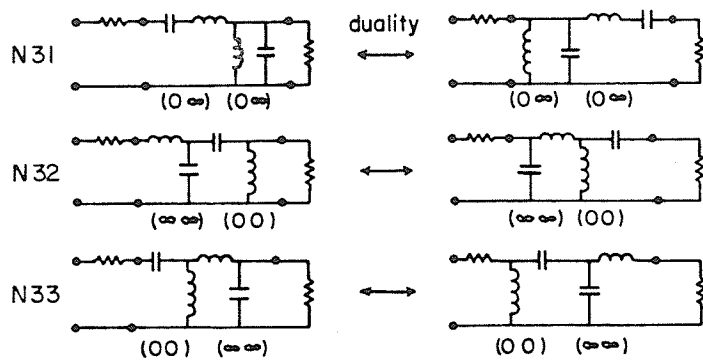
It can be easily shown that all the equivalent networks derived directly from the singly terminated networks are of normal BP type.

Since the LC two-ports in Fig. 3.7 are reciprocal, we can represent Fig. 3.7(a) by an equivalent T as shown in Fig. 3.8.

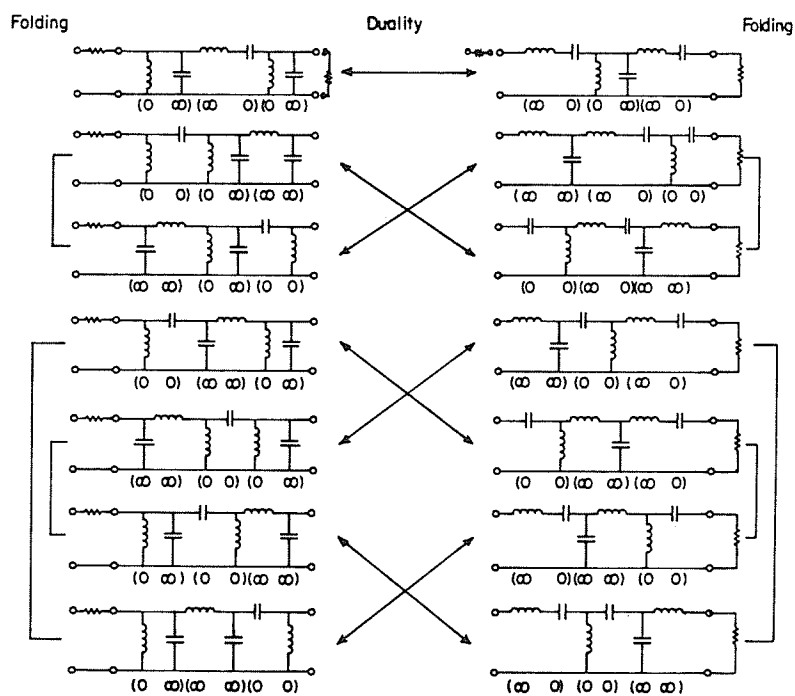
A simple analysis yields

$$H_a(s) = \frac{V_2}{V_1} = \frac{R_2 z_{12}}{z_{11} z_{22} - z_{12}^2 + R_2 z_{11} + R_1 z_{22} + R_1 R_2} . \quad (3.37)$$

Then for Fig. 3.7(b), the transfer function $H_b(s)$ is obtained by simply replacing $Z_1 \rightarrow Z_2$, $Z_2 \rightarrow Z_1$, $R_1 \rightarrow R_2$, $R_2 \rightarrow R_1$, $Z_3 \rightarrow Z_3$ in (3.37).

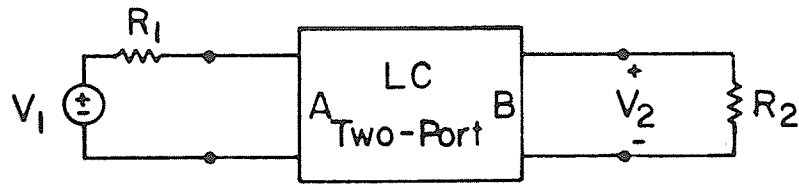


$$(a) \quad n=2 \quad \frac{V_2}{V_1} = \frac{K s^2}{s^4 + a s^3 + b s^2 + a s + 1}$$

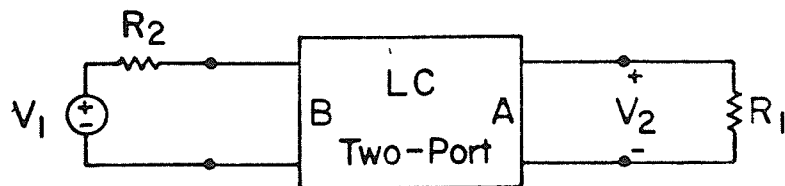


$$(b) \quad n=3 \quad \frac{V_2}{V_1} = \frac{K s^3}{s^6 + a s^5 + b s^4 + c s^3 + b s^2 + a s + 1}$$

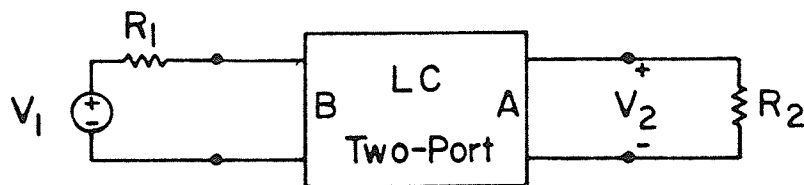
Fig. 3.6 Equivalent normal BP canonic networks (a) for $n=2$
(b) for $n=3$.



$$(a) \quad \frac{V_2}{V_1} = H_a(s)$$



$$(b) \quad \frac{V_2}{V_1} = H_b(s)$$



$$(c) \quad \frac{V_2}{V_1} = H_c(s)$$

Fig. 3.7 Doubly terminated networks with interchanged LC two-ports and terminations

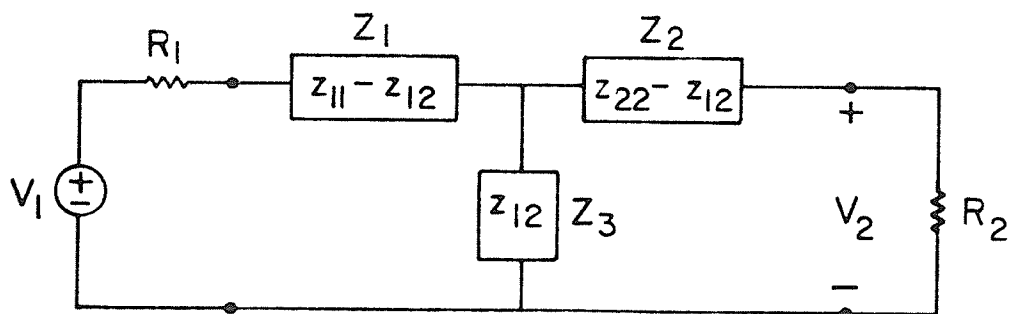


Fig. 3.8 Equivalent T network of Fig. 3.7(a)

$$H_b(s) = \frac{R_1 z_{12}}{z_{11}z_{22} - z_{12}^2 + R_2 z_{11} + R_1 z_{22} + R_1 R_2} = \frac{R_1}{R_2} H_a(s) \quad (3.38)$$

Similarly, by replacing $Z_1 \rightarrow Z_2$, $Z_2 \rightarrow Z_1$, $Z_3 \rightarrow Z_3$, and retaining R_1 and R_2 in (3.37) we write the transfer function for Fig. 3.7(c) as

$$H_c(s) = \frac{R_2 z_{12}}{z_{11}z_{22} - z_{12}^2 + R_1 z_{11} + R_2 z_{22} + R_1 R_2} \neq H_a(s) \quad (3.39)$$

The implication of (3.38) is that if the realization exists in configuration of Fig. 3.7(a), we can physically rotate the network 180° about the vertical axis to realize the same transfer function, with a scaling factor of R_1/R_2 . On the other hand, (3.39) implies that if we keep R_1 and R_2 fixed and rotate the LC two-port alone, the denominator changes as shown. Consequently, a new set of element values for the LC two-port results. The dual networks can be obtained readily by inspection as shown in Fig. 3.6. It should be noted that the dual networks realize the given normal BP transfer function within the multiplicative constant.

The preceding development confirms the fact that all the equivalent networks generated directly from the single termination cases are conformable to the BP transfer function. Then, one may ask "Is the set of equivalent doubly terminated canonic ladder networks complete and exhaustive?" The affirmative answer can be derived as follows.

If there are to be any more equivalent networks, the LC two-port part must be generated at the expense of violating the rules of interconnecting the reduction cycles. Then the order of the driving-point parameters of the

two-port is reduced in (3.37) - (3.39). As a consequence, no additional equivalent canonic networks can be generated.

3.3.4 Constraint on Terminating Resistances

Once a $\rho(s)$ is determined, it is straightforward to determine $Z_{in}(s)$ and carry out continued fraction expansion on $Z_{in}(s)$ in accordance with the given canonic ladder networks. To determine the value R of the terminating resistor for a given choice of $Z_{in}(s)$, for the LP and HP network, we can find easily by

$$R = Z_{in}(\infty) \text{ for HP}$$

and

$$R = Z_{in}(0) \text{ for LP} \quad . \quad (3.40)$$

However, for the normal BP network, there is no simple way of determining R . It should be noted that since R_1 is normalized, R actually represents a resistance ratio. The determination of constraints on R in conjunction with the equivalent canonic ladder networks can be best explained by examples.

Example 3.2

Let us first consider the maximally flat 4th order normal BP transfer function which is given in (3.12).

Step 1: Determination of $\rho(s)$.

From (3.26) we have,

$$\begin{aligned} \rho(s) \rho(-s) &= \frac{s^8 + 4s^6 + (6 + B_n^4 - \frac{4}{R}K^2)s^4 + 4s^2 + 1}{s^8 + 4s^6 + (6 + B_n^4)s^4 + 4s^2 + 1} \\ &= \frac{p(s) p(-s)}{q(s) q(-s)} \quad . \end{aligned} \quad (3.41)$$

There is no freedom in the choice of the denominator of $\rho(s)$ because its roots must lie in the left half plane. However, since as given in (3.23), only the squared magnitude of $\rho(j\omega)$ is fixed by the specification of the transmission coefficient, the zero distribution of $p(s)$ is optional, as long as $\rho(j\omega) \rho(-j\omega)$ represents the numerator of $|\rho(j\omega)|^2$. Since the numerator is a reciprocal polynomial of order 8, the root distribution would appear as shown in Fig. 3.9.

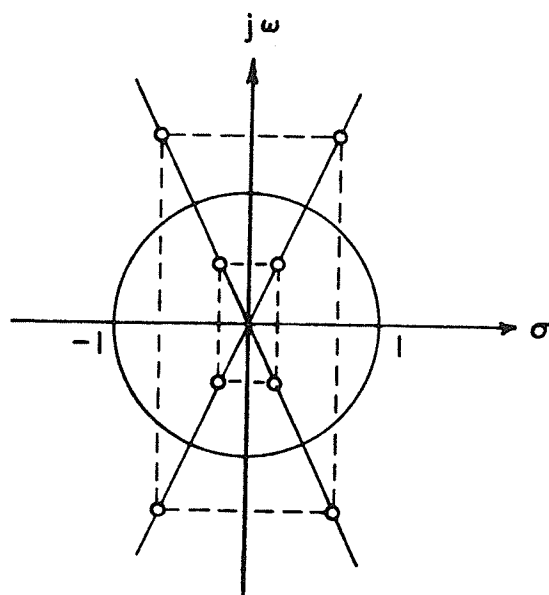


Fig. 3.9 Zero-pair distribution of $\rho(s)$.

Thus, $p(s)$ with all its roots in the left half plane, yields a uniquely defined minimum phase $\rho(s)$; the other root distributions may be obtained from this one by replacing any pair of complex conjugate roots by its mirror image.

Since for a $p(s)$ corresponding to $\rho(s)$, the root distribution $p(-s)$ corresponds to the reflection coefficient of the other part of the same network [4], each different network corresponds to a pair of root distributions. Therefore, it can be easily shown that for integer n , $2^{(n-1)}$ different combinations of pairs of root distributions exist. An actual partition of the 8th order numerator into $p(s) p(-s)$ can be carried out either by using computer or by analytic method as follows:

From (3.41), we can write

$$\begin{aligned} s^8 + 4s^6 + (6 + B_n^4 - \frac{4}{R} K^2) s^4 + 4s^2 + 1 \\ = (s^4 + \alpha s^3 + \beta s^2 + \alpha s + 1) (s^4 - \alpha s^3 + \beta s^2 - \alpha s + 1) . \end{aligned} \quad (3.42)$$

By matching coefficient of each term, we have

$$\begin{aligned} \alpha &= \sqrt{2} \cdot (B_n^4 - \frac{4}{R} K^2)^{\frac{1}{4}} \\ \beta &= 2 + \sqrt{B_n^4 - \frac{4}{R} K^2} . \end{aligned}$$

Let

$$A \triangleq \sqrt{B_n^4 - \frac{4}{R} K^2} \quad (3.43)$$

then

$$\begin{aligned} \alpha &= \sqrt{2} \sqrt{A} \\ \beta &= 2 + A . \end{aligned} \quad (3.44)$$

Now, from (3.41) and (3.42), we can identify the minimum phase function $\rho(s)$

as

$$\rho(s) = \frac{s^4 + \sqrt{2} \sqrt{A} s^3 + (2 + A) s^2 + \sqrt{2} \sqrt{A} s + 1}{s^4 + \sqrt{2} B_n s^3 + (2 + B_n^2) s^2 + \sqrt{2} B_n s + 1}. \quad (3.45)$$

Step 2: Determination of $Z_{in}(s)$.

From (3.25) and (3.45), we have either

$$Z_{in}(s) = \frac{2s^4 + \sqrt{2} (B_n + \sqrt{A}) s^3 + (4 + B_n^2 + A) s^2 + \sqrt{2} (B_n + \sqrt{A}) s + 2}{\sqrt{2} (B_n - \sqrt{A}) s^3 + (B_n^2 - A) s^2 + \sqrt{2} (B_n - \sqrt{A}) s} \quad (3.46)$$

or

$$Z_{in}(s) = \frac{\sqrt{2} (B_n - \sqrt{A}) s^3 + (B_n^2 - A) s^2 + \sqrt{2} (B_n - \sqrt{A}) s}{2s^4 + \sqrt{2} (B_n + \sqrt{A}) s^3 + (4 + B_n^2 + A) s^2 + \sqrt{2} (B_n + \sqrt{A}) s + 2}. \quad (3.47)$$

Note that (3.46) is the dual of (3.47).

Step 3: Realization of $Z_{in}(s)$ into N_{31} , N_{32} , N_{33} networks shown in Fig. 3.6(a).

If we use the divide-and-invert procedure to find the necessary continued fraction expansion of $Z_{in}(s)$ such that the final element is R , we can find that the proper $Z_{in}(s)$ is (3.46), the last element being for N_{31}

$$(B_n^2 + A)/(B_n^2 - A) \quad (3.48)$$

for N_{32}

$$(B_n^2 + 2 + A)^2/(B_n^4 - A^2) \quad (3.49)$$

for N_{33}

$$(B_n^2 + 2 + A)^2 / (B_n^4 - A^2) . \quad (3.50)$$

Since N_{31} is the direct transform from the LP realization, the gain K is

$$K = B_n^2 \left(\frac{R}{1 + R} \right) . \quad (3.51)$$

Substituting (3.51) into A , we can check that (3.48) is indeed R . For other structures, we must select K and R values such that

$$\frac{(B_n^2 + 2 + A)^2}{B_n^4 - A^2} = R . \quad (3.52)$$

Substituting A into (3.52), we obtain

$$\left(B_n^2 + 2 + \sqrt{B_n^4 - 4K^2/R} \right)^2 = (2K)^2$$

$$\therefore 2K = B_n^2 + 2 + \sqrt{B_n^4 - 4K^2/R} .$$

Rearranging, we have

$$2K - (B_n^2 + 2) = \sqrt{B_n^4 - 4K^2/R} . \quad (3.53)$$

Let us choose R and K such that $B_n^4 - 4K^2/R = 0$.

Then, we have

$$K = \frac{B_n^2 + 2}{2}$$

$$R = \frac{(2 + B_n^2)^2}{B_n^4} . \quad (3.54)$$

Table 3.4 shows the element values in terms of B_n with other parameters.

Table 3.4 Equivalent Networks and their Parameters - Doubly Terminated

	EQUIVALENT NETWORKS	L_1	L_2	C_1	C_2	ΣL_i	ΣC_i	K
N_{31}		$\frac{\sqrt{Z}}{B_n - \sqrt{A}}$	$\frac{B_n^2 + A}{\sqrt{Z}(B_n - \sqrt{A})}$	$\frac{B_n - \sqrt{A}}{\sqrt{Z}}$	$\frac{\sqrt{Z}(B_n - \sqrt{A})}{B_n^2 + A}$	$\frac{B_n^2 + A + 2}{\sqrt{Z}(B_n - \sqrt{A})}$	$\frac{B_n^2 + A + 2}{\sqrt{Z}(B_n + \sqrt{A})}$	$\frac{(2+B_n^2)^2 \times 10^{-2}}{2B_n^4 + 4B_n^2 + 4}$
N_{32}		$\frac{\sqrt{Z}}{B_n}$	$\frac{(2+B_n^2)^2}{\sqrt{Z}B_n^3}$	$\frac{\sqrt{Z}B_n}{2+B_n^2}$	$\frac{B_n^3}{\sqrt{Z}(2+B_n^2)}$	$\frac{B_n^4 + 6B_n^2 + 4}{\sqrt{Z}B_n^3}$	$\frac{B_n}{\sqrt{Z}}$	$1 + \frac{B_n^2}{2}$
N_{33}		$\frac{2+B_n^2}{\sqrt{Z}B_n}$	$\frac{\sqrt{Z}(2+B_n^2)}{B_n^3}$	$\frac{B_n}{\sqrt{Z}}$	$\frac{\sqrt{Z}B_n^3}{(2+B_n^2)^2}$	$\frac{(2+B_n^2)^2}{\sqrt{Z}B_n^3}$	$\frac{B_n[(2+B_n^2)^2 + 2B_n^2]}{\sqrt{Z}(2+B_n^2)^2}$	$1 + \frac{B_n^2}{2}$

$$* A = B_n^2 \frac{(R-1)}{(R+1)}$$

$$R = \frac{(2+B_n^2)^2}{B_n^4}$$

There are three points to be noted.

Firstly, the value of A defined in (3.43) must always be positive real. Therefore, the gain and the terminating resistance are constrained by

$$\frac{K^2}{R} \leq \frac{B_n^4}{4} \quad (3.55)$$

Secondly, the element values of network N_{33} can be obtained from those of N_{32} by inspection due to a coefficient symmetry in $Z_{in}(s)$, i.e., C_1 in N_{33} is the inverse of L_1 in N_{32} , C_2 in N_{33} the inverse of L_2 in N_{32} ,

etc. Also, three other equivalent networks are the duals of those shown in Table 3.4, therefore, element values are readily obtainable by simple inspection.

Thirdly, the other possible choice for $\rho(s)$ produces a $Z_{in}(s)$ that does not have a coefficient symmetry. As a result, the continued fraction expansion procedure in accordance with the given canonic networks fails. However, it should be noted that the choice of the zero distribution of the reflection coefficient does not affect the minimum phase property of the transfer function.

Example 3.3

As a second example, let us consider a maximally flat 6th order normal BP transfer function. We start with 3rd order Butterworth LP function

$$H_{LP}(p) = \frac{k}{p^3 + 2p^2 + 2p + 1} \quad (3.56)$$

and apply the transformation $p \rightarrow \frac{s^2 + 1}{B_n s}$, where B_n is the normalized bandwidth. For convenience, let us assign $B_n = 0.1$. Then the required BP function is

$$H(s) = \frac{K s^3}{s^6 + 0.2s^5 + 3.02s^4 + 0.401s^3 + 3.02s^2 + 0.2s + 1} \quad (3.57)$$

Step 1: Determination of $\rho(s)$.

From (3.26), we obtain

$$\rho(s) \rho(-s) = \frac{s^{12} + 6s^{10} + 15s^8 + (20 - 10^{-6} + \frac{4}{R^2})s^6 + 15s^4 + 6s^2 + 1}{s^{12} + 6s^{10} + 15s^8 + (20 - 10^{-6})s^6 + 15s^4 + 6s^2 + 1}$$

$$= \frac{p(s) p(-s)}{q(s) q(-s)} \quad (3.58)$$

Since the numerator is a reciprocal polynomial of order 12, the root distribution pattern would appear as shown in Fig. 3.10.

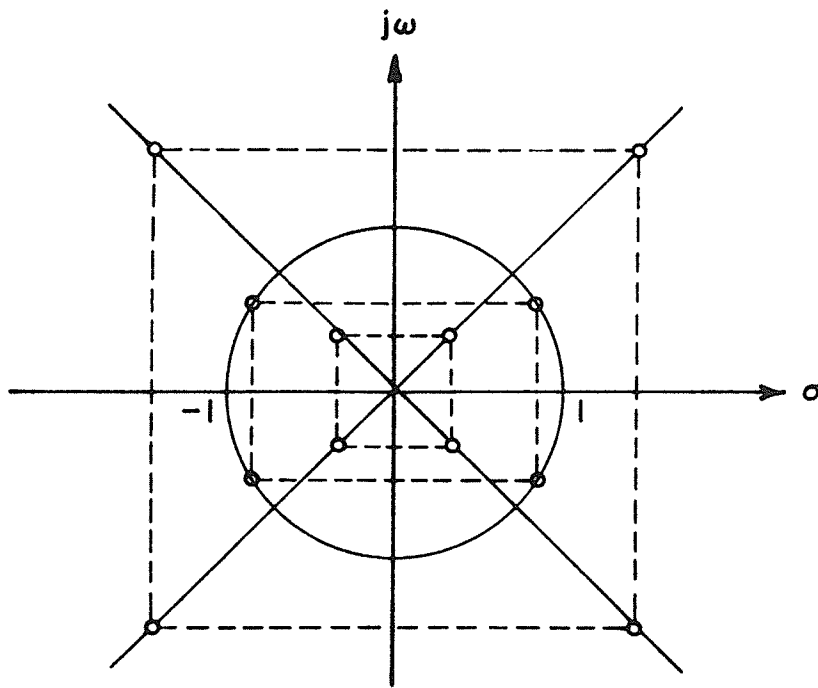


Fig. 3.10 Zero-pair distribution of $\rho(s)$.

Then, there are four different ways to choose $\rho(s)$. Again using an analytical procedure, we can partition the numerator $N(s)$ of (3.58) as,

$$N(s) = (s^6 + as^5 + bs^4 + cs^3 + bs^2 + as + 1)(s^6 - as^5 + bs^4 - cs^3 + bs^2 - as + 1).$$

Matching the coefficients of each term, we obtain

$$2b - a^2 = 6 \quad (3.59a)$$

$$2b - 2ac + b^2 = 15 \quad (3.59b)$$

$$2 + 2b^2 - 2a^2 - c^2 = 20 - Y \quad (3.59c)$$

where
$$Y = 10^{-6} - \frac{4}{R} K^2.$$

Because $|\rho(j\omega)|^2 \leq 1$, Y must be in the range of

$$0 \leq Y \leq 10^{-6}.$$

Therefore, R and K must satisfy the relation,

$$0 \leq \frac{4}{R} K^2 \leq 10^{-6}. \quad (3.60)$$

To find the positive and real values of a , b and c in (3.59) in terms of Y requires the solution of the fourth order polynomial equation. Two sets of solutions are found to be:

$$a = 0, b = 3, c = Y^{3/6} \quad (3.61)$$

and

$$a = 2Y^{1/6}, b = 3 + 2Y^{2/6}, c = 4Y^{1/6} + Y^{3/6}. \quad (3.62)$$

Therefore, we can identify for (3.61),

$$\rho_I = \frac{s^6 + 3s^4 + \gamma^{1/2}s^3 + 3s^2 + 1}{s^6 + 0.2s^5 + 3.02s^4 + 0.401s^3 + 3.02s^2 + 0.2s + 1} \quad (3.63)$$

for (3.62),

$$\rho_{II} = \frac{s^6 + 2\gamma^{1/6}s^5 + (3+2\gamma^{1/3})s^4 + (4\gamma^{1/6} + \gamma^{1/2})s^3 + (3+2\gamma^{1/3})s^2 + 2\gamma^{1/6}s + 1}{s^6 + 0.2s^5 + 3.02s^4 + 0.401s^3 + 3.02s^2 + 0.2s + 1} \quad (3.64)$$

Two other possible choices are excluded, because they fail to produce $\rho(s)$ with coefficient symmetry.

Step 2: Determination of $Z_{in}(s)$.

From (3.63) and (3.64), we can identify, respectively,

$$Z_I = \frac{2s^6 + 0.2s^5 + 6.02s^4 + (0.401 + \gamma^{1/2})s^3 + 6.02s^2 + 0.2s + 2}{0.2s^5 + 0.02s^4 + (0.401 - \gamma^{1/2})s^3 + 0.02s^2 + 0.2s} \quad (3.65a)$$

or

$$\hat{Z}_I = \frac{1}{Z_I} \quad (3.65b)$$

and

$$Z_{II} = \frac{2s^6 + (0.2 + 2\gamma^{1/6})s^5 + (6.02 + 2\gamma^{1/3})s^4 + [0.401 + (4\gamma^{1/6} + \gamma^{1/2})]s^3 + (6.02 + 2\gamma^{1/3})s^2 + (0.2 + 2\gamma^{1/6})s + 2}{(0.2 - 2\gamma^{1/6})s^5 + (0.02 - 2\gamma^{1/3})s^4 + [0.401 - (4\gamma^{1/6} + \gamma^{1/2})]s^3 + (0.02 - 2\gamma^{1/3})s^2 + (0.2 - 2\gamma^{1/6})s} \quad (3.66a)$$

or

$$\hat{Z}_{II} = \frac{1}{Z_{II}} \quad (3.66b)$$

Step 3: Realization of $Z_{in}(s)$ into canonic ladder networks listed in Fig. 3.6(b).

Element values can readily be obtained by continued fraction expansion on impedances in accordance with the configurations. It is to be noted that due to duality relations and coefficient symmetry shown in impedance expressions, it is sufficient to calculate element values for network N_1 , N_3 , N_4 and N_6 . For example, due to coefficient symmetry, in the continued fraction expansion for the N_3 and N_2 , the quotients are exactly the same. The same statement holds true for the pairs of N_4 - N_5 and N_6 - N_7 . The element values of the other seven networks can be obtained by inspection due to duality. In order to develop these networks such that the last resistance element is R , the proper choice of impedances is of (3.65b) and (3.66b).

The last resistance elements are found to be:

for $\hat{Z}_I(s)$

$$N_1 \quad R = \frac{10^{-3} - \gamma^{1/2}}{10^{-3} + \gamma^{1/2}}$$

$$N_2 \text{ \& } N_3 \quad R = \frac{(0.201 - \gamma^{1/2})^2 (10^{-3} + \gamma^{1/2})}{(0.201 + \gamma^{1/2})^2 (10^{-3} - \gamma^{1/2})}$$

$$N_4 \text{ \& } N_5 \quad R = \frac{10^{-6} - \gamma}{(0.201 + \gamma^{1/2})^2}$$

$$N_6 \text{ \& } N_7 \quad R = \frac{(0.201 - Y^{1/2})^2}{10^{-6} - Y} .$$

for $\hat{Z}_{II}(s)$

$$N_1 \quad R = \frac{10^{-3} - Y^{1/2}}{10^{-3} + Y^{1/2}}$$

$$N_2 \text{ \& } N_3 \quad R = \frac{(2.01 + 0.1Y^{1/6} + Y^{2/6})^2 (0.01 - 0.1Y^{1/6} + Y^{2/6}) (0.1 - Y^{1/6})}{(2.01 - 0.1Y^{1/6} + Y^{2/6})^2 (0.01 + 0.1Y^{1/6} + Y^{2/6}) (0.1 + Y^{1/6})}$$

$$N_4 \text{ \& } N_5 \quad R = \frac{(0.1 - Y^{1/6}) (0.01 - 0.1Y^{1/6} + Y^{2/6}) (0.01 + 0.1Y^{1/6} + Y^{2/6})}{(0.1 + Y^{1/6}) (2.01 + 0.1Y^{1/6} + Y^{2/6})^2}$$

$$N_6 \text{ \& } N_7 \quad R = \frac{(2.01 + 0.1Y^{1/6} + Y^{2/6})^2 (0.1 - Y^{1/6})}{(0.01 + 0.1Y^{1/6} + Y^{2/6}) (0.01 - 0.1Y^{1/6} + Y^{2/6}) (0.1 + Y^{1/6})} .$$

As in Example 3.2, we can choose R and K such that the terminating resistance is R. This process is omitted for brevity.

3.3.5 Sensitivity Considerations in Doubly Terminated Networks

The characteristics of active and passive elements used in a filter design may vary from their nominal values because of aging, environmental changes, and other causes. These variations may cause a network to depart significantly from its desired performance. It is of little use to expend effort to obtain an ideal transfer function only to find, after the filter has been constructed using practical components, that the filter performance does not satisfy the specifications. For example, in an active filter, the

gain of active element may change to the extent that the transfer function poles are shifted to the right half s -plane, resulting in instability.

In filter synthesis, once a transfer function is obtained, the solution of synthesis problem is not unique. Different networks can be realized to produce the same input-output relationship. As long as ideal elements are used under ideal conditions, one network works just as well as the other. In practice, however, one network may outperform another because it is less sensitive to element variations and to environmental changes. This network may be no more expensive to construct than the other. Therefore, a quantitative measure is needed not only to compare networks with regard to element variations but also to make an appropriate allowance for component variations in realizing a transfer function. Sensitivity functions are used for this purpose. These functions provide a numerical measure of how much an important aspect of the network or response varies as an element or a combination of elements varies from the nominal design values.

In the following, definition of sensitivity function is introduced, and sensitivity comparisons are made between singly terminated and doubly terminated LC ladders.

3.3.5.1 Definitions

The sensitivity function plays an important practical and conceptual role in transfer function variability studies, and it is a measure of the change of the overall transfer function with respect to change of an element or parameter of interest in the network. We define the measure of the change Δy in some performance characteristic y , resulting from a change Δx in a network parameter x , to be the sensitivity of y with respect to x , given by

$$S_x^y = \lim_{\Delta x \rightarrow 0} \frac{\Delta y/y}{\Delta x/x} = \lim_{\Delta x \rightarrow 0} \frac{x}{y} \frac{\Delta y}{\Delta x} . \quad (3.67)$$

Thus the changes in x and y have been normalized, i.e., S_x^y is a ratio of normalized changes or percentages. For sufficiently small Δx_i and well behaved higher order derivatives, we may make the first order approximation,

$$\Delta y \doteq \sum_{i=1}^n \frac{\partial y}{\partial x_i} \cdot \Delta x_i \quad (3.68)$$

to obtain the deviation. It should be noted that the validity of (3.68) depends on Δx_i being "small" and the higher order derivatives being "well behaved". This may not always be the case and the first order approximation may not be relied upon when such pathological cases arises. From (3.67) and (3.68), we have

$$S_{x_i}^y = \frac{x_i}{y} \frac{\partial y}{\partial x_i} = \frac{\partial [\ln y]}{\partial [\ln x_i]} . \quad (3.69)$$

3.3.5.2 Transfer Function Sensitivity

Let us consider a transfer function

$$H(s) = \frac{N(s)}{D(s)} . \quad (3.70)$$

For sinusoidal inputs, we are more concerned with the variation of $H(j\omega)$ with respect to the variation of the parameter x . For $s = j\omega$, we have

$$H(j\omega) = |H(j\omega)| e^{j\phi(\omega)} \quad (3.71)$$

where

$$\phi(\omega) = \arg [H(j\omega)] .$$

Then

$$\ln H(j\omega) = \ln |H(j\omega)| + \ln [e^{j\phi(\omega)}] . \quad (3.72)$$

In (3.72) $\ln |H(j\omega)|$ and $\phi(\omega)$ are known as the gain function and phase function, respectively. From the definitions (3.69) and (3.72), we have

$$\begin{aligned} S_x^{H(j\omega)} &= S_x^{|H(j\omega)|} + S_x^{e^{j\phi(\omega)}} \\ &= S_x^{|H(j\omega)|} + j\phi(\omega) S_x^{\phi(\omega)} . \end{aligned} \quad (3.73)$$

If x is real (which is true in most cases), then $S_x^{|H(j\omega)|}$ and $S_x^{\phi(\omega)}$ are real and by (3.73), we obtain

$$S_x^{|H(j\omega)|} = \operatorname{Re} [S_x^{H(j\omega)}] \quad (3.74)$$

$$S_x^{e^{j\phi(\omega)}} = \operatorname{Im} [S_x^{H(j\omega)}] \quad (3.75)$$

Thus the gain and phase sensitivity may be calculated directly by definition or they may be obtained from $S_x^{H(j\omega)}$ using (3.74) and (3.75).

3.3.5.3 Loss Sensitivities in LC Filters

It is well known that the loss of a doubly terminated LC filter is far less sensitive than the loss of singly terminated one. This is the main reason why high quality filters meeting stringent specifications rely heavily

on the doubly terminated LC ladder structure [3-5, 24-30].

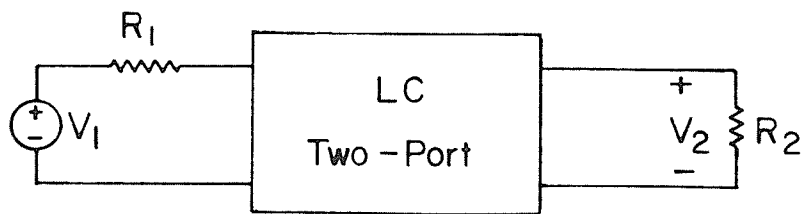
The primary objectives in a filter design are to obtain a passband whose loss remains constant within prescribed limits over its assigned frequency interval and one or two stopbands where the loss, relative to that in the passband, exceeds some prescribed discrimination by an amount whose precise value is unimportant as long as it remains constant. The important point to note about the behavior in the passband is that the response is required to be flat, and that the flatness is specified by upper and lower limits between which the response must lie. What is not so important is the absolute level at which these limits occur. If, due to component variations, the loss increases or decreases by the same amount at all frequencies, the flatness of the passband will be unchanged and the resulting small level shift, (which is merely equivalent to inserting an attenuator), while not desirable, is not particularly troublesome. But if the component variations cause the passband loss to develop a systematic ripple, it will almost certainly prove objectionable to the user and may make the loss exceed the prescribed limits on flatness.

We now examine how the component variations affect the loss of both doubly terminated and singly terminated LC filters.

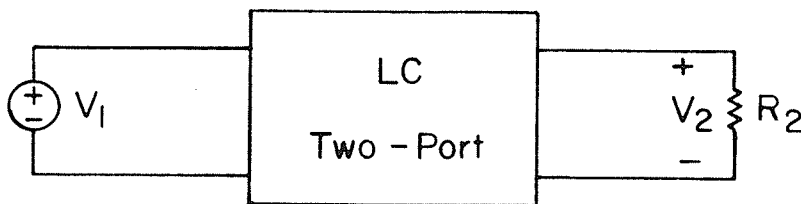
(i) Doubly Terminated Filters.

First, for the circuit shown in Fig. 3.11, we define the transducer function $T(s)$, the loss α (in nepers), and the phase β (in radians) by [30],

$$\begin{aligned}\alpha + j\beta &= \ln T(j\omega) \\ &= \ln \frac{V_1}{V_2} \sqrt{\frac{R_2}{R_1}}\end{aligned}\tag{3.76}$$



(a)



(b)

Fig. 3.11 (a) Doubly terminated and (b) Singly terminated filter.

Note that

$$\begin{aligned}
 2\alpha &= \ln |T(j\omega)|^2 \\
 &= \ln \frac{|V_1|^2/4R_1}{|V_2|^2/R_2} = \ln \frac{P_{\max}}{P_2} \geq 1
 \end{aligned}
 \tag{3.77}$$

where P_{\max} is the maximum power available from the source R_1 and P_2 is the power dissipated in R_2 . As the two-port is assumed passive, the loss α is always non-negative and is equal to zero when $P_2 = P_{\max}$. From (3.18), we can identify that

$$|t(j\omega)|^2 = e^{-2\alpha} \leq 1 \quad . \tag{3.78}$$

The logarithmic sensitivity of the loss $\alpha(j\omega)$ to changes of the inductance L_i and capacitance C_k are given as follows:

$$L_i \frac{\partial \alpha}{\partial L_i} = - \frac{\omega}{P_2} \operatorname{Im} [\bar{\rho} L_i I_i^2 / 2] \quad (3.79a)$$

$$C_k \frac{\partial \alpha}{\partial C_k} = \frac{\omega}{P_2} \operatorname{Im} [\bar{\rho} C_k V_k^2 / 2] \quad (3.79b)$$

where ρ is the input reflection coefficient defined in (3.23).

To establish the bound on these sensitivities, let us examine the behavior of $\rho(j\omega)$. Consider a filter with a transducer loss response which varies between α_0 and $\alpha_0 + \alpha\rho$ in the passband. Then, from (3.78) the locus of $\rho(j\omega)$ must be contained in a ring-shaped area with an inside radius,

$$|\rho|_{\min} = \sqrt{1 - e^{-2\alpha_0}} \quad (3.80)$$

as shown in Fig. 3.12.

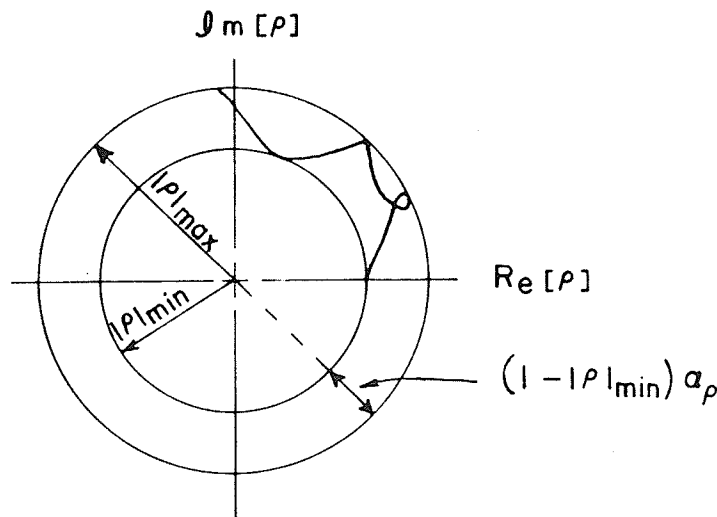


Fig. 3.12 Locus of $\rho(j\omega)$.

Then, from (3.79a) and (3.79b), recognizing the fact that $L_i I_i^2/2$ and $C_k V_k^2/2$ are the average magnetic energy and average electric energy stored in L_i and C_k , respectively, the worst case sensitivity of the loss response to variations of any reactance element x_i can be written,

$$\left| x_i \frac{\partial \alpha}{\partial x_i} \right| \leq \frac{\omega \epsilon_i}{P_2} \sqrt{1 - e^{-2\alpha}} \quad (3.81)$$

where ϵ_i is the average energy stored in the component x_i . Similarly, the worst case loss sensitivity to R_1 and R_2 can be obtained as,

$$\left| R_i \frac{\partial \alpha}{\partial R_i} \right| \leq \frac{1}{2} \sqrt{1 - e^{-2\alpha}} \quad i=1, 2 \quad (3.82)$$

Therefore, if one designs a conventional equi-ripple passband filter with the usual magnitude of ripple and arranges to get maximum transfer of power at the frequencies of minimum loss, then both α and $\partial \alpha / \partial x_i$ are exactly zero at these frequencies, and because of small passband ripple, $\partial \alpha / \partial x_i$ also remains small everywhere else in the passband. This is the basis of the low sensitivity of conventional doubly terminated LC filters.

If V_2 is the output quantity of interest, from (3.76), we obtain,

$$S_{x_i}^{V_2} = - x_i \frac{\partial \alpha}{\partial x_i} \quad (3.83)$$

if x_i is any element inside the two-port, then

$$S_{R_1}^{V_2} = - R_1 \frac{\partial \alpha}{\partial R_1} - \frac{1}{2} \quad (3.84a)$$

$$S_{R_2} |V_2| = -R_2 \frac{\partial \alpha}{\partial R_2} + \frac{1}{2} \quad (3.84b)$$

for R_1 and R_2 respectively. Thus $|V_2|$ will share the zero sensitivity of α with respect to all the elements inside the two-port, but due to the terms $\pm 1/2$ in (3.84a) and (3.84b), a change in either R_1 or R_2 will produce a frequency independent shift in $|V_2|$ in addition to the small effects proportional to $\partial \alpha / \partial R_i$. As mentioned previously, these frequency independent shifts have no effect on the quality of the passband and are normally of no consequence.

(ii) Singly Terminated Filters.

Now, we consider the case of Fig. 3.11(b), and define the transducer function $T(j\omega)$, the loss α , and the phase β by

$$\alpha + j\beta = \ln T(j\omega) = \ln (V_1/V_2) \quad (3.85)$$

It must be noted here that there is no upper limit to the power that can be dissipated in R_2 and so there is no possibility of desensitizing the loss by working at maximum transfer of power. We can derive a formula similar to (2.81) and (3.83) for case where x_i represents an element inside the two-port, namely

$$S_{x_i} |V_2| \leq \frac{\omega \epsilon_i}{P_2} \quad (3.86)$$

The absence from (3.86) of the factor $\sqrt{1 - e^{-2\alpha}}$ that appears in (3.81) clearly shows that the sensitivity in the singly terminated filter will be many times greater than in the doubly terminated filter.

To examine the sensitivity with respect to R_2 , let $Y_2 = jB_2$ be the output admittance seen into port 2 with the source V_1 set to zero. Then, we can obtain

$$S_{R_2}^{|V_2|} = \frac{R_2}{|V_2|} \frac{\partial |V_2|}{\partial R_2} = \frac{1}{1 + R_2^2 B_2^2} \quad (3.87)$$

Y_2 is a positive real odd function and most of its poles and zeros will lie in the passband and so, as one traverses the passband, Y_2 will oscillate back and forth through positive values between zero and infinity. Hence the sensitivity will oscillate between zero, at the poles of Y_2 and unity at the zeros of Y_2 . Thus we find that an error in R_2 will produce in the output voltage a systematic ripple whose maxima and minima coincide with the zeros and poles of Y_2 .

3.3.6 Comparison of Equivalent Networks

We have made comparison of equivalent networks for singly terminated maximally flat 4th order filter in section 3.2.3. A similar comparison for doubly terminated filters which are shown in table 3.4 may be made with respect to specified criteria.

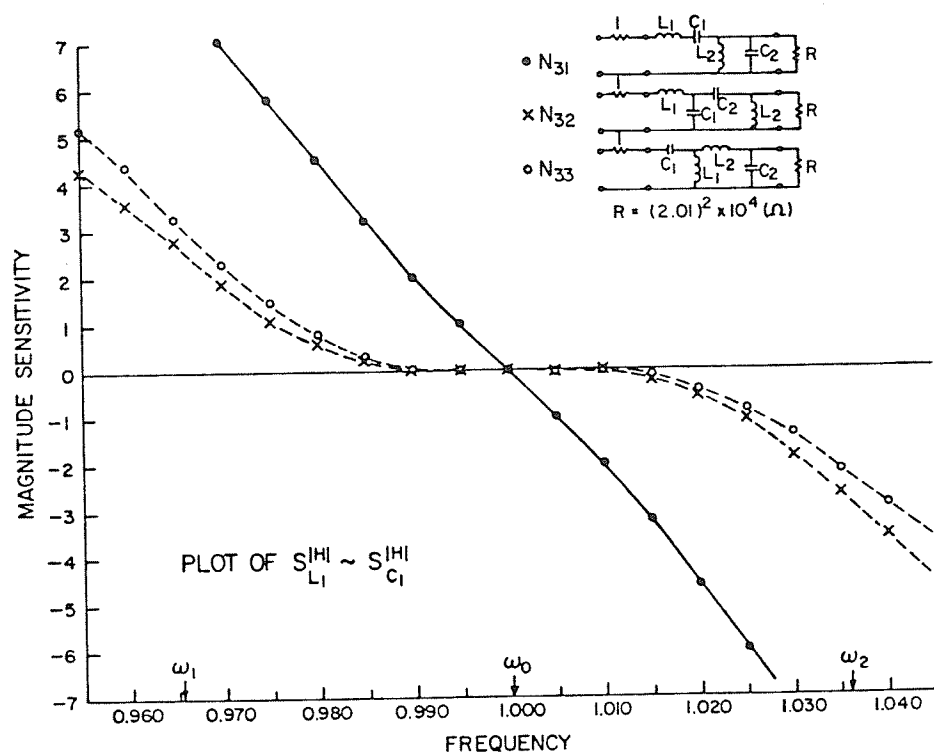
For the normalized bandwidth $B_n = 0.1$, we have found that the N_{31} (conventional network) requires a total inductance about two orders of magnitude more than those of non-conventional ones. However, for a total capacitance requirement, the statement is reversed, i.e., non-conventional ones require approximately two orders of magnitude more. Two non-conventional filters are comparable in this respect.

The gain of N_{31} is much lower than that of networks N_{32} , and N_{33} . The gain of the non-conventional ones is identical but much higher than that of the conventional network N_{31} . Thus, in terms of the gain, the two non-conventional networks are preferable to the conventional one.

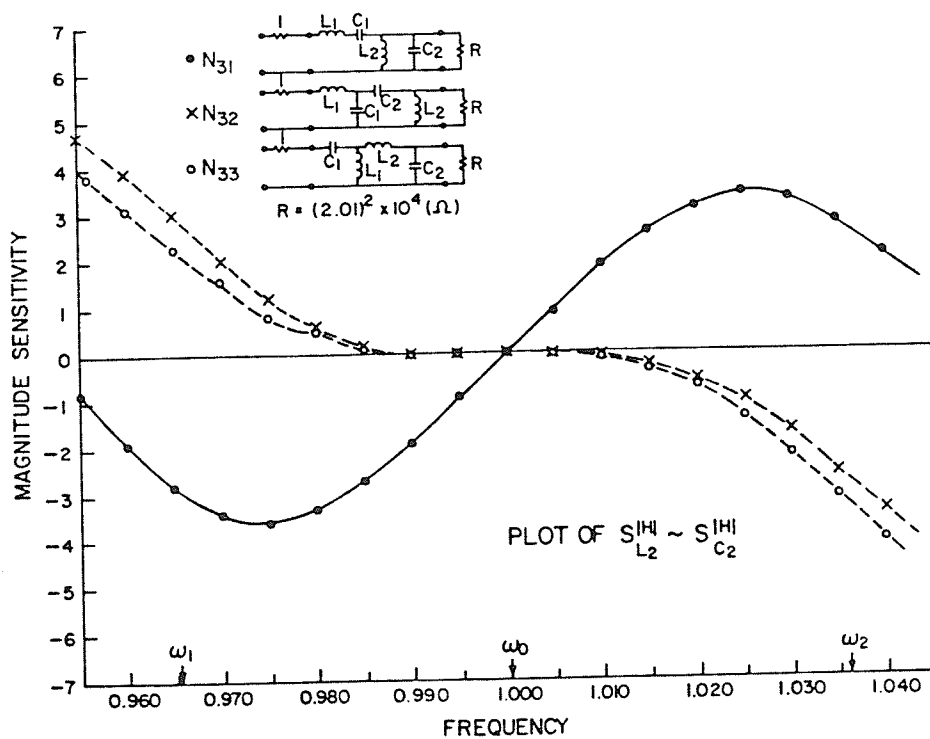
A further advantage of non-conventional filters is observed when we compare the transfer function magnitude sensitivity with respect to element variations.

As shown in Fig. 3.4 the magnitude sensitivities with respect to the LC component variations in a singly load-terminated case are roughly comparable among equivalent networks. This is also true for the case of singly source-terminated networks. Therefore, we conclude that as far as the magnitude transfer function sensitivity is concerned, there is no real preference in choosing one network over another.

To make comparisons for the case of doubly terminated structures, the magnitude sensitivities with respect to LC components are calculated, and the results are plotted in Fig. 3.13 for the value of $B_n = 0.1$. As can be seen the networks N_{32} and N_{33} exhibit much better sensitivity performance than that of network N_{31} .



(a)



(b)

Fig. 3.13 Plot of magnitude sensitivity - Doubly terminated

CHAPTER IV

DIRECT CONVERSION TO ACTIVE AND DIGITAL FILTERS IN CANONIC LADDER STRUCTURES

Electrical filters may be classified in a number of ways. Analog filters are used to process analog signals or continuous-time signals; digital filters are used to process digital signals (discrete-time signals with quantized magnitude levels). Analog filters may be classified as lumped or distributed depending on the frequency ranges for which they are designed. Finally, analog filters may also be classified as passive or active depending on the type of elements used in their realization. So far we have dealt with analog, passive and lumped filters with a specific structure, i.e., canonic ladder filter networks.

The doubly terminated canonic ladders (so called LC prototypes or reference networks) may be directly converted to active and digital filters in canonic ladder structures sustaining all the desirable features of LC prototypes. In this chapter, using the component simulation technique, equal number of active ladder networks are generated. In particular, implementation of the Generalized Immittance Converter (GIC) [6, 35, 38, 39, 43, 56] is studied. Since the number of required GIC's depends on the relative location of inductance, e.g., ladder imbedding, in the reference networks, economic filters with optimum design of GIC are sought among the active counterparts.

The digital filters with true ladder configuration [67] are also directly obtainable from the reference equivalent networks using wave digital filter realization method [62]. A new analysis method for the magnitude sensitivity

of the transfer function with respect to multiplier coefficients is presented and equivalent wave digital filters are compared from a sensitivity point of view.

4.1 ACTIVE CANONIC FILTERS

It is well known that among passive elements the inductor is the most non-ideal one. This is especially true at low frequencies where inductors become impractical because of their bulky size and considerable departure from ideal behavior. This fact coupled with other technology development led circuit designers to the investigation of inductorless networks. Particularly, research in active RC filters initiated more than two decades ago, matured quickly with the advent of integrated circuit technology in the mid and late sixties [40]. As most of the communication and instrumentation systems became smaller in size, the filters' part appeared to be the bulkiest. More seriously, inductors are not readily adaptable to integration which dominates most of today's systems. Attempts to produce integrated circuit inductor have generally failed. The search, therefore, started for developing methods of retaining the effect of inductors while avoiding their actual use. The methods come under the general heading of active filter synthesis, in which the circuit elements used are resistors, capacitors and one or more active devices [31-58].

There are basically two distinct approaches to the design of active filters with an order greater than 2. The first approach starts directly from realizing the given transfer function $H(s)$ as the voltage transfer function of a feedback structure containing amplifiers and RC networks [6, 37, 44-46].

It turns out, however, that if one attempts a direct realization of even a moderately higher order transfer function in one feedback loop, the resulting network is quite sensitive to component variations. For this reason, a more practical and simpler technique, namely the cascaded realization of biquad, had been developed. Due to sensitivity considerations, however, its utility is limited to filter functions of moderate stringency [41, 46, 47, 52].

The other major approach is based on the simulation of LC ladder filters. The starting point is an LC ladder prototype which may be readily obtainable from the wealth of knowledge in the analysis, design and manufacture of LC filters. As previously demonstrated, doubly terminated passive LC ladders designed by Darlington's method exhibit excellent sensitivity performance over the filter passband. One of the reasons for the reduced transfer function sensitivity with respect to each ladder component is that the ladder transfer function is dependent on all the network components. Hence, the transfer function is spread out, with each individual sensitivity being small in value. This spreading out of sensitivity functions in an LC ladder may be visualized as if the ladder possesses internal negative feedback that reduces the transfer function sensitivity to each component. This point of view had led to the coupled biquad structures, which indeed have lower sensitivities than the cascaded structures [6, 50].

Also, the low sensitivity performance of LC ladders provided a strong motivation to seek methods for designing active filters based on simulating LC ladder prototypes [24, 42]. The simplest of these methods, at least

conceptually, is the component simulation method. The component simulation method is based on replacing the inductors by simulated inductors [31-43, 48, 52-54, 57]. An alternative method exists that simulates the operation of the LC ladder rather than simulating an inductor in the LC ladder. This method is generally termed operational simulation against component simulation for the former case [6, 51]. It is generally recognized that the design method based on LC ladder simulation method should be used whenever the filter specifications are stringent.

4.1.1 Component Simulation - Optimum GIC

The use of more than one amplifier to realize an RC-active filter is now economically viable because of the relatively low cost of high performance operational amplifiers. As a result, the topic of multiple-amplifier RC active filter design has become increasingly important in recent years; this is basically because multiple-amplifier RC active filters may be designed so that the magnitude transfer function is highly insensitive to the tolerance errors associated with the RC elements and to the imperfections of the op amp's. The major technique that is currently used most to implement high-quality RC active filters is to simulate the behavior of doubly terminated LC filters by directly replacing inductors by simulated inductors. A number of circuits for inductor simulation has been proposed [31-34, 57]. The use of the Generalized Immittance Converter (GIC), particularly the Antoniou GIC is the most widely accepted for the simulation of inductors and for the design of high quality RC active filters in general.

Fig. 4.1 shows the Antoniou GIC embeded in an arbitrary network. Assuming ideal op amps with finite gains, A_1 and A_2 , a straightforward

analysis yields

$$\frac{I_1}{V_1} = \frac{I_2}{V_2} \frac{Y_1 Y_3}{Y_2 Y_4} \frac{1 + \frac{1}{A_1} \left(1 + Y_4 \frac{V_2}{I_2} \right) + \frac{1}{A_2} \frac{Y_2}{Y_3} \left(1 + Y_4 \frac{V_2}{I_2} \right) + \frac{1}{A_1 A_2} \left(1 + \frac{Y_2}{Y_3} \right) \left(1 + Y_4 \frac{V_2}{I_2} \right)}{1 + \frac{1}{A_1} \frac{Y_3}{Y_2} \left(1 + \frac{1}{Y_4} \frac{I_2}{V_2} \right) + \frac{1}{A_2} \left(1 + \frac{1}{Y_4} \frac{I_2}{V_2} \right) + \frac{1}{A_1 A_2} \left(1 + \frac{Y_3}{Y_2} \right) \left(1 + \frac{1}{Y_4} \frac{I_2}{V_2} \right)} \quad (4.1)$$

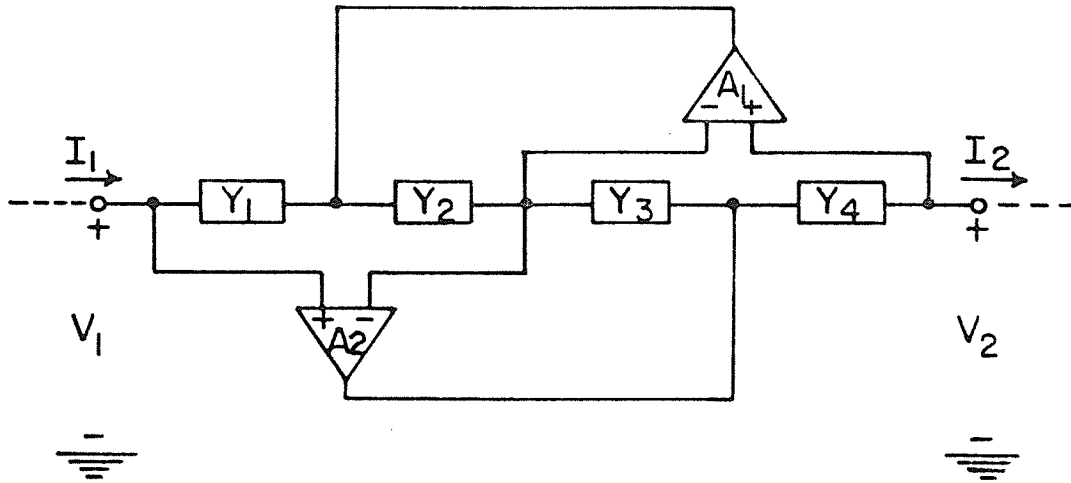


Fig. 4.1 The Antoniou GIC embedded in an arbitrary network.

If we represent op amps by the one-pole rolloff model, and further approximate

$$A_1 \cong \frac{\omega_{t1}}{j\omega} \quad , \quad A_2 \cong \frac{\omega_{t2}}{j\omega} \quad \text{and} \quad \omega \ll \omega_t \quad ,$$

where ωt_1 and ωt_2 are the gain bandwidth products, then, ignoring the terms $(\frac{\omega}{\omega_t})^2$, we have

$$\frac{I_1}{V_1} \cong \frac{I_2}{V_2} \frac{Y_1 Y_3}{Y_2 Y_4} \cdot \left[1 + j \left(\frac{\omega}{\omega_{t_1}} \right) \left(1 - \frac{Y_3}{Y_2} + Y_4 \frac{V_2}{I_2} - \frac{Y_3}{Y_2 Y_4} \frac{I_2}{V_2} \right) + j \left(\frac{\omega}{\omega_{t_2}} \right) \left(\frac{Y_2}{Y_3} - 1 + \frac{Y_2 Y_4}{Y_3} \frac{V_2}{I_2} - \frac{1}{Y_4} \frac{I_2}{V_2} \right) \right]. \quad (4.2)$$

For ideal performance it is desired to have

$$\frac{I_1}{V_1} = \frac{I_2}{V_2} \cdot \frac{Y_1 Y_3}{Y_2 Y_4} \quad (4.3)$$

independent of ωt_1 and ωt_2 . Thus, from (4.2), it is required that

$$1 - \frac{Y_3}{Y_2} + Y_4 \frac{V_2}{I_2} - \frac{Y_3}{Y_2} \frac{1}{Y_4} \frac{I_2}{V_2} = 0 \quad (4.4)$$

$$\frac{Y_2}{Y_3} - 1 + \frac{Y_2 Y_4}{Y_3} \frac{V_2}{I_2} - \frac{1}{Y_4} \frac{I_2}{V_2} = 0. \quad (4.5)$$

Since in general $\frac{V_2}{I_2}$ is a function of frequency and takes on a complex value, $(1 - \frac{Y_3}{Y_2})$ term must be linearly independent of $(Y_4 \frac{V_2}{I_2} - \frac{Y_3}{Y_2} \cdot \frac{1}{Y_4} \cdot \frac{I_2}{V_2})$. Thus, from (4.4) or (4.5), we can see that it is necessary to have $(1 - \frac{Y_3}{Y_2}) = 0$ which implies

$$Y_2 = Y_3. \quad (4.6)$$

Substituting (4.6) into either (4.4) or (4.5), we see that it is also

necessary to have

$$\frac{V_2}{I_2} = \frac{1}{Y_4} \quad (4.7)$$

(4.6) is easily satisfied by letting $Y_2 = Y_3 = g$ where g is real. However, satisfying (4.7) is seldom possible as $\frac{V_2}{I_2}$ has in general components orthogonal to $\frac{1}{Y_4}$. Substituting (4.6) into (4.2) results in

$$\frac{I_1}{V_1} = \frac{I_2}{V_2} \frac{Y_1}{Y_4} \left\{ 1 + j \left(\frac{\omega}{\omega_{t_1}} + \frac{\omega}{\omega_{t_2}} \right) \left[Y_4 \frac{V_2}{I_2} - \frac{1}{Y_4} \frac{I_2}{V_2} \right] \right\}. \quad (4.8)$$

For the best performance, we make the quantity $M = Y_4(V_2/I_2) - (1/Y_4)$ (I_2/V_2) as small as possible at the most critical frequency, ω_c , in the filter transfer function. This frequency is the one where the greatest group delay occurs and is usually close to the passband edge.

Letting $Y_4 = j\omega C_4$ where C_4 is real, M is minimized if

$$\omega_c C_4 = \left| \frac{I_2}{V_2} \right|_{\omega = \omega_c}. \quad (4.9)$$

The corresponding value for the GIC transfer function is

$$\frac{I_1}{V_1} = \frac{I_2}{V_2} \frac{Y_1}{Y_4} \left[1 - 2 \left(\frac{\omega}{\omega_{t_1}} + \frac{\omega}{\omega_{t_2}} \right) \cos \theta \right] \quad \text{at } \omega = \omega_c. \quad (4.10)$$

From (4.9), we may write that for most ideal performance one selects

$$\left| Y_4 \right|_{\omega = \omega_c} = \left| \frac{I_2}{V_2} \right|_{\omega = \omega_c} . \quad (4.11)$$

Taking the absolute value of both sides of (4.10) at $\omega = \omega_c$ and assuming $\omega \ll \omega_{t_1}$, $\omega \ll \omega_{t_2}$, we see that satisfying equation (4.11) is approximately equivalent to making

$$\left| Y_4 \right|_{\omega = \omega_c} = \left| \frac{I_1}{V_1} \right|_{\omega = \omega_c} . \quad (4.12)$$

We can interpret (4.11) and (4.12) as follows: at the critical frequency ω_c the magnitude of the end-admittance Y_4 on one side of the GIC must be matched to the magnitude of the admittance $\frac{I_2}{V_2}$, seen by that side of the GIC. The magnitude of the other end-admittance Y_1 will then be approximately matched to the magnitude of the admittance $\frac{I_1}{V_1}$, seen by the other side of the GIC. It must be noted that this condition implies some sort of "proper termination of" the GIC; and this together with the fact that $Y_2 = Y_3$ ensures optimum GIC performance.

Now let us simulate a grounded inductor with an optimum GIC. The circuit for simulating an inductor is shown in Fig. 4.2.

Setting $Y_2 = Y_3$ means that

$$R_2 = R_3 \quad (4.13)$$

Also, setting $\left| Y_4 \right|_{\omega = \omega_c} = \left| \frac{I_2}{V_2} \right|_{\omega = \omega_c}$ implies that

$$\omega_c C_4 R_5 = 1 \quad (4.14)$$

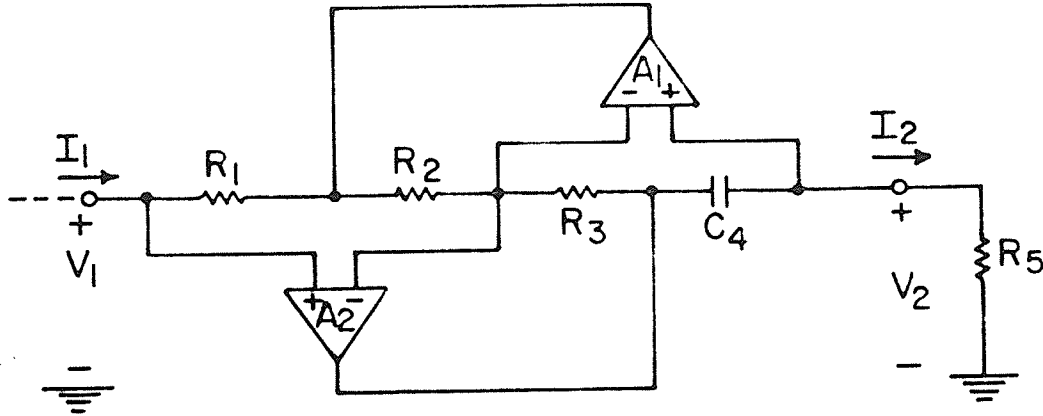


Fig. 4.2 The Antoniou GIC used to realize a grounded inductor.

Substituting (4.9), (4.17) and $\frac{V_2}{I_2} = R_5$ into (4.8), we have

$$\left. \frac{I_1}{V_1} \right|_{\omega = \omega_c} \cong jR_1 \left[1 + 2 \left(\frac{\omega_c}{\omega_{t1}} + \frac{\omega_c}{\omega_{t2}} \right) \right] \quad (4.15)$$

which implies that at $\omega = \omega_c$ the input inductance has infinite Q-factor but undergoes a deviation in value given by

$$\left. \frac{\Delta L}{L} \right|_{\omega = \omega_c} \cong \left(\frac{\omega_c}{\omega_{t1}} + \frac{\omega_c}{\omega_{t2}} \right) \quad (4.16)$$

(4.15) also suggests that R_1 may be used to adjust or trim the value of the input inductance.

In practice, $\omega_c \ll \omega_t$, therefore, it can be seen that an accurate and high Q inductor can be simulated with the GIC circuit.

4.1.2 Active Realizations - GIC Ladder Embedding Technique

The LC ladder realizations of BP filters have, by necessity, floating inductors. Although a number of circuits has been proposed for simulating ungrounded inductors [32, 33, 53, 57], none has been found to be practically viable [6]. Although no practical op. amp. implementation of a floating inductor exists, a number of techniques have been developed for the realization of BP filters using GICs. All these techniques involve a complex frequency transformation of a part, or parts, of the LC ladder prototypes [35, 36, 38].

Gorski-Popiel's ladder embedding method has laid the foundation for the realization of LP and general BP filters using GICs. Let us now refer to Fig. 4.3. The resistive n-port N' is connected to the multi-GIC network N_1 to form the composite n-port N . Note that N_1 is formed of n identical (ks) GICs of the current-transformation type, i.e., the i th GIC is described by $V_i = V_i'$ and $I_i = \frac{1}{ks} I_i'$.

Let N' be characterized by

$$\bar{V}' = \bar{Z}' \bar{I}' ,$$

then we may write

$$\bar{V} = \bar{V}' = \bar{Z}' \bar{I}' = \bar{Z}' (ks) \bar{I} = (ks \bar{Z}') \bar{I} .$$

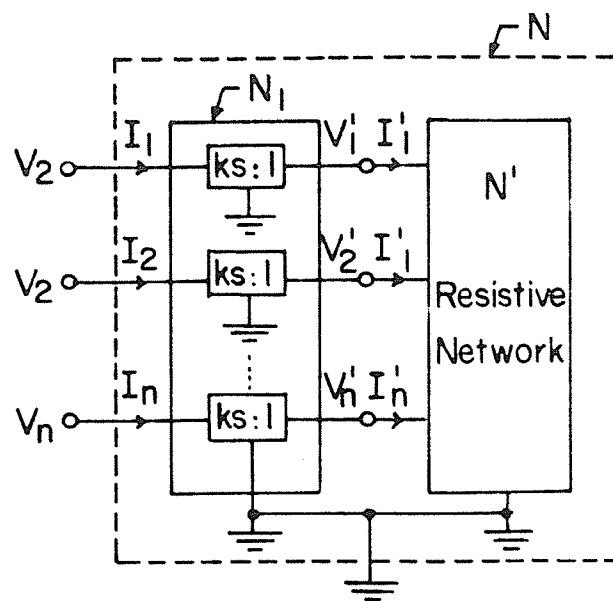


Fig. 4.3 Simulation of an inductive network N through the connection of a topologically identical resistive network N' and n GICs.

Thus, the composite n -port network N will be characterized by an impedance matrix \bar{Z} given by

$$Z = ks Z' .$$

Since Z' describes a resistive network, then Z describes a topologically identical inductive network with each inductance in N equal to the resistance of the corresponding resistor in N' multiplied by the constant k . Note that the number of GICs required, and correspondingly the number of capacitors, is not equal to the number of inductors in the subnetwork being simulated. Rather, it is equal to the number of terminals that connects the inductance subnetwork to the rest of the LC ladder network, discounting ground. A

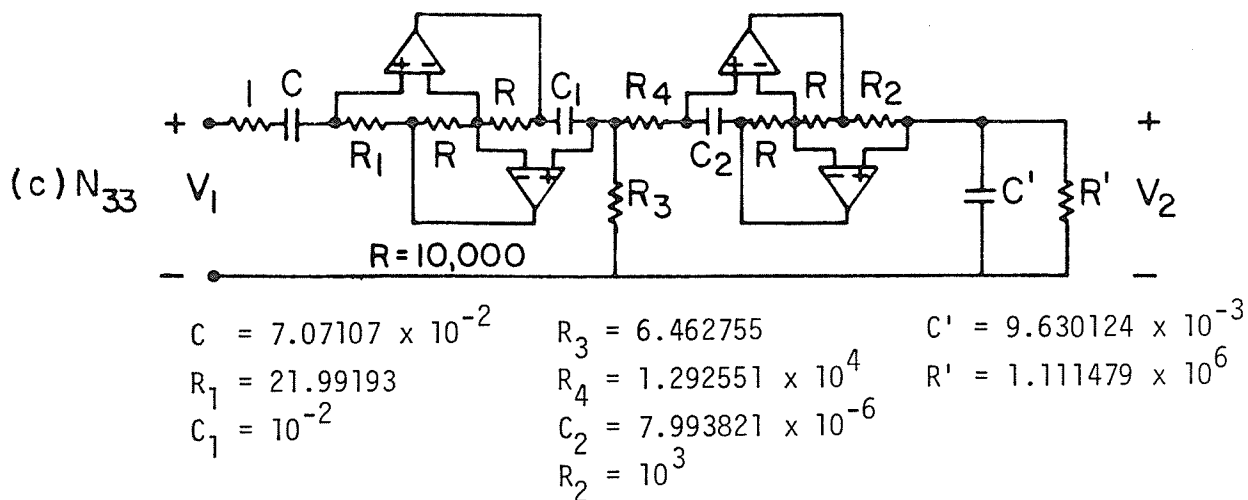
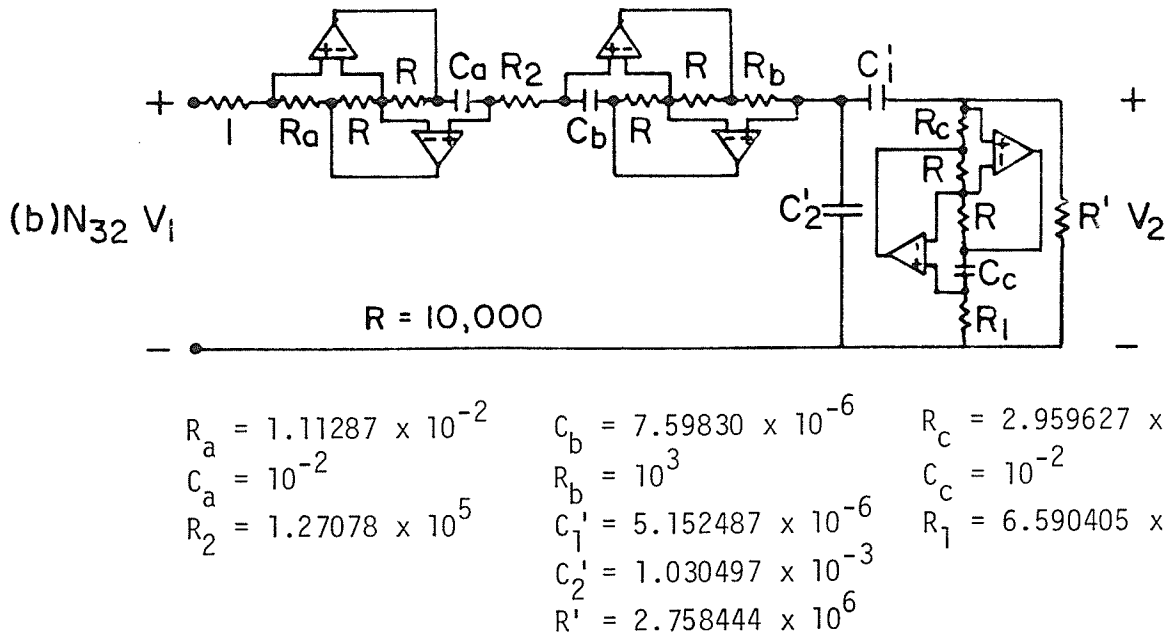
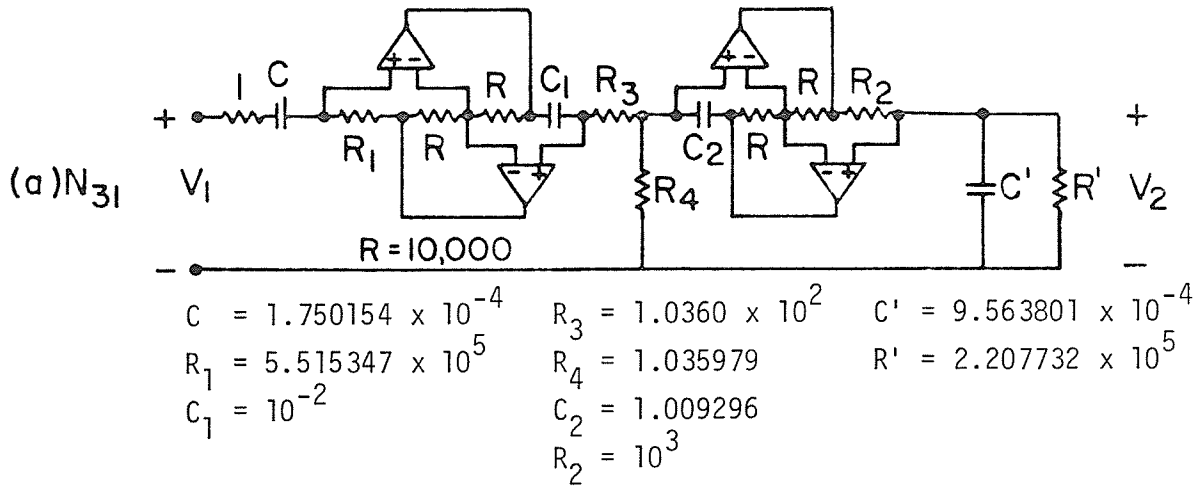


Fig. 4.4 Active realizations with optimum GICs for $B_n = 0.1$ (Element values in Ohm and Farad).

floating inductor has to be considered as a two-port and realized using two GIC s, with two capacitors.

A possible realization of three equivalent doubly terminated LC ladder networks developed in the previous chapter for $n=2$, $B_n=0.1$ is shown in Fig. 4.4 using ladder embedding technique. As can be noted, the network N_{32} requires three GIC s where others require only two. The resulting networks are optimum in the sense of minimized dependence on the op. amps. frequency response. This is achieved by ensuring that each GIC is properly terminated as mentioned previously. Also, N_{31} and N_{33} are canonic in the sense of minimum number of GICs required. It should be noted that the dual of N_{32} requires only two GICs whereas the dual of N_{33} requires three GIC s. Since the non-conventional equivalent reference networks N_{32} and N_{33} are less sensitive to inductance deviations as compared to the conventional prototype N_{31} , it is equally valid to conclude that their counterparts N_{32} and N_{33} in Fig. 4.4 are less sensitive than N_{31} with respect to GIC coefficients.

For the case when $n=3$, each one from N_1 to N_7 in Fig.3.6 requires three GIC s, however, the duals of N_2 to N_7 requires four GIC s, while the dual of N_1 requires only two.

4.2 Digital Canonic Filters

Digital filtering is the process of spectrum shaping using digital hardware as the basic building block. Thus the aim of digital filtering is the same as that of analog filtering, but the physical realization is different.

Real-time digital filters have several advantages over analog filters [59]. A greater degree of accuracy can be attained in the digital filter realization.

A great variety of digital filters, can be built, since certain realization problems associated with negative element value do not arise.

No special components are required to realize filters with time varying coefficients. No aging process can affect the parameters of the digital filters. In addition, they can operate down to extremely low frequencies (e.g. 0.01 to 1 Hz) where the size of analog components becomes appreciable.

As is in the case of analog filters, the design of digital filters involves the process of finding appropriate transfer functions to meet the required specifications. These specifications are often given in the frequency domain in the same way as those for analog filters.

There are at least three techniques for designing infinite impulse response recursive digital filters, which are derived from a transformation of the transfer function of analog filters: the impulse invariance, the bilinear transformation and the matched z -transform technique [66]. Since there are many transformations, so are many network realizations of the same transfer function. In practise, there are a number of basic network structures commonly encountered, such as, direct form, canonic form, cascade form, parallel form and so forth [69, 70]. One consideration in the choice between these different structures is computational complexity, i.e., networks with the fewest constant multipliers and the fewest delay branches are often most desirable. On the other hand, the effects of finite register length in actual hardware realizations of digital filters depend on the structure, and it is sometimes desirable to use a structure that does not have the minimum number of multipliers and delays but is less sensitive to finite-register-length effects. It is to be expected that some of these structures will be less

sensitive than others to quantization of the parameters [64]. Unfortunately, no systematic method has yet been developed for determining the best realization, under given constraints on the number of multipliers, word length and the number of delays. In place of a detailed mathematical analysis of the parameter-sensitivity problem, a common practical approach is the use of simulations for determining acceptable quantization of the parameters of a given network. Another aspect is that due to the finite word length, zero input limit cycles and overflow oscillations can occur in recursive digital filters [60, 61]. Some structures have been reported which are free of limit cycles when magnitude truncation is used for quantization, and which do not have overflow oscillations [73]. However, due to the complexity of the mathematics involved, the important results have so far been limited to sections of order not exceeding two. This is sufficient, in principle, since conventional digital filters are built by cascading first- and second-order sections.

An alternative way to overcome these sensitivity and stability problems was proposed by Fettweis [62]. Fettweis has derived a class of digital filters which has the low passband insensitivity which doubly terminated LC filters are known to have. These filters, known as wave digital filters (WDF), have been essentially derived from analog reference networks by applying the bilinear transformation directly to the circuit elements.

4.2.1 Wave Digital Filter

The design procedure for WDFs imitating ordinary LC ladder filters is based on the voltage wave scattering representation of the reference analog

filter structure together with the application of the bilinear z-transformation [62]. With this method, the frequency s in the analog filter is replaced by the frequency variable ψ defined by

$$\psi = \frac{1 - e^{-sT}}{1 + e^{-sT}} = \frac{1 - z^{-1}}{1 + z^{-1}} = \tanh\left(\frac{sT}{2}\right) \quad (4.17)$$

where $T = \frac{1}{f_s}$ is the sampling interval, and z is the discrete-time domain complex frequency variable. Voltage waves are used as the signal variables so that the reactance elements are characterized by a delay. For $s = j\omega$, we thus can write

$$\psi = j\phi \quad \phi = \tan\left(\frac{\omega T}{2}\right) \quad (4.18)$$

where ϕ is the analog frequency and ω is the digital frequency.

A list of some basic circuit elements with their corresponding wave flow diagrams as derived by Fettweis is given in Appendix II.

By means of wave adaptors such as the two-port adaptor, the n-port parallel adaptor and the n-port series adaptor, Fettweis and Sedlmeyer have obtained a true ladder wave digital structure from a doubly terminated LC ladder network [67, 74]. Such a wave digital realization is elegant in the sense that it is not only simple in concept and implementation but also has salient advantages over the conventional digital realizations. Namely, due to the insensitivity of the doubly terminated ladder networks, the coefficient sensitivity is much smaller, which in turn implies that a significant reduction in the coefficient word length is possible [63, 76, 77]. Also,

it has been shown by Fettweis and Meerkötter [65, 72] that it is stable and much easier to eliminate parasitic oscillations, both granularity and overflow, in such a structure. Furthermore, it is relatively simple to translate any well-known classical ladder filter directly into a WDF form when compared with other approaches [71, 78].

4.2.2 Wave Digital Filter Realization

4.2.2.1 Wave Transfer Function

The Darlington circuit structure, which is reproduced in Fig. 4.5 for convenience, is the most preferred analog filter structure. Such a structure is normally described by either its voltage transfer function,

$$H(\psi) = \frac{V_2(\psi)}{V_1(\psi)} \quad (4.19)$$

or by its transmission coefficient

$$t(\psi) = 2 \left(\frac{R_1}{R_2} \right)^{\frac{1}{2}} H(\psi) \quad (4.20)$$

where ψ is the continuous-time domain complex frequency variable.

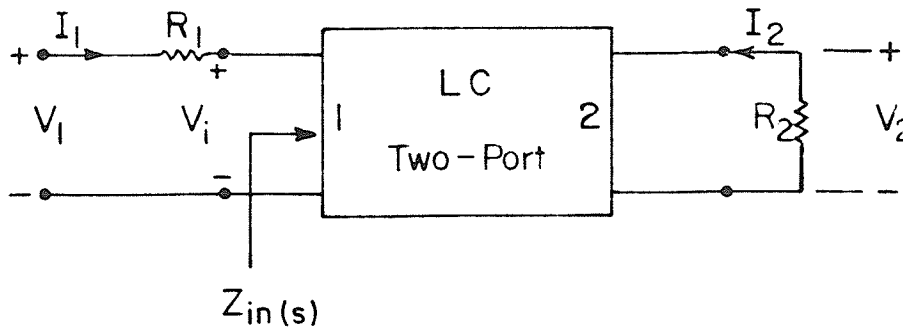


Fig. 4.5 Doubly terminated lossless network.

For a given port with associated references for voltage $v(t)$ and the current $i(t)$ as shown in Fig. 4.6, we define the incident and reflected voltage waves $a(t)$ and $b(t)$ respectively by,

$$a(t) = v(t) + R i(t) \quad (4.21a)$$

$$b(t) = v(t) - R i(t) \quad (4.21b)$$

or in the complex frequency domain,

$$A = V + RI \quad (4.22a)$$

$$B = V - RI \quad (4.22b)$$

where A , B , V and I are the complex amplitudes of the signals and R is the reference resistance, normally positive, chosen for the port.

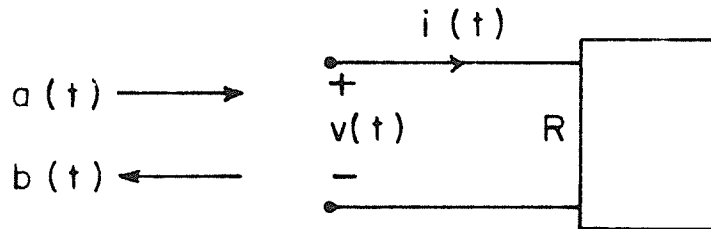


Fig. 4.6 Definition of port variables.

By using these definitions, from the Fig. 4.5 we can obtain,

for port 1,

$$A_1 = V_i + R_1 I_1 = V_1 \quad (4.23)$$

for port 2,

$$A_2 = V_2 + R_2 I_2 \quad (4.24)$$

$$B_2 = V_2 - R_2 I_2 \quad (4.25)$$

Since $V_2 = -R_2 I_2$, from (4.24) and (4.25), we have

$$A_2 = 0$$

$$B_2 = 2 V_2$$

respectively.

Substituting these into (4.24) and (4.25), we obtain,

$$W(\psi) = \frac{B_2}{A_1} \quad (4.26a)$$

$$= \frac{2 V_2}{V_1} \quad (4.26b)$$

where $W(\psi)$ is the voltage wave transfer function by definition.

Thus, from (4.19), (4.20) and (4.26), we have

$$W(\psi) = 2 H(\psi) \quad (4.27a)$$

$$= \left(\frac{R_2}{R_1} \right)^{\frac{1}{2}} t(\psi) \quad (4.27b)$$

It is important to note that the magnitude of $H(\psi)$, $t(\psi)$ and $W(\psi)$ differ by, at most, a frequency independent constant, and hence a realization

of any of these functions produces the desired frequency response.

As previously mentioned, the WDF design technique is essentially based on the analog filter configuration by applying the bilinear transformation (defined in (4.17)) directly to the circuit elements of the analog reference network and by connecting each transformed element (see Appendix II) through wave adaptors [62, 67, 74]. An alternative wave digital structure in the form of a single n-port adaptor terminated with feedback through memory has been proposed by Martens, et.al. [75, 79]. Unlike the procedure taken by Fettweis et.al., this method utilizes the voltage wave scattering matrix of the n-port consisting of the reference network interconnections which results in a wave digital n-port adaptor directly. This method is not restricted to the transformation of ladder prototypes. However, it should be noted that both approaches result in exactly the same multiplier coefficients. It is the direct transformation of the elements that differs from the conventional recursive digital filter design techniques where the transformation into the discrete-time domain is made directly on the transfer function [66, 69, 70].

4.2.2.2 Wave Adaptors

The adaptors form the main building blocks in a WDF design. Parallel adaptors serve to simulate the parallel connections and series adaptors the corresponding series connections [74]. Since the elements in a ladder structure are arranged in a series-parallel form, it is straightforward to replace them with elementary three-port series and parallel wave adaptors. These adaptors are described in detail in Appendix III.

4.2.2.3 Canonic WDF Realization

We have seen how various circuit elements (inductance, capacitance, resistance and source), and adaptors (three-port parallel and series), can be built which serve as building blocks for the wave flow diagrams to be realized. When interconnecting these building blocks, the following principle must be observed [62]:

- 1) The building blocks are interconnected port by port, i.e., the two wave terminals of one wave port are connected with the two wave terminals of precisely one other wave port.
- 2) The waves corresponding to any two wave terminals that are joined together are compatible, i.e., they flow in the same direction.
- 3) The port resistance of two wave ports that are interconnected are the same.

In earlier publications, Fettweis has introduced a cascaded unit element to satisfy the realizability condition for the resulting signal flow diagram, i.e., to satisfy the requirement that no closed loop without a delay may occur when the adaptors and elements are interconnected. Although, the unit elements introduced can be used perfectly well for improving the filtering capabilities, filters of that type do not really correspond to what are commonly considered to be true ladder filters.

This drawback has been overcome in a later publication by Sedlmeyer and Fettweis [67] by introducing the concept of a wave adaptor with a reflection free port. Also, it has been shown that by means of reflection free wave

adaptors, any LC ladder filter can very easily be transformed into a corresponding digital structure in which the number of multipliers corresponds to the number of degrees of freedom in the original LC filter.

By using the above mentioned rules and building blocks, for WDF obtained from doubly terminated LC canonic ladder networks, it can be easily shown that,

- (1) the realization is always possible with only three-port wave adaptors,
- (2) the number of three-port adaptors required is the same as the number of energy storage elements in the original LC network,
- (3) only one of those three-port adaptors used in the realization does not have a reflection free port,
- (4) the number of dependent ports is equal to the number of the three-port adaptors used, and
- (5) the number of required multipliers is equal to the number of the three-port adaptors used plus one.

Therefore, the WDF resulting from a canonic ladder network is also canonic in the sense that the number of required multipliers and the number of required wave adaptors is minimum.

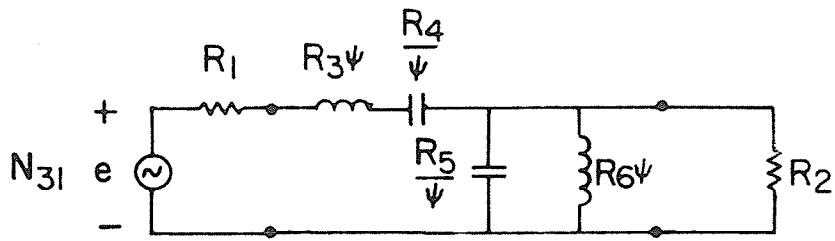
Three different structures of fourth order bandpass canonic ladder networks with their corresponding WDF realizations are shown in Figs. 4.7, 4.8 and 4.9. As can be noted in Fig. 4.7, the conventional BP network can be realized with either two four-port adaptors or four three-port adaptors, and in either case, the number of multiplier required is the same, i.e., both are canonic.

In Fig. 4.8 and 4.9, it can be seen that two WDF realizations are exactly the same except for the positions of the inverted delay elements. This is due to the LP-HP frequency transformation, i.e., the reference network N_{32} can be obtained from N_{33} by L-C interchange which in effect exchanges the role of each reactive element.

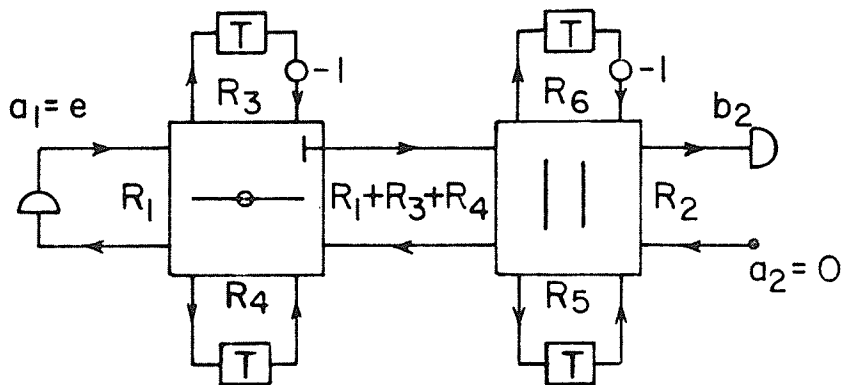
4.2.3 Sensitivity Considerations and Comparisons

Since wave digital ladder filters are designed in such a way that they imitate the behavior of doubly terminated LC ladder filters, it is possible to achieve the extremely low sensitivity characteristic with respect to parameter variations [79]. Although tolerance problems as such do not exist for digital filters in general, major problems occur due to coefficient word length limitation and roundoff or truncation noise generation [60, 61, 69, 70].

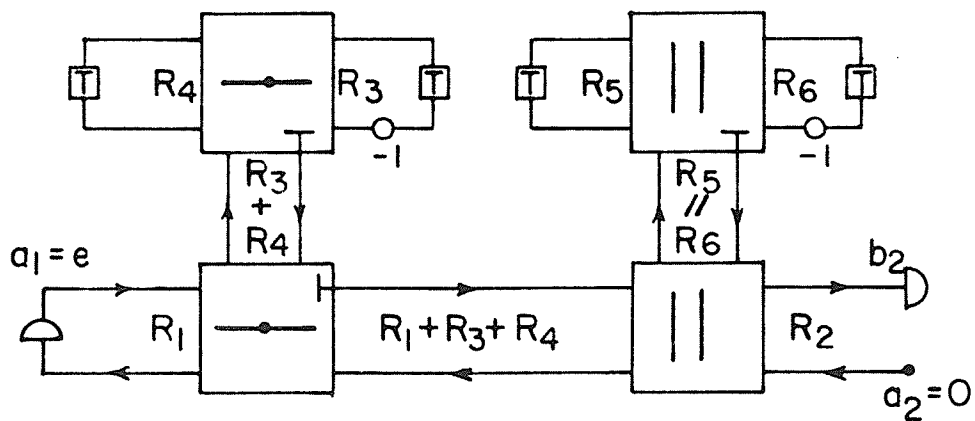
It has been shown by Fettweis [63] that for digital filters there exists a direct and an indirect connection between the generation of roundoff noise by a multiplier and the effect that the coefficient word length limitation of this multiplier has upon the response characteristic: rounding can be interpreted as coefficient fluctuation, and any design method requiring fewer digits for the multipliers makes it possible to increase the signal word lengths without an increase in overall complexity. It confirms why digital filters with reduced attenuation sensitivity, such as ladder WDF, also produce less roundoff noise. Subsequently, Fettweis has proved the stability property of the WDF's in a direct way, i.e., without being inferred from certain analogies with analog filters [65].



(a)



(b)



(c)

Fig. 4.7 (a) Fourth order canonic bandpass filter
 (b) Corresponding wave digital filter using two four-port wave adaptors
 (c) Corresponding wave digital filter using four three-port wave adaptors.

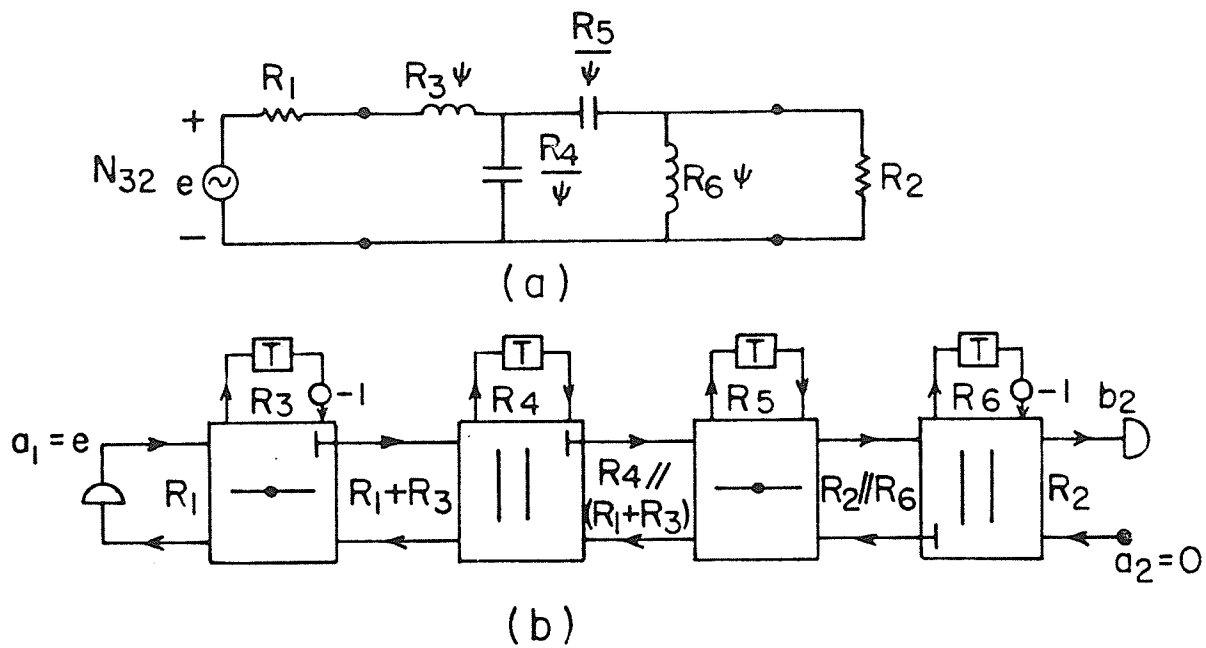


Fig. 4.8 (a) Fourth order canonic bandpass filter
(b) Corresponding wave digital filter.

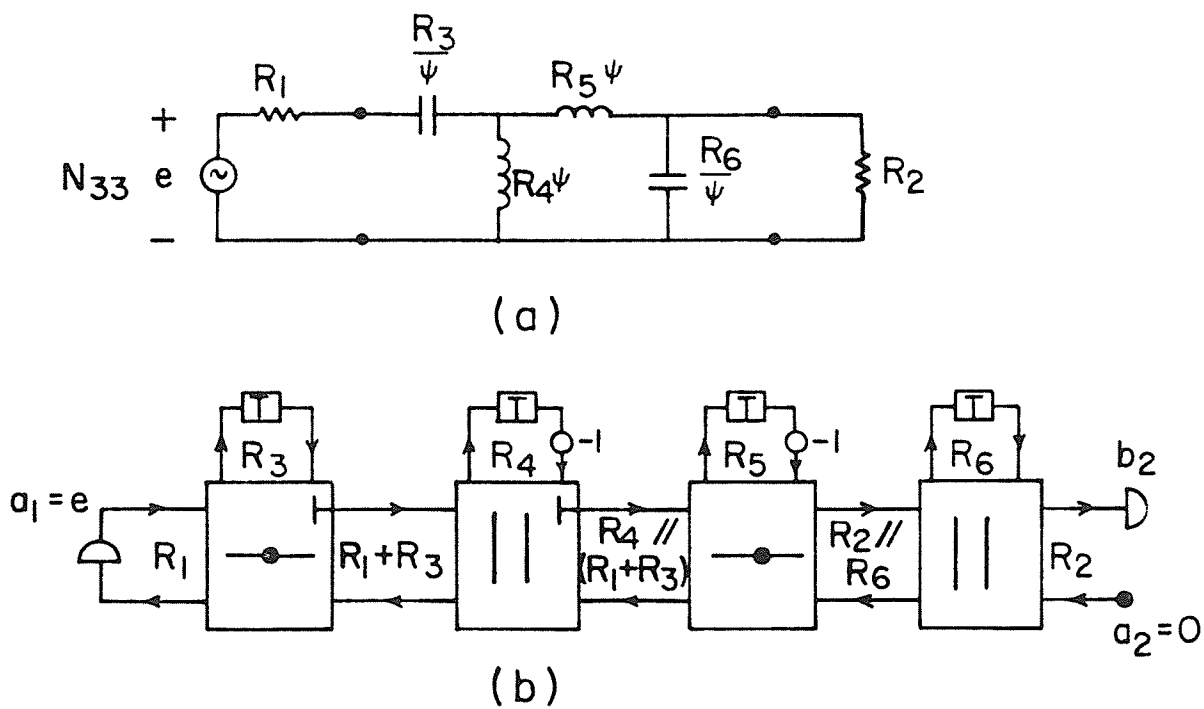


Fig. 4.9 (a) Fourth order canonic bandpass filter
(b) Corresponding wave digital filter.

Furthermore, using simple arithmetic operation Fettweis and Meerkötter have been able to guarantee the absence of parasitic nonlinear oscillations, such as, limit cycle oscillations and overflow oscillations in the WDF structures for which all port resistances are positive [72].

It appears then that in WDF realizations, the sensitivity with respect to variations of the multiplier coefficients is the most important design criteria. We have shown in Chapter III that the non-conventional canonic BP ladder networks tend to have better sensitivity performance. As expected, this tendency is consistent with WDF realizations [80].

To compare the sensitivity characteristics of WDF directly derived from the doubly terminated canonic ladder filters, a new analysis method is given below.

From WDF realizations such as shown in Fig. 4.7, 4.8, 4.9, it is straightforward to obtain multiplier coefficients in terms of element values. Let us consider a reference network with n elements in it, say, R_i . By taking ratios of element values, say $\rho_i = \frac{R_i}{R_j}$ ($i \neq j$), we can always reduce the degree of freedom by one.

For convenience, let us normalize the element values with respect to R_1 , i.e., $\rho_i = \frac{R_{i+1}}{R_1}$ ($i \leq n-1$), then the transfer function can be written as

$$H(\psi) = H(\psi, \rho_1, \rho_2, \dots, \rho_{n-1}) \quad (4.28)$$

to show the explicit dependence on the ρ_i .

Recalling the fact that in the canonic realization the number of multiplier coefficients required is $(n-1)$, let us designate multiplier

coefficients as α_k , $k = 1, 2, 3, \dots, n-1$. Then each α_k is a function of element values R_i . Thus, it is always possible to represent ρ_i as a function of α_k , i.e.,

$$\rho_i = \rho_i(\alpha_1, \alpha_2, \alpha_3, \dots, \alpha_{n-1}), \quad i = 1, 2, \dots, n-1. \quad (4.29)$$

Now, suppose that the functions in (4.29) have partial derivatives $\frac{\partial \rho_i}{\partial \alpha_k}$ with respect to each variable α_k , then on fixing in (4.29) all variables except α_k , we obtain a composite function $H(\psi)$ of just one variable α_k . Thus, the derivative of $H(\psi)$ with respect to α_k can be computed by the chain rule, and we obtain,

$$\begin{aligned} \frac{\partial H}{\partial \alpha_k} &= \frac{\partial H}{\partial \rho_1} \cdot \frac{\partial \rho_1}{\partial \alpha_k} + \frac{\partial H}{\partial \rho_2} \cdot \frac{\partial \rho_2}{\partial \alpha_k} + \dots + \frac{\partial H}{\partial \rho_{n-1}} \cdot \frac{\partial \rho_{n-1}}{\partial \alpha_k} \\ &= \sum_{i=1}^{n-1} \frac{\partial H}{\partial \rho_i} \cdot \frac{\partial \rho_i}{\partial \alpha_k}. \end{aligned} \quad (4.30)$$

This is valid whenever $H(\psi)$ is differentiable and the derivatives $\frac{\partial \rho_i}{\partial \alpha_k}$ exist, which is true in our case.

The sensitivity function of $H(\psi)$ with respect to α_k is by definition,

$$S_{\alpha_k}^{H(\psi)} \triangleq \frac{\alpha_k}{H} \cdot \frac{\partial H}{\partial \alpha_k}. \quad (4.31)$$

Substituting (4.28) into (4.31) we have

$$\begin{aligned}
 S_{\alpha_k}^H &= \frac{\alpha_k}{H} \cdot \sum_{i=1}^{n-1} \frac{\partial H}{\partial \rho_i} \cdot \frac{\partial \rho_i}{\partial \alpha_k} \\
 &= \sum_{i=1}^{n-1} \frac{\alpha_k}{H} \cdot \frac{\partial H}{\partial \rho_i} \cdot \frac{\partial \rho_i}{\partial \alpha_k} .
 \end{aligned} \tag{4.32}$$

By manipulating (4.32), and from the definition of sensitivity function, we obtain

$$\begin{aligned}
 S_{\alpha_k}^H &= \sum_{i=1}^{n-1} \frac{\rho_i}{H} \cdot \frac{\partial H}{\partial \rho_i} \cdot \frac{\alpha_k}{\rho_i} \cdot \frac{\partial \rho_i}{\partial \alpha_k} \\
 &= \sum_{i=1}^{n-1} S_{\rho_i}^H \cdot S_{\alpha_k}^{\rho_i} .
 \end{aligned} \tag{4.33}$$

That is, the transfer function sensitivity with respect to multiplier coefficient α_k can be represented as a multiplication of two sensitivity functions, $S_{\rho_i}^{H(\psi)}$ and $S_{\alpha_k}^{\rho_i}$, summed over the number of normalized elements in the network. This can be represented conveniently in a matrix form as below.

$$\begin{bmatrix} S_{\alpha_1}^H \\ S_{\alpha_2}^H \\ \vdots \\ S_{\alpha_{n-1}}^H \end{bmatrix} = \begin{bmatrix} S_{\alpha_1}^{\rho_1} & S_{\alpha_1}^{\rho_2} & \dots & S_{\alpha_1}^{\rho_{n-1}} \\ S_{\alpha_2}^{\rho_1} & S_{\alpha_2}^{\rho_2} & \dots & S_{\alpha_2}^{\rho_{n-1}} \\ \vdots & \vdots & & \vdots \\ S_{\alpha_{n-1}}^{\rho_1} & S_{\alpha_{n-1}}^{\rho_2} & & S_{\alpha_{n-1}}^{\rho_{n-1}} \end{bmatrix} \begin{bmatrix} S_{\rho_1}^H \\ S_{\rho_2}^H \\ \vdots \\ S_{\rho_{n-1}}^H \end{bmatrix} . \tag{4.34}$$

Using this analysis method, the WDF realization of two equivalent reference networks, N_{31} and N_{33} , in Table 3.4 has been examined. Figs. 4.10(a) and 4.10(b) show the magnitude sensitivities of the transfer functions with respect to multiplier coefficients in the passband as a function of digital frequency. It can be noted that the non-conventional reference network yields much better characteristics. In particular, we note that the sensitivity curves in Fig. 4.10(b) in contrast to those in Fig. 4.10(a) are almost constant across the passband and hence multiplier quantization will have little effect on the shape of the frequency response producing only a change in gain. This is confirmed by Fettweis' [68] observation with respect to multiplier coefficients.

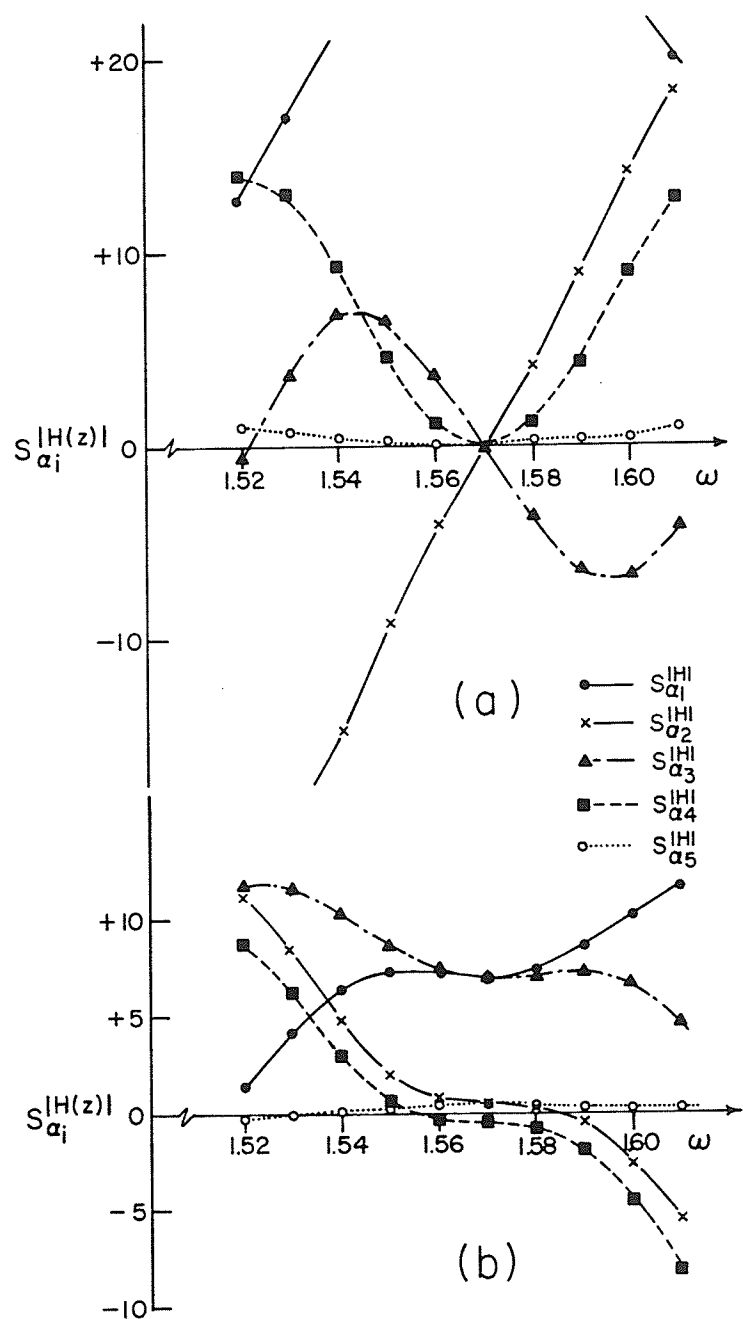


Fig. 4.10 Magnitude sensitivity with respect to multiplier coefficients; (a) for N_{31} , (b) for N_{33} .

CHAPTER V

CONCLUSION

A novel approach, based on the removal sequences of the transmission zeros, has been taken to generate all equivalent networks in canonic ladder configurations. Theorems have been developed to generate independent sequences of transmission zero removal, and the unique relationship between the independent sequences and the equivalent canonic networks has been demonstrated by means of six basic sections which are responsible for the removal of pairs of transmission zeros. A new straightforward procedure has been developed that synthesizes the two-element-kind driving-point immittance functions in all possible ladder configurations using a minimum number of elements.

The procedure has been applied to the realization of singly terminated, equivalent, canonic ladder networks. A closed form formula has been advanced, which determined the exact number of equivalent canonic ladder networks for a given bandpass type transfer function. An illustrative example is provided to compare all equivalent networks with respect to certain specified design criteria. A possible cost minimization scheme has also been suggested. A method of deriving the doubly terminated equivalent canonic networks directly from singly terminated networks has been developed. Using duality, it is shown that the total number of doubly terminated canonic ladder networks, is twice the number of singly terminated networks. A proof has been given regarding the completeness of the set of equivalent canonic networks. Equivalent networks are compared with particular emphasis on the transfer

function magnitude sensitivity with respect to variations of element values. An illustrative example is provided using a maximally flat fourth order bandpass filter. In general, it has been shown that the newly generated non-conventional networks require lower ΣL and render better sensitivity performance. It has been pointed out, that for realizability, the value of the terminating resistance is subject to certain constraints. These constraints are illustrated for the cases of maximally flat fourth and sixth order bandpass functions respectively.

Subsequently, these doubly terminated canonic ladder networks are used as reference prototypes for conversion into a corresponding set of RC active filters and a set of digital filters. They are all in canonic ladder structure, and retain all the excellent features of the reference networks. For the RC active filters, the component simulation technique, that utilizes a ladder embedding technique of optimum GICs, is studied, and an example of three equivalent realizations for the given function is presented. In digital filter realization, a wave digital filter concept is adopted, and only three-port, series and parallel adaptors are utilized. It has been shown, that all the reference canonic networks result in canonic wave digital filters, in the sense of a minimum number of multiplier as well as adaptors. To compare the transfer function magnitude sensitivities with respect to variations of the multiplier coefficients, a new analysis method is proposed. Three canonic wave digital filters obtained from three reference canonic networks of order four are compared, based on this method. As expected, the wave digital filter obtained from the non-conventional reference network exhibits better performance than the conventional counterpart.

The new canonic reference networks discovered in this study, having ladder structures, may also serve as the prototype in the design of precision monolithic high-order filters [81, 82] using MOS switched capacitor techniques.

APPENDIX I

Element values in terms of the 6th order BP transfer function,

$$H(s) = \frac{K s^3}{s^6 + a_1 s^5 + a_2 s^4 + a_3 s^3 + a_2 s^2 + a_1 s + 1} .$$

Table 1 Gain Values

Network	Values of K
N_1	$a_3 - a_1$
N_2	$\frac{(a_3 - a_1)(a_1 a_2 - a_3 - a_1)}{a_1 a_2 - a_3}$
N_3	$a_3 - a_1$
N_4	$\frac{(a_3 - a_1)(a_1 a_2 - a_3 - a_1)}{a_1 a_2 - a_3}$
N_5	$\frac{(a_3 - 2a_1)(a_1 a_2 - a_3 - a_1)}{a_1 a_2 - a_3}$
N_6	$\frac{(a_3 - a_2^2)(a_1 a_2 - a_3 - a_1)}{a_1 a_2 - a_3}$
N_7	$a_3 - 2a_1$

Table 2. Inductance Values

Network	L_1	L_2	L_3	ΣL_i
N_1	$\frac{1}{a_1}$	$\frac{a_1 a_2 - a_3 - a_1}{a_1^2}$	$\frac{(a_3 - 2a_1)(a_1 a_2 - a_3 - a_1)}{a_1(a_3 - a_1)^2}$	$\frac{a_1 a_3^2 + 2a_1^3 - a_3^3 + a_1 a_2 a_3^2 - a_1^2 a_2 a_3 - a_1^3}{a_1^2(a_3 - a_1)^2}$
N_2	$\frac{a_1 a_2 - a_3}{a_1^2}$	$\frac{a_1 a_2 - a_3}{a_1(a_1 a_2 - a_3 - a_1)}$	$\frac{(a_1 a_2 - a_3)^2(a_3 - 2a_1)}{a_1(a_3 - a_1)^2(a_1 a_2 - a_3 - a_1)}$	$\frac{(a_1 a_2 - a_3)^2(a_3^2 - a_1 a_2 - a_1^2)}{a_1^2(a_3 - a_1)^2(a_1 a_2 - a_3 - a_1)}$
N_3	$\frac{1}{a_1}$	$\frac{a_1 a_2 - a_3 - a_1}{a_1(a_3 - a_1)}$	$\frac{(a_3 - 2a_1)(a_1 a_2 - a_3 - a_1)}{a_1^2(a_3 - a_1)}$	$\frac{a_1 a_2 - a_3}{a_1^2}$
N_4	$\frac{1}{a_1}$	$\frac{(a_1 a_2 - a_3)^2}{a_1(a_3 - a_1)(a_1 a_2 - a_3 - a_1)}$	$\frac{(a_1 a_2 - a_3)^2}{a_1^2(a_3 - a_1)(a_1 a_2 - a_3 - a_1)}$	$\frac{a_1^2 a_2^2 + a_1^2 a_2 - a_1^2 - a_1 a_3 - 2a_1 a_2 a_3 + a_3^2}{a_1^2(a_1 a_2 - a_3 - a_1)}$
N_5	$\frac{a_1 a_2 - a_3}{a_1^2}$	$\frac{a_1 a_2 - a_3}{a_1(a_1 a_2 - a_3 - a_1)}$	$\frac{(a_1 a_2 - a_3)^2}{a_1(a_3 - 2a_1)(a_1 a_2 - a_3 - a_1)}$	$\frac{(a_1 a_2 - a_3)^2(a_2 - a_1)}{a_1^2(a_3 - 2a_1)(a_1 a_2 - a_3 - a_1)}$
N_6	$\frac{1}{a_1}$	$\frac{(a_1 a_2 - a_3)^2}{a_1(a_3 - 2a_1)(a_1 a_2 - a_3 - a_1)}$	$\frac{(a_1 a_2 - a_3)^2}{a_1(a_3 - 2a_1)(a_1 a_2 - a_3 - a_1)}$	$\frac{1}{a_1} + \frac{(a_3 - a_1)(a_2 a_1 - a_3)^2}{a_1^2(a_3 - 2a_1)(a_1 a_2 - a_3 - a_1)}$
N_7	$\frac{1}{a_1}$	$\frac{a_1 a_2 - a_3 - a_1}{a_1^2}$	$\frac{a_1 a_2 - a_3 - a_1}{a_1(a_3 - 2a_1)}$	$\frac{a_1 a_2 a_3 - a_3^2 - a_1^2 a_2 + a_1 a_3 - a_1^2}{a_1^2(a_3 - 2a_1)}$

Table 3. Capacitance Values

Network	C_1	C_2	C_3	ΣC_i
N_1	a_1	$\frac{a_1(a_3-a_1)}{a_1a_2-a_3-a_1}$	$\frac{a_1^2(a_3-a_1)}{(a_3-2a_1)(a_1a_2-a_3-a_1)}$	$\frac{a_1^2(a_2a_3-a_3-2a_1a_2+3a_1)}{(a_3-2a_1)(a_1a_2-a_3-a_1)}$
N_2	a_1	$\frac{a_1(a_3-a_1)(a_1a_2-a_3-a_1)}{(a_1a_2-a_3)^2}$	$\frac{a_1^2(a_3-a_1)(a_1a_2-a_3-a_1)}{(a_3-2a_1)(a_1a_2-a_3)^2}$	$\frac{a_1+a_1(a_3-a_1)^2(a_1a_2-a_3-a_1)}{(a_3-2a_1)(a_1a_2-a_3)^2}$
N_3	a_1	$\frac{a_1^2}{a_1a_2-a_3-a_1}$	$\frac{a_1(a_3-a_1)^2}{(a_1a_2-a_3-a_1)(a_3-2a_1)}$	$\frac{a_1^2(a_2a_3-2a_1a_2+a_1)}{(a_1a_2-a_3-a_1)(a_3-2a_1)}$
N_4	$\frac{a_1^2}{a_1a_2-a_3}$	$\frac{a_1(a_1a_2-a_3-a_1)}{a_1a_2-a_3}$	$\frac{a_1(a_3-a_1)^2(a_1a_2-a_3-a_1)}{(a_3-2a_1)(a_1a_2-a_3)^2}$	$\frac{a_1+a_1(a_3-a_1)^2(a_1a_2-a_3-a_1)}{(a_3-2a_1)(a_1a_2-a_3-a_1)}$
N_5	a_1	$\frac{a_1(a_1a_2-a_3-a_1)}{(a_1a_2-a_3)^2}$	$\frac{a_1(a_3-2a_1)(a_1a_2-a_3-a_1)}{(a_1a_2-a_3)^2}$	$\frac{a_1^2(a_1a_2^2+a_1-a_2a_3-a_1a_2)}{(a_1a_2-a_3)^2}$
N_6	$\frac{a_1^2}{a_1a_2-a_3}$	$\frac{a_1(a_1a_2-a_3-a_1)}{a_1a_2-a_3}$	$\frac{a_1(a_3-2a_1)(a_1a_2-a_3-a_1)}{(a_1a_2-a_3)^2}$	$\frac{a_1^2(a_1a_2^2-a_2a_3+a_3-2a_1a_2+2a_1)}{(a_1a_2-a_3)^2}$
N_7	a_1	$\frac{a_1^2}{a_1a_2-a_3-a_1}$	$\frac{a_1(a_3-2a_1)}{a_1a_2-a_3-a_1}$	$\frac{a_1^2(a_2-2)}{a_1a_2-a_3-a_1}$

APPENDIX II

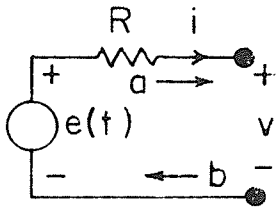
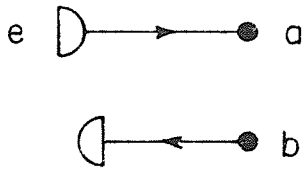
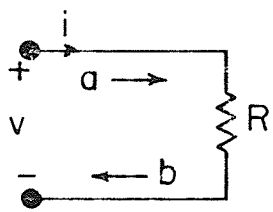
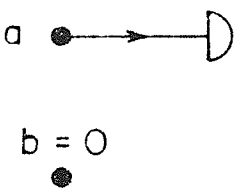
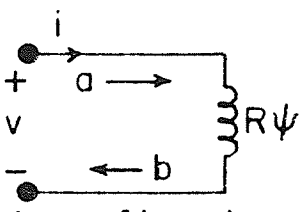
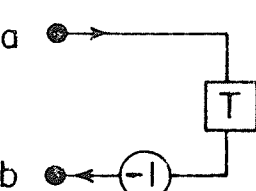
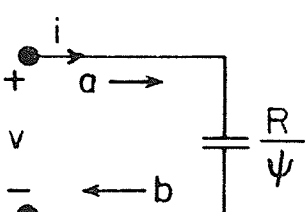
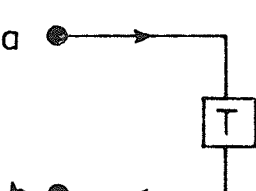
Wave Flow Diagrams of Basic Circuit Elements

This appendix presents the wave flow diagrams of some basic circuit elements as derived by Fettweis upon applying directly the bilinear transformation to these elements. For a given port with associated references for the voltage $v(t)$ and the current $i(t)$, the instantaneous incident wave $a(t)$ and the reflected wave $b(t)$ are defined as follows;

$$a(t) = v(t) + R i(t)$$

$$b(t) = v(t) - R i(t)$$

where R is the reference resistance constant, normally positive, chosen for the port. The following table gives the wave flow diagrams of such basic elements as a resistive source, a resistance, an inductance and a capacitance together with the difference equations which result from the wave digital realization.

ELEMENT	WAVE FLOW DIAGRAM	DIFFERENCE EQUATION
 <p>Resistive source</p>		$a(t) = e(t)$
 <p>Resistance R</p>		$b(t) = 0$
 <p>Inductance of impedance $R\psi$</p>		$b(t) = -a(t-T)$
 <p>Capacitance of impedance R/ψ</p>		$b(t) = a(t-T)$

APPENDIX III

Wave Adaptors

This appendix presents the description of elementary three-port wave adaptors that are required for the WDF realization of the canonic LC ladder reference networks.

(1) Three-port Parallel Adaptor

Consider three ports with port resistances R_1 , R_2 , and R_3 , respectively, and assume these three ports are connected in parallel as shown in Fig. A.1(a).

The incident waves a_n and reflected waves b_n are related to the voltage v_n and current i_n by

$$\begin{aligned} a_n &= v_n + R_n i_n & b_n &= v_n - R_n i_n \\ n &= 1, 2, 3. \end{aligned} \quad (\text{A.1})$$

From the equalities $v_1 = v_2 = v_3$ and $i_1 + i_2 + i_3 = 0$, we obtain the adaptor equations

$$b_n = (\alpha_1 a_1 + \alpha_2 a_2 + \alpha_3 a_3) - a_n \quad (\text{A.2})$$

where

$$\alpha_n = \frac{2 G_n}{G_1 + G_2 + G_3}, \quad G_n = \frac{1}{R_n} \quad (\text{A.3})$$

$$\alpha_1 + \alpha_2 + \alpha_3 = 2. \quad (\text{A.4})$$

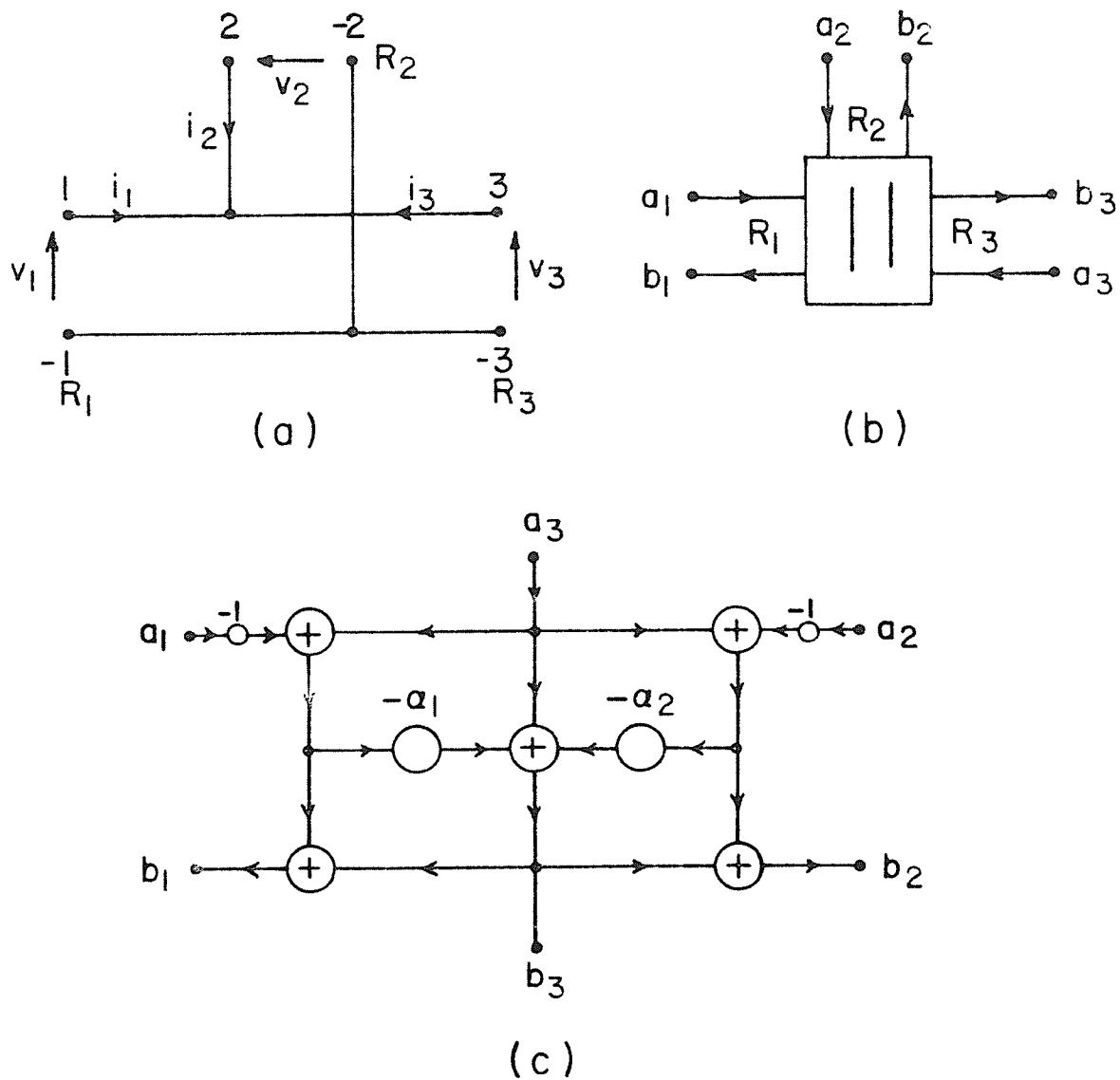


Fig. A.1 (a) Parallel connection of three ports
 (b) Corresponding adaptor
 (c) Signal flow diagram corresponding to this adaptor with port 2 chosen as dependent port.

By making use of (A.4), the coefficient α_n of one of the ports, called the dependent port, can be eliminated. By choosing port 3 as dependent port, i.e., $\alpha_3 = 2 - (\alpha_1 + \alpha_2)$, (A.2) can be rewritten as

$$\begin{aligned} b_1 &= b_3 + (a_3 - a_1) \\ b_2 &= b_3 + (a_3 - a_2) \\ b_3 &= a_3 - \alpha_1 (a_3 - a_1) - \alpha_2 (a_3 - a_2) . \end{aligned} \tag{A.5}$$

Fig. A.1(b) is a symbol of three-port parallel adaptor and Fig. A.1(c) represents a signal flow diagram of three-port adaptor with port 3 being a dependent port. As can be seen, this adaptor requires two multipliers and has six adders since one of the five adders has three inputs. Of particular interest are parallel adaptors for which one of the ports, say port 3, is reflection free. In this case we must have,

$$\begin{aligned} \alpha_3 &= 1 \\ \text{i.e.} \quad G_3 &= G_1 + G_2 . \end{aligned} \tag{A.6}$$

Therefore, we have

$$\alpha_1 + \alpha_2 = 1 \tag{A.7}$$

$$\alpha_1 = \frac{G_1}{G_3} , \quad \alpha_2 = \frac{G_2}{G_3} . \tag{A.8}$$

Then, by choosing port 2 as the dependent port, i.e., $\alpha_2 = 1 - \alpha_1$, we have

$$b_1 = b_2 + (a_2 - a_1)$$

$$b_2 = b_0 + a_3$$

$$b_3 = b_0 + a_2$$

where

$$b_0 = -\alpha_1 (a_2 - a_1) .$$

Note that the output wave b_3 is independent of the input wave a_3 .

Fig. A.2(a) is a symbol of three-port parallel adaptor with the port 3 reflection free and the port 2 being the dependent port, and Fig. A.2(b) is

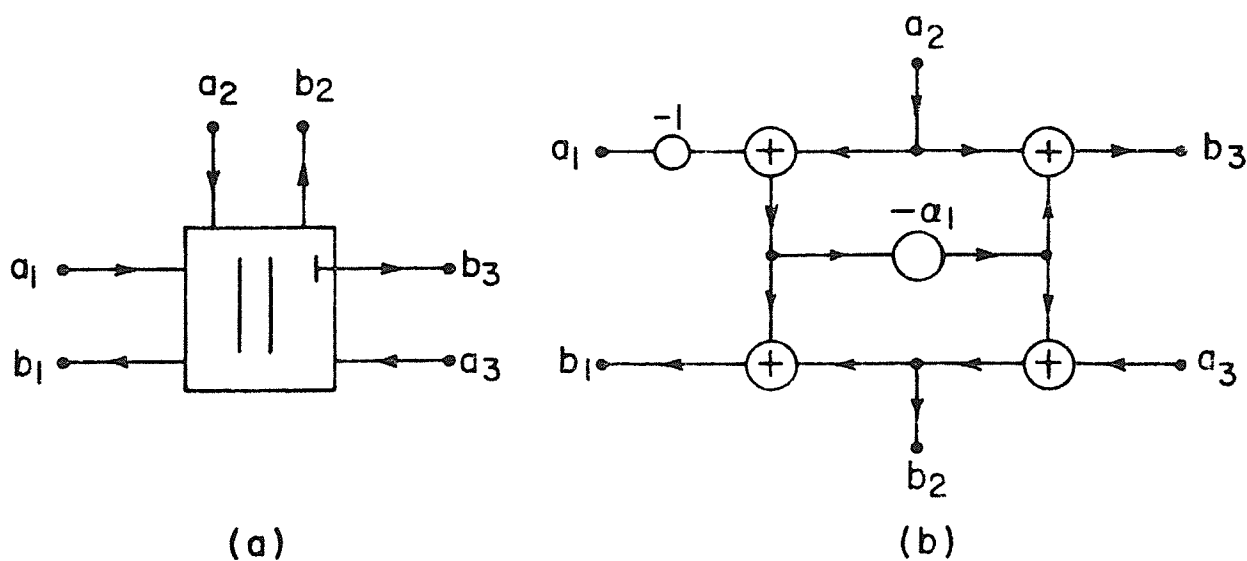


Fig. A.2 (a) Three-port parallel adaptor with port 3 reflection free, and port 2 being dependent
(b) Signal flow diagram corresponding to this adaptor.

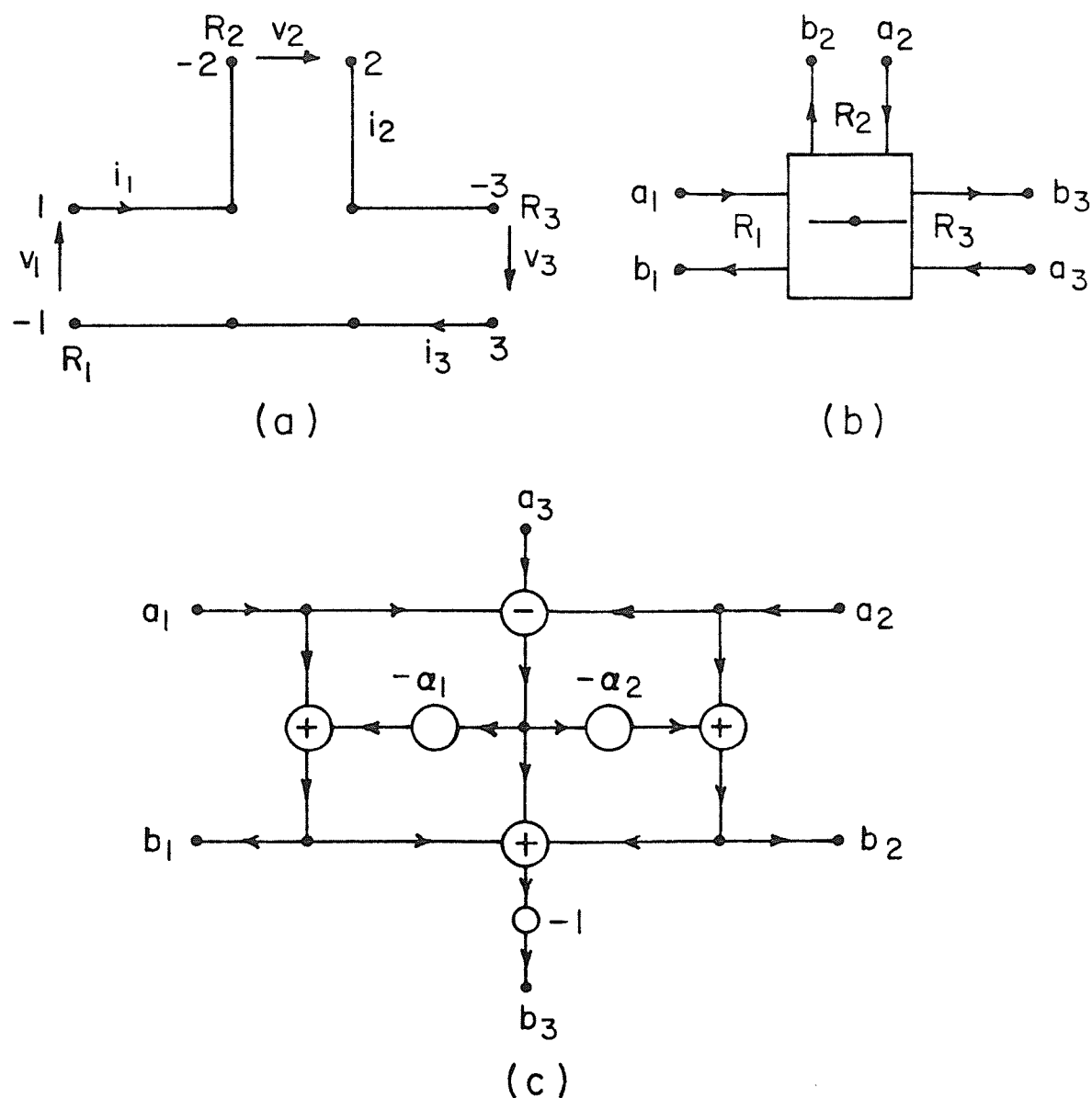


Fig. A.3 (a) Series connection of three ports
 (b) Corresponding three-port series adaptor
 (c) Signal flow diagram corresponding to this adaptor with port 2 chosen as dependent port.

the signal flow diagram of the corresponding adaptor. This adaptor requires only one multiplier and four adders.

(2) Three-port Series Adaptor

Consider three ports with port resistances R_1 , R_2 , and R_3 , respectively, and assume these three ports are connected in series as shown in Fig. A.3(a). The incident and reflected waves are again given by (A.1). However, in this case, from the equalities $i_1 = i_2 = i_3$ and $v_1 + v_2 + v_3 = 0$, we obtained different adaptor equations as follows:

$$b_n = a_n - \alpha_n (a_1 + a_2 + a_3) \quad (\text{A.9})$$

where

$$\alpha_n = \frac{2 R_n}{R_1 + R_2 + R_3} \quad (\text{A.10})$$

with (A.4) still holding.

The dependent port is again that port for which the corresponding α_n is eliminated by means of (A.4). Fig. A.3(b) is the symbol for a three-port series adaptor and Fig. A.3(c) is a signal flow diagram of the three-port adaptor with port 3 being the dependent port. This adaptor requires two multipliers and six adders since two of the four adders have three inputs.

Of particular interest are series adaptors for which one of the ports, say port 3, is reflection free. In this case, we must have,

$$\alpha_3 = 1 \quad (\text{A.11})$$

i.e.

$$R_3 = R_1 + R_2 \quad (\text{A.12})$$

Thus, we have

$$\alpha_1 + \alpha_2 = 1 \quad (\text{A.13})$$

$$\alpha_1 = \frac{R_1}{R_3}, \quad \alpha_2 = \frac{R_2}{R_3} \quad (\text{A.14})$$

Then, by choosing port 2 as the dependent port,

i.e., $\alpha_2 = 1 - \alpha_1$, we have

$$b_1 = a_1 - \alpha_1 (a_1 + a_2 + a_3)$$

$$b_2 = - (a_3 + b_1)$$

$$b_3 = - (a_1 + a_2) \quad .$$

Note that the output wave b_3 is independent of the input wave a_3 .

The symbol for the three-port series adaptor with port 3 reflection free is shown in Fig. A.4(a), and Fig. A.4(b) is the signal flow diagram of the corresponding adaptor with port 2 chosen as the dependent port. Again, this adaptor requires only one multiplier and four adders.

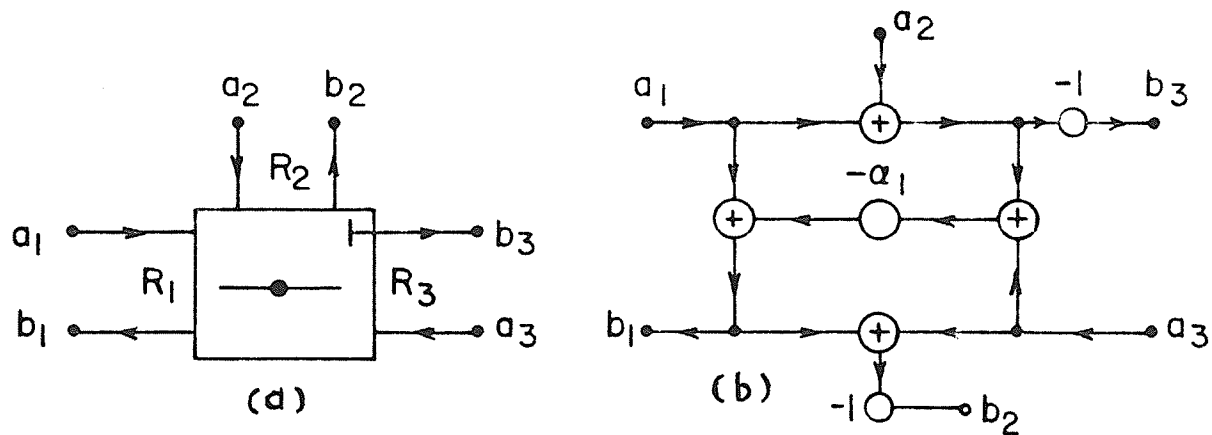


Fig.A.4 (a) Series adaptor with port 3 reflection free, port 2 being dependent
(b) Signal flow diagram corresponding to this adaptor.

REFERENCES

- [1] M.E. Van Valkenburg, Introduction to Modern Network Synthesis, New York: John Wiley & Sons, Inc., 1962.
- [2] L. Weinberg, Network Analysis and Synthesis, New York: McGraw-Hill Book Co., 1962.
- [3] G.C. Temes and S.K. Mitra, Modern Filter Theory and Design, New York: John Wiley & Sons, Inc., 1973.
- [4] A. Budak, Passive and Active Network Analysis and Synthesis, Boston: Houghton Mifflin Co., 1974.
- [5] D.E. Johnson, Introduction to Filter Theory, New Jersey: Prentice-Hall, Inc., 1976.
- [6] A.S. Sedra, P.O. Brackett, Filter Theory: Active and Passive, Champaign: Matrix Publishers, Inc., 1978.
- [7] H.Y-F. Lam, Analog and Digital Filters: Design and Realization, New Jersey: Prentice-Hall, Inc., 1979.
- [8] H.B. Lee, "A new canonic realization procedure," IEEE Trans. Circuit Theory, CT-10, pp. 81-85, 1963.
- [9] _____, "An additional realization cycle for LC impedance," IEEE Trans. Circuit Theory, CT-12, pp. 435-437, 1965.
- [10] V. Ramachandran and M.N.S. Swamy, "A new canonic realization of lossless immittance functions using six element sections," Circuit Theory and Applications, vol. 4, pp. 43-53, 1976.
- [11] S. Darlington, "Synthesis of reactance 4-poles which produce prescribed insertion loss characteristics," J. Math. Phys., vol. 18, pp. 257-353, Sept. 1939.
- [12] A.D. Fialkow and I. Gerst, "The transfer function of general two terminal-pair RC networks," Quart. Appl. Math., vol. 10, pp. 113-127, 1952.
- [13] F.J. MacWilliams, "An iterative method for the direct Hurwitz factorization of a polynomial," IRE Trans. Circuit Theory, pp. 347-352, Dec. 1958.
- [14] H. Watanabe, "Synthesis of band-pass ladder network," IRE Trans. Circuit Theory, pp. 256-264, Dec. 1958.

- [15] R. Saal and E. Ulbrich, "On the design of filters by synthesis," IRE Trans. Circuit Theory, vol. CT-5, pp. 284-327, Dec. 1958.
- [16] J.L. Herreo and G. Willoner, Synthesis of Filters, New Jersey: Prentice-Hall, Inc., 1966.
- [17] N. Ming, "Simultaneous realization of the transfer and reflection factors of two-ports and n-ports," IEEE Trans. Circuit Theory, vol. CT-15, Dec. 1968.
- [18] H.J. Orchard and G.C. Temes, "Filter design using transformed variables," IEEE Trans. Circuit Theory, CT-15, pp. 385-408, Dec. 1968.
- [19] J.K. Skwirzynski, "On synthesis of filters," IEEE Trans. Circuit Theory, vol. CT-18, pp. 152-163, Jan. 1971.
- [20] H.K. Kim and A. Ali, "Cost function minimization in RC ladder networks," IEEE Trans. on Circuits and Systems, vol. CAS-23, pp. 39-45, Jan. 1976.
- [21] W. Chan, "Explicit formulas for the synthesis of optimum broad-band impedance-matching networks," IEEE Trans. Circuits and Systems, vol. CAS-24, April 1977.
- [22] K.J. Khatwani and R.K. Tiwari, "On lossless bandpass ladder networks," IEEE Trans. Circuits and Systems, vol. CAS-25, Oct. 1978.
- [23] H.K. Kim, "A formula for equivalent bandpass networks and their comparison," IEEE Proc., pp. 678-680, April 1979.
- [24] H.J. Orchard, "Inductorless filters," Electronics Letters, vol. 2, no. 6, pp. 224-225, June 1966.
- [25] M.L. Blostein, "Sensitivity analysis of parasitic effects in resistance terminated LC two-ports," IEEE Trans. Circuit Theory, pp. 21-25, March 1967.
- [26] G. Martinelli and M. Poggelli, "Bounds on magnitude of sensitivity to variation of component values of passive transfer voltage ratios," Electron. Lett., vol. 4, pp. 98-99, March 1968.
- [27] G.C. Temes and H.J. Orchard, "First order sensitivity and worst case analysis of doubly terminated reactance two-ports," IEEE Trans. Circuit Theory, vol. CT-20, no. 5, pp. 567-571, Sept. 1973.
- [28] L. Weyten, "Lower bounds on the summed absolute and squared voltage transfer sensitivities in RLC networks," IEEE Trans. Circuits and Systems, vol. CAS-25, no. 2, pp. 70-73, Feb. 1978.

- [29] J. Tow, "Comments on 'Lower bounds on the....'," IEEE Trans. Circuits and Systems, vol. CAS-26, no. 3, pp. 209-211, March 1979.
- [30] H.J. Orchard, "Loss sensitivities in singly and doubly terminated filters," IEEE Trans. Circuits and Systems, vol. CAS-26, no. 5, pp. 293-297, May 1979.
- [31] D.F. Sheahan and H.J. Orchard, "Bandpass realization using gyrators," Electron. Lett., vol. 3, no. 1, pp. 40-41, Jan. 1967.
- [32] R.H.S. Riordan, "Simulated inductors using differential amplifiers," Electron. Lett., vol. 3, no. 2, pp. 50-51, Feb. 1967.
- [33] G.J. Deboo, "Applications of a gyrator-type circuit to realize ungrounded inductors," IEEE Trans. Circuit Theory, CT-14, pp. 101-102, March 1967.
- [34] A. Antoniou, "Gyrators using op. amplifiers," Electron. Lett., vol. 3, pp. 350-352, Aug. 1967.
- [35] J. Gorski-Popiel, "RC active synthesis using positive immittance convertors," Electron. Lett., vol. 3, pp. 381-382, Aug. 1967.
- [36] L.T. Bruton, "Frequency selectivity using positive impedance converter-type networks," Proc. IEEE, vol. 56, pp. 1378-1379, Aug. 1968.
- [37] S.K. Mitra, Analysis and Synthesis of Linear Active Networks, New York: John Wiley & Sons, Inc., 1969.
- [38] L.T. Bruton, "Network transfer functions using the concept of frequency dependent negative resistance," IEEE Trans. Circuit Theory, vol. CT-16, pp. 406-408, Aug. 1969.
- [39] A. Antoniou, "Realization of gyrators using op. amplifiers and their use in RC active network synthesis," Proc. IEE, vol. 116, no. 11, pp. 1838-1850, Nov. 1969.
- [40] G.S. Moschytz, "Inductorless filters: A survey I. Electromechanical filters, II. Linear active and digital filters," IEEE Spectrum, vol. 7, no. 8, pp. 30-36 and no. 9, pp. 63-75, 1970.
- [41] P.R. Geffe, "Toward high stability in active filters," IEEE Spectrum, vol. 7, pp. 63-66, May 1970.
- [42] H.J. Orchard and D.F. Sheahan, "Inductorless bandpass filter," IEEE J. of Solid State Circuits, vol. SC-5, pp. 108-118, June 1970.
- [43] L.T. Bruton, "Nonideal performance of two amplifier positive-impedance converters," IEEE Trans. Circuit Theory, vol. CT-17, no. 4, pp. 541-549, Nov. 1970.

- [44] L.C. Thomas, "The biquad: Part I-Some practical design considerations," IEEE Trans. Circuit Theory, vol. CT-18, pp. 350-357, May 1971.
- [45] L.C. Thomas, "The biquad: Part II-A multipurpose active filtering system," IEEE Trans. Circuit Theory, vol. CT-18, pp. 358-361, May 1971.
- [46] G.S. Moschytz, "Gain-sensitivity product - A figure of merit for hybrid-integrated filters using op. amplifiers," IEEE J. of Solid State Circuits, vol. SC-6, no. 3, pp. 103-110, June 1971.
- [47] M.A. Soderstrand and S.K. Mitra, "Gain and sensitivity limitations of active RC filters," IEEE Trans. Circuit Theory, vol. CT-18, no. 6, Nov. 1971.
- [48] L.T. Bruton and A.B. Haase, "Sensitivity of generalized immittance converter-embedded ladder structures," IEEE Trans. Circuits and Systems, vol. CAS-21, no. 2, pp. 245-250, March 1974.
- [49] H.K. Kim and E. Kim, "An approach to the continuous decomposition of second-order polynomials," IEEE Trans. Circuits and Systems, vol. CAS-21, Nov. 1974.
- [50] K.R. Laker, M.S. Ghausi and J.J. Kelly, "Minimum sensitivity active (leapfrog) and passive ladder bandpass filters," IEEE Trans. Circuits and Systems, vol. CAS-22, pp. 670-677, Aug. 1975.
- [51] P.O. Brackett and A.S. Sedra, "Direct SFG simulation of LC ladder networks with applications to active filter design," IEEE Trans. Circuits and Systems, vol. CAS-23, no. 2, pp. 61-67, Feb. 1976.
- [52] P.O. Brackett and A.S. Sedra, "Active compensation for high frequency effects in op-amp circuits with applications to active RC filters," IEEE Trans. Circuits and Systems, vol. CAS-23, no. 2, pp. 68-72, Feb. 1976.
- [53] Le Qui The and T. Yanagisawa, "Some new lossless floating inductance circuits," Proc. IEEE, pp. 1071-1072, July 1977.
- [54] K. Martin and A.S. Sedra, "Optimum design of active filters using the generalized immittance converters," IEEE Trans. Circuits and Systems, vol. CAS-24, no. 9, Sept. 1977.
- [55] D. Dubois and J. Neiryneck, "Synthesis of a leapfrog configuration equivalent to an LC-ladder filter between generalized terminations," IEEE Trans. Circuits and Systems, vol. CAS-24, no. 11, Nov. 1977.
- [56] L.T. Bruton, "Multiple amplifier RC-active filter design with emphasis on GIC realizations," IEEE Trans. Circuits and Systems, CAS-24, pp. 830-845, Oct. 1978.

- [57] Raj Senani, "Realization of single-resistance-controlled lossless floating inductance," Electron. Lett., vol. 14, no. 25, pp. 828-829, Dec. 1978.
- [58] Euiwon Kim and H.K. Kim, "Equivalent canonic ladder networks," Proc. Midwest Symp. on Circuits and Systems, pp. 408-412, Philadelphia, June 1979.
- [59] C.M. Rader and B. Gold, "Digital filter design techniques in the frequency domain," Proc. IEEE, vol. 55, pp. 149-171, Feb. 1967.
- [60] L.B. Jackson, "An analysis of limit cycles due to multiplication rounding in recursive digital filters," Proc. 7th Annual Allerton Conf. Circuit and System Theory, pp. 69-78, 1969.
- [61] P.M. Ebert, J.E. Mazo and M.G. Taylor, "Overflow oscillations in digital filters," Bell Sys. Tech. J., vol. 48, pp. 2999-3020, Nov. 1969.
- [62] A. Fettweis, "Digital filter structures related to classical filter networks," Arch. Elek. Übertragung., vol. 25, pp. 79-89, Feb. 1971.
- [63] _____, "On the connection between multiplier word length limitation and roundoff noise in digital filters," IEEE Trans. Circuit Theory, vol. CT-19, pp. 486-491, Sept. 1972.
- [64] R.E. Crochiere, "Digital ladder structures and coefficient sensitivity," IEEE Trans. Audio and Electroacoustics, vol. AU-20, pp. 240-246, Oct. 1972.
- [65] A. Fettweis, "Pseudopassivity, sensitivity and stability of wave digital filters," IEEE Trans. Circuit Theory, vol. CT-19, pp. 668-673, Nov. 1972.
- [66] G.C. Temes and S.K. Mitra, Modern Filter Theory and Design, pp. 505-557, New York: John Wiley & Sons, 1973.
- [67] A. Sedlmeyer and A. Fettweis, "Digital filters with true ladder configuration," Int. J. Circuit Theory Applications, vol. 1, pp. 5-10, 1973.
- [68] A. Fettweis, "On sensitivity and roundoff noise in wave digital filters," IEEE Trans. Acoustics, Speech, and Signal Processing, vol. ASSP-22, pp. 383-384, Oct. 1974.
- [69] L.R. Rabiner and B. Gold, Theory and Application of Digital Signal Processing, New Jersey: Prentice-Hall, 1975.
- [70] A.V. Oppenheim and R.W. Schaffer, Digital Signal Processing, New Jersey: Prentice-Hall, 1975.

- [71] L.T. Bruton, "Low sensitivity digital ladder filters," IEEE Trans. Circuits and Systems, vol. CAS-22, pp. 168-176, March 1975.
- [72] A. Fettweis and K. Meerkötter, "Suppression of parasitic oscillations in wave digital filters," IEEE Trans. Circuits and Systems, vol. CAS-22, pp. 239-246, March 1975; Also "Correction to 'Suppression of parasitic oscillations in wave digital filters'," IEEE Trans. Circuits and Systems, vol. CAS-22, p. 575, June 1975.
- [73] K. Meerkötter and W. Wegener, "New second-order digital filter without parasitic oscillations," Arch. Elek. Übertragung., vol. 29, pp. 312-314, 1975.
- [74] A. Fettweis and K. Meerkötter, "On adaptors for wave digital filters," IEEE Trans. Acoust., Speech and Signal Processing, vol. ASSP-23, no. 6, pp. 516-525, Dec. 1975.
- [75] G.O. Martens and K. Meerkötter, "On n-port adaptors for wave digital filters with application to a bridged-tee filter," Proc. IEEE Symp. Circuits and Systems, Munich, pp. 514-517, 1976.
- [76] W. Wegener, "Design of wave digital filters with very short coefficient word lengths," Proc. IEEE Symp. Circuits and Systems, Munich, pp. 473-476, 1976.
- [77] H. Leich, "On the reduction of wordlength coefficient for wave digital filters related to LC ladder network," Proc. IEEE Symp. Circuits and Systems, Munich, pp. 469-472, 1976.
- [78] L.T. Bruton and D.A. Vaughan-Pope, "Synthesis of digital ladder filters from LC filters," IEEE Trans. Circuits and Systems, vol. CAS-23, pp. 395-402, June 1976.
- [79] G.O. Martens and H.H. Lê, "Wave digital adaptors for reciprocal second-order sections," IEEE Trans. Circuits and Systems, vol. CAS-25, Dec. 1978.
- [80] H.K. Kim, E. Kim and G.O. Martens, "Equivalent bandpass filters in doubly-terminated canonic ladder structures," IEEE Int. Symp. on Circuits and Systems, to be published, Houston, Texas, U.S.A., April 28-30, 1980.
- [81] D.J. Allstot, R.W. Brodersen and P.R. Gray, "MOS switched-capacitor ladder filters," IEEE J. Solid-State Circuits, SC-13, pp. 806-814, Dec. 1978.
- [82] A. Fettweis, "Switched-capacitor filters using voltage inverter switches," Proc. ISCAS 79, pp. 910-913, July 1979.